Use of Concrete Grinding Residue as a Soil Amendment

Final Report
January 2023

IOWA STATE UNIVERSITY
Institute for Transportation

About the Program for Sustainable Pavement Engineering and Research

The overall goal of the Program for Sustainable Pavement Engineering and Research (PROSPER) is to advance research, education, and technology transfer in the area of sustainable highway and airport pavement infrastructure systems.

About the Institute for Transportation

The mission of the Institute for Transportation (InTrans) at Iowa State University is to save lives and improve economic vitality through discovery, research innovation, outreach, and the implementation of bold ideas.

Iowa State University Nondiscrimination Statement

Iowa State University does not discriminate on the basis of race, color, age, ethnicity, religion, national origin, pregnancy, sexual orientation, gender identity, genetic information, sex, marital status, disability, or status as a US veteran. Inquiries regarding nondiscrimination policies may be directed to the Office of Equal Opportunity, 3410 Beardshear Hall, 515 Morrill Road, Ames, Iowa 50011, telephone: 515-294-7612, hotline: 515-294-1222, email: eooffice@iastate.edu.

Disclaimer Notice

The contents of this report reflect the views of the authors, who are responsible for the facts and the accuracy of the information presented herein. The opinions, findings and conclusions expressed in this publication are those of the authors and not necessarily those of the sponsors.

The sponsors assume no liability for the contents or use of the information contained in this document. This report does not constitute a standard, specification, or regulation.

The sponsors do not endorse products or manufacturers. Trademarks or manufacturers' names appear in this report only because they are considered essential to the objective of the document.

Iowa DOT Statements

Federal and state laws prohibit employment and/or public accommodation discrimination on the basis of age, color, creed, disability, gender identity, national origin, pregnancy, race, religion, sex, sexual orientation or veteran's status. If you believe you have been discriminated against, please contact the Iowa Civil Rights Commission at 800-457-4416 or the Iowa Department of Transportation affirmative action officer. If you need accommodations because of a disability to access the Iowa Department of Transportation's services, contact the agency's affirmative action officer at 800-262-0003.

The preparation of this report was financed in part through funds provided by the Iowa Department of Transportation through its "Second Revised Agreement for the Management of Research Conducted by Iowa State University for the Iowa Department of Transportation" and its amendments.

The opinions, findings, and conclusions expressed in this publication are those of the authors and not necessarily those of the Iowa Department of Transportation.

Technical Report Documentation Page

1. Report No. IHRB Project TR-764	2. Government Accession No.	3. Recipient's Catalog No.
4. Title and Subtitle Use of Concrete Grinding Residue as a Soil Amendment		**5. Report Date** January 2023
		6. Performing Organization Code
7. Author(s) Patrick E. B. Bollinger (orcid.org/0000-0001-7524-3304), Md Jibon (orcid.org/0000-0003-4239-0812), Masrur Mahedi (orcid.org/0000-0002-3423-5524), Bo Yang (orcid.org/0000-0002-7774-5233), Bora Cetin (orcid.org/0000-0003-0415-7139), Halil Ceylan (orcid.org/0000-0003-1133-0366), Michael A. Perez (orcid.org/0000-0002-0309-3922)		**8. Performing Organization Report No.** InTrans Project 18-681
9. Performing Organization Name and Address Program for Sustainable Pavement Engineering & Research (PROSPER) Iowa State University 2711 South Loop Drive, Suite 4700 Ames, IA 50010-8664		**10. Work Unit No. (TRAIS)**
		11. Contract or Grant No.
12. Sponsoring Organization Name and Address Iowa Highway Research Board Iowa Department of Transportation 800 Lincoln Way Ames, IA 50010 / Recycled Materials Resource Center 2204 Engineering Hall 1415 Engineering Drive Madison, WI 53706-1691		**13. Type of Report and Period Covered** Final Report
		14. Sponsoring Agency Code RMRC Project MSN225685

15. Supplementary Notes

16. Abstract

Concrete diamond grinding on pavement projects generates a nonhazardous waste byproduct called concrete grinding residue (CGR). CGR has known cementitious characteristics that suggest a latent use as a soil-stabilizing amendment, especially for poor and problematic soils.

In this study, Western Iowa loess soil was amended with CGR and subjected to rainfall simulations and wind erosion tests to measure the erodibility of several soil mixtures. The results of the rainfall simulations showed that CGR-amended silty soil (loess) had only slightly different optimum moisture contents and maximum dry densities compared to untreated loess, while rainwater runoff samples of CGR-amended loess exhibited dramatically higher turbidity and total suspended solids. The results of the wind erosion tests showed that erosion was lower in more granular shoulder material and higher in shoulder material containing more organics. Wind erosion tests performed on CGR-amended Western Iowa loess showed modest improvement in this highly friable silty soil compared to untreated loess.

A field study conducted in Washington and Clinton Counties in Iowa compared CGR-stabilized and untreated sections to determine the effectiveness of CGR as a stabilizer for shoulder material. The CGR-stabilized sections in Washington County did not show significant improvement in strength, while the CGR-stabilized sections in Clinton County exhibited a 20% to 40% improvement in the composite elastic modulus and California bearing ratio values.

17. Key Words California bearing ratio—composite elastic modulus—concrete grinding residue—environmental impact—rainfall erosion—resilient modulus—shear strength—wind erosion		**18. Distribution Statement** No restrictions.	
19. Security Classification (of this report) Unclassified.	**20. Security Classification (of this page)** Unclassified.	**21. No. of Pages** 121	**22. Price** NA

Form DOT F 1700.7 (8-72)   **Reproduction of completed page authorized**

USE OF CONCRETE GRINDING RESIDUE AS A SOIL AMENDMENT

Final Report
January 2023

Principal Investigator
Halil Ceylan, Director
Program for Sustainable Pavement Engineering & Research (PROSPER)
Institute for Transportation, Iowa State University

Co-Principal Investigators
Bora Cetin, Associate Professor
Department of Civil and Environmental Engineering, Michigan State University

Michael A. Perez, Assistant Professor
Department of Civil Engineering, Auburn University

Research Assistants
Patrick E. B. Bollinger and Md Jibon

Authors
Patrick E. B. Bollinger, Md Jibon, Masrur Mahedi, Bo Yang, Bora Cetin,
Halil Ceylan, and Michael A. Perez

A report from
Institute for Transportation
Iowa State University
2711 South Loop Drive, Suite 4700
Ames, IA 50010-8664
Phone: 515-294-8103 / Fax: 515-294-0467
https://prosper.intrans.iastate.edu/

TABLE OF CONTENTS

LIST OF FIGURES

LIST OF TABLES

ACKNOWLEDGMENTS

Significant portions of this report were previously published as part of the following:

Bollinger, P. E. B., B. Cetin, H. Ceylan, and M. A. Perez. 2021. *Use of Concrete Grinding Residue as a Soil Amendment-Part II*. Recycled Materials Resource Center, University of Wisconsin-Madison, Madison, WI.

EXECUTIVE SUMMARY

The objective of this research was to study the behavior of concrete grinding residue (CGR) when used as a soil amendment, with the overall goal of evaluating a potential market for CGR as a soil stabilizing amendment.

A thorough literature review was conducted on concrete grinding industry standards; past and present collection and disposal practices sanctioned by federal, state, and local authorities having jurisdiction (AHJs) for the proper handling and disposal of CGRs; and laboratory testing performed to date on CGRs and CGR as an amendment to soils, concrete, and other materials. The literature review revealed a significant gap in work performed with CGR-amended soils, with soil erosivity and full-scale field implementation as stabilization agents not found in any previous research.

The laboratory portion of this research involved the evaluation of different CGR collection methods; the creation of uniform methods for the preparation, mixing, and compaction of different homogeneous CGR-amended soil mixtures; and the testing of various soil mixtures in an indoor rainfall simulator and an indoor wind erosion testing apparatus. Additionally, soil characteristic testing was conducted that involved environmental and soil strength/stiffness testing of CGR-amended soils.

Materials tested in this portion of the research included five CGR-soil amendments, one silt, and five gravel aggregates. The five CGR samples were collected from five active concrete diamond grinding projects located throughout the state of Iowa. The silt was excavated from a quarry in the Loess Hills of western Iowa. The five gravel aggregates were sampled from five rural county roads from two counties in eastern Iowa.

The results of the laboratory research suggest that amending soils with CGR and other soil amendments does have merit, but it is currently an under-researched topic. Erosion tests on soils with sustainable soil amendments like CGR appears to be discounted or overlooked although determined from this study to be an important element in the stabilization of problematic soils.

In addition to the laboratory portion of this research, methods of applying CGR dosages in the field and the usefulness of using CGR-amended soil were studied by applying different stabilization techniques at demonstration sites in Washington County and Clinton County, Iowa. The findings from the field study revealed that blending CGR with soil improved the strength of the soil significantly at the Clinton County field demonstration site. Although one of the field demonstration sites demonstrated the benefit of using CGR-amended soil, it should be confirmed by additional field demonstration.

The data and lessons learned through this research should serve as a baseline for future research performed on additional soil types with other sustainable soil amendments. Testing of other roadway construction waste byproducts (including CGR) in different dosages is expected to yield promising results.

CHAPTER 1 INTRODUCTION

1.1 Background

The first concrete road in the United States was installed in Bellefontaine, Ohio, in 1891 (Snell and Snell 2002, Pasko 1998, ASCE 2021). The first concrete highway, however, would not be installed for another 22 years, when a 24-mile, 9 ft wide, 5 in. thick stretch of roadway called "Dollarway Road" (its name based on the dollar per mile cost at the time) was installed in Pine Bluff, Arkansas, in 1913 (PCA 2021, McLaren 1999). Today there are 4.13 million miles of roads in the United States, with 2.91 million miles classified as paved (BTS 2019, FHWA 2020).

Like any manmade structure, eventual maintenance is required to extend the life of this extensive network of paved roadways. One of these maintenance methods is concrete diamond grinding to roadway surfaces. Different from concrete tining, where either transverse or longitudinal grooves are dragged through the wet concrete mix, concrete diamond grinding is performed on hardened concrete pavements. While the main purpose for tining is to provide drainage channels to improve skid resistance, longitudinal tining and concrete diamond grinding are both useful methods for reducing noise emissions from traffic over concrete pavements (Gee 2005, Rasmussen et al. 2010, Rasmussen et al. 2012, Snyder 2019). In addition to reducing noise, concrete diamond grinding has the added benefit of improving macrotexture and correcting irregularities due to faults, cracks, warping, and overall roughness of the concrete driving surface (Hibbs and Larson 1996, Rao et al. 1999, Mamo et al. 2015).

Concrete grinding on roadway surfaces was first experimented with in the late 1940s (IGGA 2019). By 1972, the International Grooving and Grinding Association (IGGA) was formed to support the concrete and concrete grinding industries. Since then, the need for grinding and grooving concrete of roadway surfaces has grown, and the practice of grinding and grooving roadway surfaces has developed into an industry standard worldwide (Kenter 2012, AC Business Media, LLC 2013, BCPA 2020, Willis 2014). Today IGGA and the American Concrete Pavement Association (ACPA) both promote best management practices (BMPs) for concrete pavements and concrete grinding and grooving for new portland cement concrete (PCC) roadways, concrete pavement preservation (CPP) projects, and concrete pavement restoration (CPR) projects (IGGA 2013).

The greatest fear authorities have in terms of concrete grinding is environmental concerns with the disposal of concrete grinding residue (CGR), which is primarily discharged directly onto adjacent roadway shoulders and the surrounding landscape and to a lesser degree disposed of in landfills (Ceylan et al. 2019, Luo 2019, Yang et al. 2019a). Chief among the concerns for disposal along roadsides is the chemistry and mineral composition of the CGR and the caustic nature of this highly alkaline waste product (Mamo et al. 2015, Ceylan et al. 2019, Kluge et al. 2017, Luo et al. 2019).

The crux of the argument from an environmental and health perspective is the effect of CGR discharge (or slurry) spread onto sensitive areas, including roadside vegetation, soil, or nearby streams and bodies of water (Dispenza 2020). The United States Environmental Protection

Agency (U.S. EPA) classifies hazardous waste as a substance that is ignitable, corrosive, reactive, or toxic (EPA 2022a). Although CGR is not ignitable or reactive, the question of the corrosiveness and the toxicity of CGR has been a source of consternation because of the known high pH and high alkalinity of the wastewater and solids in a typical CGR slurry. As a result, many states have developed regulations and standards limiting or prohibiting discharge of CGR onto roadway shoulders, medians, or embankments (Yang et al. 2019a). Two additional environmental concerns revolve around the question of trace metals and potential leachate concerns with CGR when in contact with water and soil (Mamo et al. 2015, Kluge et al. 2017). Kluge et al. (2017) and Yang et al. (2019a) also found that state regulations varied greatly by region, with 41 out of 50 states having regulations regarding CGR (Kluge et al. 2017) and 19 states requiring "continuous removal" of CGR (Yang et al. 2019a) from roadway surfaces during concrete grinding operations.

In 1990, a failed roadway overlay on a large-scale (and very public) PCC pavement project resulted in an environmental firestorm that led to significant changes in the way the Federal Highway Administration (FHWA) and state departments of transportation (DOTs) still view and handle the treatment and disposal of CGR on roadway projects today. On this Utah project, an experimental thin bonded portland cement (PC) overlay on a 12-mile stretch of Utah's I-15 failed after one month, with 15% delamination reported after only four months (Goodwin and Roshek 1992). This initiated a large-scale concrete diamond grinding project, with direct disposal of CGR discharge onto the roadway shoulders and median swales, which was consistent with Utah's current CGR disposal regulations at the time. Grab samples taken from the initial CGR discharge from this remediation project revealed a highly caustic CGR discharge with a pH of 12.0 (above regulation limits), which promptly caused the project to be halted to address this environmental problem and modify the disposal procedures for this project. The unique aspect of this project was that the PC overlay was thick, with an average depth of ¾ in. being removed. It was later determined that this project generated 891,000 gal of alkaline wastewater and 3,200 yd^3 of alkali solids, which at the time was an environmental nightmare for the Utah Division of Environmental Health and the Utah DOT due to the unknown long-term effects of CGR on soil and vegetation (Goodwin and Roshek 1992).

PCC overlays are not new, and both unbonded overlays (PC over PC) and bonded overlays (PC over asphalt concrete) have been installed successfully over aging roads for decades (McGhee 1994). Additionally, concrete diamond grinding has also been around this long, dating back to at least 1965 when the purported first large-scale concrete diamond grinding project was performed on the San Bernardino Freeway (I-10) in southern California to eliminate excessive faulting between PCC roadway slabs (Rao et al. 1999, Neal and Woodstrom 1976). Through the years, removal and disposal challenges similar to those experienced during the Utah project have undoubtedly been faced by state DOTs as their roads have required similar concrete pavement preservation or restoration.

The pH of CGR has been studied vigorously since the initial 1965 San Bernardino project, with high pH values above 11.0 reported in many studies (Holmes and Narver 1997, Yonge and Shanmugam 2005, DeSutter et al. 2011a, Yang et al. 2019b). In addition to high pH values, Holmes and Narver (1997) also found high cation and anion concentrations of aluminum, iron, and sulfate above California drinking water standards, and DeSutter et al. (2011a, 2011b) also

found concerning but not toxic levels of various minerals, including arsenic, chromium, and lead, in CGR samples tested. The high pH in CGR is the result of hydroxide ions formed from the metal oxides present in the CGR discharge, with lime (CaO) and magnesium oxide (MgO) contributing to both the high pH and high alkalinity of the CGR discharge (Mamo et a. 2015). The high metals content in CGR (including chromium and iron) is attributed to the use of portland cement replacement pozzolans like fly ash and steel slag in cement production and concrete mix preparation (Yang et al. 2019b).

In addition to studies on the pH of CGR, numerous studies have classified CGR as a nonhazardous material by U.S. EPA standards (Mamo et a. 2015, Yang et al. 2019a, Holmes and Narver 1997, Correa and Wong 2020). The study by Holmes and Narver (1997) also concluded that the effects of CGR on fish were minimal, with a reported 100% survival rate for fish tested with both solid and slurry filtrate samples of CGR, and that CGR was compliant with California Title 22 wastewater treatment standards.

Additional research on CGR has also focused on environmental effects from CGR on soils and plants. With respect to the effects of CGR on soils and existing vegetation, several recent studies have affirmed that CGR has a positive impact on plant growth (Mamo et al. 2015, Ceylan et al. 2019, Luo 2019, Luo et al. 2019, DeSutter et al. 2011a, Yang et al., 2019b). Mamo et al. (2015), in particular, studied the effects of CGR on established vegetation on roadway foreslopes, with research focused on how existing vegetation, soil chemistry, and water quality from stormwater runoff might be affected by CGR. This important study concluded that CGR did not have an adverse effect on existing vegetation, soil chemistry, or water runoff volume or soil chemistry. The arduous debate on any long-term environmental effects from CGR discharge onto soils and vegetation were largely put to rest by two environmental studies by Mamo et al. (2015) and Ceylan et al. (2019), which both concluded that CGR did not cause any long-term negative effects to existing vegetation or soil chemistry. Additionally, Ceylan et al. (2019), Yang et al. (2019), and Luo et al. (2019) studied vegetated test plots with various dosages of CGR and found only short-term increases in pH and no long-term detrimental effect to the soil and vegetation, including changes in infiltration and plant biomass with the addition of CGR to the soil.

Studies have also been performed on CGR as an additive in various applications. In a 2017 study, CGR was used as a mortar amendment, with results demonstrating that the use of CGR as a replacement for portland cement generally decreased the compressive strength of the mortar with an increase in the amount of CGR (Kluge et al. 2017). However, one CGR sample with finer gradation (and an average particle size of 27 μm) at 5% portland cement replacement outperformed the control mortar with no CGR (Kluge et al. 2017). With respect to CGR used as a soil amendment, DeSutter et al. (2011a) amended a silty clay and a fine sandy loam with CGR and found no appreciable change in the infiltration for these two soils. Yonge and Shanmugam (2005) studied the pH neutralization and soil metal concentration changes when CGR was mixed with organic composts. Results from this study demonstrated that compost did help reduce the pH levels of the CGR but that changes in metal concentrations were negligible. Yang et al. (2019b) further tested the chemical changes (including pH, electroconductivity [EC], alkalinity, metal concentrations, and cation exchange) resulting from the addition of CGR in different dosages to a sandy loam (clayey sand). Results demonstrated that CGR showed no long-term detrimental effects to the soils amended with CGR (Yang et al. 2019b).

Research into CGR as a soil amendment for the purpose of soil stabilization is currently minimal. Yang et al. (2019b) added CGR to two different soils, a clayey sand and a sandy silt. Two strength tests, including unconfined compressive strength (UCS) and California bearing ratio (CBR), were performed with dosages of CGR ranging from 0% to 40% (amended to these two soils). Results showed increases in UCS and CBR with the addition of CGR, with the highest improvement exhibited by the soils with 20% CGR dosages. No other research was found where strength tests were performed with CGR used as a soil amendment. Additionally, no soil erosion studies were found involving CGR used as a soil amendment, and no research was found on CGR as a soil stabilizing amendment with other types of soils.

Since testing soil amendments with a wide range of soils and testing soil amendments for both strength and erosivity are important measures for soil stabilizing amendments, the purpose of the present study was to evaluate the effects of CGR on several different soils. Soil erosivity in particular was the primary focus of the research in this study. By evaluating erosion by both wind and rain, this study aimed to explore aspects of CGR-amended soils not previously studied and add to the mechanical characteristics already known about CGR from the Yang et al. (2019b) study.

The research performed in this study involved both a rainfall erosion study and a wind erosion study. In the rainfall erosion study, western Iowa loess was tested with two different CGRs with 20% CGR dosages. Total suspended solids (TSS), water quality (turbidity), and pH tests were performed in this first study. In the wind erosion study, tests were performed on the same CGR-amended soil mixtures used in the rainfall erosion study along with additional tests on five Iowa shoulder aggregates combined with two different CGRs at two different CGR dosages (20% and 40%). The wind erosion test consisted of three phases, with soil loss measurements taken for each phase of the wind erosion cycle.

An important aspect of checking the effectiveness of using CGR in pavement shoulder material stabilization is to assess the performance of CGR-amended soils at field test sites. Since no previous study was available regarding the field implementation of CGR for shoulder stabilization, the field demonstration sites were constructed based on the optimum dosage of CGR identified from the unconfined compressive strength tests in the erosion studies. The performance of CGR-stabilized shoulder material was investigated at the field demonstration sites through lightweight deflectometer (LWD) and dynamic cone penetrometer (DCP) tests.

1.1.1 Concrete Diamond Grinding

Thousands of roadway construction projects are completed each year. On PCC roadway projects where surface repairs are required, concrete diamond grinding is commonly included in the scope of work. While CGR generated from these projects is often discharged onto adjacent roadway embankments, current environmental concerns have pushed 29 states to restrict roadside disposal in favor of offsite CGR disposal (Yang et al. 2019a). This is because many environmental authorities, including the U.S. EPA, state departments of natural resources, and state departments of public health, view CGR solely as a pernicious waste byproduct (Ceylan et al. 2019, Yang et al. 2019a, Townsend et al. 2016). A key goal of this research, therefore, was to

further evaluate the potential of recycling uses for CGR, namely in the stabilization of roadway embankments, underlying soils, and/or subgrades, as suggested in previous studies by Yang et al. (2019b) and Kluge et al (2017).

Pavements rely on subgrades and confining slopes. Permeability and drainage are important/key factors for subgrades (Ceylan et al. 2013, Coban 2017), while strength and stiffness are primary critical design criteria for embankments (Sawangsuriya and Edil 2016, Schaefer et al. 2008). Side-slope erosion and long-term infiltration are also important design factors with embankments (Christopher et al. 2006, Kinnell 2000), and exposed embankments with little or no vegetation are particularly vulnerable to erosion from wind and rain (Benik et al. 2003, Ricks et al. 2019). Such erosion, whether the result of new construction or due to exposure caused by natural elements like wind and rain, can lead to slope failures or structural confinement issues (Schaefer et al. 2008), while slopes comprised of collapsible soils (e.g., silts and loess deposits) are susceptible to failure due to sudden changes in volume when exposed to moisture (Christopher et al. 2006).

While amending soils with lime or portland cement are two of the more common methods for combatting some of the more worrisome material characteristics of poor soils (White and Vennapusa 2013, Bruce et al. 2013), exploring the use of waste byproducts for stabilizing soils would provide a more sustainable solution (Kestler 2009, Christopher et al. 2006). Venn diagrams are commonly used to show the holistic approach for sustainable design. The 3 R's (reduce, reuse, and recycle) when incorporated into an engineering design determine the extent that an engineering design or construction process is "green" or sustainable (Brusseau 2019). Often referred to as the "triple bottom line" approach, recycling responsibly looks at environmental and societal impacts, not just the monetary cost of the project (Brusseau 2019). Products like reclaimed asphalt pavement (RAP), reclaimed portland cement concrete (RPCC), high-carbon fly ash (HCFA), and CGR are examples of waste products produced in abundance that, if integrated into roadway projects, could not only reduce the bottom-line costs of a project but also significantly reduce the burden on landfills (Brusseau 2019, Robinson et al. 2004, Cetin et al. 2010, Jones and Cetin 2017, Li et al. 2018, Cline et al. 2020, Chesner et al. 1998).

CPR projects that include diamond grinding vary significantly in size and scope, and although the selection of grinding equipment for a project is often based on the size of the grinding job, disposal procedures are often prescriptively dictated by county, state, and/or federal guidelines (Yang et al. 2019a). With only general regulations for project execution left at the discretion of the contractor, offsite disposal of CGR discharge remains somewhat arbitrary (Correa and Wong 2001). For example, on a project where the collection of CGR discharge is required, a ready-mix truck or tanker truck might be used for transport and offsite disposal to a third party's sedimentation pit.

CPR projects with diamond grinding to make roadway surface corrections (primarily to remove roadway bumps) are generally referred to as "bump grinding" jobs. Smaller bump grinding jobs vary from simply correcting high spots in a single roadway intersection to leveling miles of multilane highway pavement sections. Diamond Products Limited out of St. Elyria, Ohio, is one of the largest grinding equipment manufacturers in the concrete grinding industry. Included in

the Diamond Products (DP) commercial product line are the 1500 Series, 4500 Series, and 6000 Series (drivable) grooving and grinding equipment rigs. The 1500 Series grinding rig has a 38 in. (~3 ft) grinding drum/head with a series of parallel grinding blades, while the larger 4500 and 6000 Series rigs each have 50 in. (~4 ft) grinding heads. Unless a project has space restrictions, Section 2532 of the Iowa DOT's *Standard Specifications for Highway and Bridge Construction* specifies that a 3 ft minimum grinding head is required on roadway projects (Iowa DOT 2020). Companies including Cedar Falls Construction, Manatt's Inc., and West Fork Grinding, for example, each specialize in smaller bump grinding projects. On the bump grinding jobs visited during this research in Palo, Iowa (Cedar Falls Construction), in Des Moines, Iowa (Manatt's Inc.), and in Ruthven, Iowa (Cedar Falls Construction), smaller 1500 Series DP grinders were utilized.

Concrete diamond grinding projects on larger county, state, or Interstate roadway projects are commonly referred to as mainline surface repair projects (or simply "mainline" jobs). Mainline jobs typically utilize one or more larger concrete grinding rigs, each with 4 ft (grinding) heads, to perform the required roadway profile improvements. Mainline grinding jobs can be as short as a few miles on smaller two-lane rural roads to as long as 10 to 20 miles on larger four-lane (or wider) undivided and divided highways. National firms including Penhall, Interstate Improvement, and Diamond Surfacing, Inc., for example, each have multiple DP 6000 Series (or similar) mainline grinding rigs. These larger firms often deploy three larger grinding rigs (with 4 ft grinding heads) in series to grind the full surface across 12 ft driving lanes. This is accomplished by operating three machines in tandem with a small overlap of the edge of each successive grinding strip, which allows grinding of a full driving lane in a single pass with three trucks. It is not uncommon for several lane miles of grinding to be completed per workday in this manner. Larger mainline rigs can also be used on smaller bump grinding jobs when time is a factor to meet compressed project schedules. Smaller grinding rigs with 3 ft heads are typically used on smaller projects, while larger mainline rigs (with 4 ft grinding heads) are used on larger highway projects. On a mainline grinding project in Muscatine, Iowa, for example, West Fork Grinding (as detailed in the following chapter) deployed a larger DP 6000 Series grinder to handle grinding along a multi-mile section of a two-lane undivided highway, completing surface corrections to several lane miles in a single workday.

1.1.2 Erosion

Rain erosion is simply defined as the detachment of soil particles due to the impact of raindrops on the soil, followed by the transport and deposition of these particles away from the source (USDA 2011). This erosion can be categorized into four types: splash erosion, sheet erosion, rill erosion, and gully erosion (National Geographic n.d.). As raindrops impact the ground, inter-rill erosion starts as the drops strike the ground (OSU n.d.), which leads to sheet erosion (or overland flow) and concentrated flows in rivulets/small channels that lead to the creation of grooves or rill erosion (OSU n.d., Zhang et al. 2019). Conservative estimates of soil loss due to sheet and rill erosion in the United States are appraised at 3.4 billion tons/year (Olson et al. 1994). This is three times the annual erosion rates due to wind erosion in the United States, which accounts for an additional 1.2 billion tons/year in transported soil from farmlands alone (Olson et al. 1994). Erosion of sediment from local heavy rainstorms is dependent on a number of factors, including rainfall characteristics, topography, soil type, and soil conservation practices (Cruse et al. 2006).

In Iowa, average rainfall varies for a given 24-hour rainfall event but falls generally into a range of 0.5 to 3 in., with estimated average runoffs during this period around 2 in. (Cruse et al. 2006). However, climate modeling in the United States has shown increases in heavy precipitation from 1958 to 2007 in all regions of the country, including a 15% increase in the Midwest (including Iowa) to as much as a 67% increase in the Northeast (Berendzen et al. 2011). In more recent data, the 2015 Iowa Statewide Urban Design and Specifications (SUDAS) manual divided the state into nine climatic sections. Using data from the National Oceanic and Atmospheric Administration (NOAA) for these nine Iowa regions, the average rainfall for a 24-hour storm event was estimated to be 3.07 in. with a standard deviation of 0.09 in. across the state (Iowa SUDAS 2015). This confirmed the 2010 climate change estimates reported by the Iowa Climate Change Impacts Committee (ICCIC) in its report to the Governor and the Iowa General Assembly at that time (Berendzen et al. 2011), which postulated that this increased rainfall would lead to continued erosion and soil loss in exposed and vulnerable lands despite current soil conservation practices. Cruse et al. (2006) estimated current sheet and rill erosion at 5.1 tons/acre annually for the state of Iowa. This erosion rate is supported by the 2017 data from the National Resources Inventory (NRI), which estimated a loss of 5.6 tons/acre/year for the state of Iowa (USDA 2020) or approximately 3,600 tons/mi^2/year. With an area of just over 56,000 mi^2 in Iowa, this translates to an alarming 201 million tons of rain-eroded soil per year for the state.

Wind erosion is a complex physical phenomenon that, until the Dust Bowl of the 1930s, was viewed primarily as a regional problem during periods of drought (Argabright 1991). Some of the earliest research and quantifiable methods for predicting wind erosion were developed by Chepil (1958) at the United States Department of Agriculture (USDA). Chepil (1958) developed a byzantine wind erosion equation, later coined WEQ (Woodruff and Siddoway 1965), in an effort to develop a method to predict wind erosion. Chepil's (1958) soils research determined that the "most erodible discrete soil particles" had diameters of approximately 0.1 mm and that "relatively few particles greater than 0.5 mm" (in diameter) were displaced by everyday wind events. Saltation (movement and airborne spreading) of these small 0.1 to 0.5 mm airborne soil particles accounts for between 50% to 80% of erosion by wind (USDA 2011). Since wind erosion involves soil particle detachment, transport, and deposition (Smith and English 1982), this range of particle size is an important soil characteristic, especially for loess and other silty soils, which have a median particle size of 0.01 mm (Knappett and Craig 2012) or 1/100th of the 0.1 mm soil particle size most susceptible to wind erosion identified by Chepil (1958).

The median particle size for the western Iowa loess used in the initial rainfall testing portion of the present study was 0.03 mm, with 99.9% of the particles in this soil measuring less than 0.5 mm (Coban 2017). The first batch of loess was from Monona County, Iowa, while the second batch of loess was collected from Crescent Quarry in nearby Pottawattamie County, Iowa. A sieve analysis was not performed on this second batch of soil from Crescent Quarry, but it is believed to share the same soil properties and particle size distribution as other loess samples. Further analysis for the Monona County loess (with similar results assumed for the Crescent Quarry loess) classified the western Iowa loess as an inorganic silt, with Unified Soil Classification System (USCS) soil classification ML and American Association of State Highway and Transportation Officials (AASHTO) soil classification A-4 (Coban 2017). This soil was further characterized to contain 0% gravel, 1% sand, 87% silt, and 12% clay-sized particles (Coban 2017). Based on particle size alone, western Iowa loess is a highly erodible soil.

The median particle size for the Clinton and Washington County, Iowa, Class A-1 shoulder aggregates used in this study was much larger, at 4.5 mm and 3.7 mm, respectively, with only 16.3% and 18.9% of the particles in these soils measuring less than 0.5 mm, respectively. This shows that the Class A-1 shoulder aggregates have a much lower propensity to erode compared to the western Iowa loess specimens. However, these percentages still translate to significant amounts of erodible soil particles under 0.5 mm for these Class A-1 shoulder aggregates.

Unpaved, compacted, gravel shoulders also suffer from erosion from both wind and rain. Guidelines for the proper installation and maintenance of gravel roadways exist for every state as well as the FHWA. One of the more comprehensive unpaved gravel road manuals used today is the FHWA's *Gravel Roads Construction and Maintenance Guide* (FHWA 2015). This comprehensive and prescriptive guide details some of the more common problems found in unpaved gravel roads and shoulders caused by both wind and rain erosion. The wind-scouring of roadway soils due to the passage of larger trucks traveling at high speeds along unpaved roads or paved roads with unpaved gravel shoulders (i.e., wind whip) is a significant contributor to erosion. The laboratory-based wind erosion testing performed at Michigan State University (MSU) described in this report reproduced and analyzed wind whip on a smaller scale, which in turn allowed for the measurement of wind erosion of different soils in a laboratory-controlled environment.

1.2 Problem Statement

Diamond grinding is a widely used rehabilitation technique commonly referred to as the resurfacing of PCC pavement. As a maintenance operation, diamond grinding can provide a smooth PCC surface with enhanced texture and skid resistance and reduced road noise. Typically, this operation uses a truck equipped with grinding heads at ground level to saw a thin layer of concrete, grinding it into fine particles, while mixing with water to cool the grinding blades and reduce dust. This process generates a slurry byproduct known as CGR.

The majority of current maintenance practice involves the spreading of fresh CGR along roadsides, resulting in potential environmental concerns regarding vegetation growth. This becomes a more critical issue when the disposal of CGR slurries is adjacent to sensitive areas such as farmlands, water bodies, or areas with high groundwater tables. CGR disposal may lead to reduced density of vegetation, which may result in increased erosive risks.

The composition of CGR can vary widely due to the use of different portland cement products and admixture materials in concrete. Generally, CGR is characterized as having a high pH and is rich in metal content (e.g., chromium [Cr] and iron [Fe]) due to the addition of fly ash and/or steel slag during cement production or concrete mix preparation. Thus, the inappropriate disposal of CGR may cause critical environmental issues at or near sensitive areas. On the other hand, CGR has a significant potential for reuse as construction material, liming product, or soil stabilizer due to its high pH and rich calcium oxide (CaO) content.

A comprehensive literature review conducted during this study showed that CGR may pose some environmental concerns, even though in some cases it seems to be environmentally friendly. A

state-of-the-practice survey of regulations governing CGR management practices in all 50 US states was conducted to understand issues and concerns regarding CGR use in the concrete industry and state highway agencies (SHAs). In considering the properties of CGR, recycling of slurry waste in soil, concrete, and other applications could be an attractive alternative for ultimately improving roadway sustainability and field performance and reducing the life-cycle cost of pavement designs.

The present study evaluated the possibilities for reuse of CGR in several applications. In particular, this study explored CGR recycling opportunities for soil stabilization and erosion mitigation by conducting both laboratory and full-scale field studies. The laboratory tests included UCS, surface runoff tests, Atterberg limits, alkalinity, EC, pH, and leaching tests. The field demonstration sites were constructed with the aim of studying the benefits of using CGR in unbound material stabilization, assessing the performance of CGR-amended soils in the field, and selecting the best CGR application rates and construction practices.

1.3 Objectives

The main goal of this research was to develop a new cost-effective market for soil liming agents for transportation projects and to reduce stockpiles of diamond grinding wastes. To achieve this goal, laboratory experiments and full-scale field studies were conducted to investigate the performance of soils treated with CGR and to provide guidance about the use of CGR as a stabilizing agent. The specific research objectives are listed below:

1. Determine the erosion resistance of soils mixed with CGRs
2. Determine the stiffness/strength of soils mixed with CGRs
3. Determine the environmental impact of these soil-CGR mixtures
4. Determine the optimum amount of CGR in these soil-CGR mixtures based on mechanical and environmental evaluations
5. Measure the performance of CGR-stabilized soil at field demonstration sites
6. Assess different methods of applying CGR in the field

1.4 Research Plan

The research consisted of seven tasks, as described below:

Task 1: Kick-Off Meeting to Review the Project Scope and Work Plan
Task 2: Collection of Materials
Task 3: Laboratory Testing for Index and Engineering Properties of Materials and Mixtures
Task 4: Erosion Testing
Task 5: Environmental Analyses
Task 6: Field Demonstration
Task 7: Final Report

1.5 Research Benefits

The results of this study will contribute to knowledge about CGR-related practices and the environmental impacts of CGR. Currently, there are no guidance documents on the utilization of CGR in soil improvement applications. Current design recommendations use standard recipes without regard for the pH adjustments or buffer requirements necessitated by the use of CGR. The results of this project are expected to lead to changes in standard specifications for chemical soil stabilization and field implementation.

The outcome of this study is expected to lead to a stronger understanding of the potential use and management of CGR waste materials in a sustainable way. It is expected that successful implementation of CGR in soil stabilization applications would eliminate environmental concerns and improve the performance of pavement foundation materials. The results of the field implementation study can help guide construction techniques and confirm the benefit of CGR as a stabilization agent in the field.

CHAPTER 2 RAIN EROSION STUDY

2.1 Materials

The soil used in the rainfall erosion portion of this study was loess from the Loess Hills of western Iowa. In addition to the loess, five CGRs were collected from active concrete diamond grinding projects located in eastern, western, northern, central, and south central Iowa.

2.1.1 Western Iowa Loess

Western Iowa loess soil (hereafter referred to as loess) was selected as the base soil (control) to amend with CGR for this study. Loess was chosen for evaluation with CGR due to its abundance, its poor compaction characteristics, and its high degree of erodibility. Two batches of loess were needed for this project. The first batch of loess was transported by ISU's Department of Civil, Construction, and Environmental Engineering from a farm in the Loess Hills (in Monona County, Iowa) located in western Iowa. No other details were available about the collection of this first truckload of loess.

The second batch of loess was also sourced from the Loess Hills but was collected from Crescent Quarry located in the city of Crescent, Iowa (in Pottawattamie County), owned and operated by Schildberg Construction Company (Figure 1).

Figure 1. Crescent Quarry (Pottawattamie County, Iowa)

During the mining process for aglime and crushed aggregates, stockpiles of loess soils are generated. In Crescent Quarry, these stockpile deposits have grown over time into a mountain of unused loess surrounding the quarry. This soil is seeded to help mitigate erosion of this highly friable soil. The loess sampled from Crescent Quarry was excavated using a Caterpillar CAT 980B front-end loader with a 5 yd^3 bucket. The loader operator excavated the soil from a section of stockpiled loess, first scarifying the top 2 to 3 ft of soil from the stockpile to minimize any small roots and vegetation from getting into the desired soil. A total of 62 5 gal buckets (or

approximately 1.8 tons of soil) was loaded and transported back to ISU. While unloading the loess at the civil engineering laboratory, any remaining visible small roots and vegetation were removed. No stones or rocks were found in the soil collected. The general appearance of the loess from both Monona County and Crescent Quarry had the same royal brown color with a soft, velvety composition and appeared free from contamination from other soils or foreign matter, namely gravel, peat, and vegetation.

2.1.2 Concrete Diamond Grinding

Five CGRs (designated CGR-1 through CGR-5) were collected for research and testing in this study. On each of the grinding projects where CGR was generated and collected, Diamond Products grinding rigs were used exclusively. The DP 1500 Series, DP 4500 Series, and DP 6000 Series grinding rigs used on the projects visited were each operated by a single driver. These rigs have the versatility of grinding (or texturing) PCC roadway surfaces using closely spaced blades or grooving the roadway surface (to improve traction) with blades spaced slightly farther apart. Grinding (not grooving) was performed on the five grinding jobs visited for this project. Each of the grinding jobs visited had water trucks following the grinding rigs with pumps supplying up to 5 lb/in^2 of pressurized water, at a rate of approximately 8 gal per minute, to cool the blades on the grinding heads. As a result, a wet discharge mixture of sediment-laden water with concrete grindings (hereafter referred to as CGR discharge) was generated. CGR discharge collection was done by hand into 5 gal buckets for each of the five CGRs collected. Results are shown in Table 1.

Table 1. Concrete grinding project details

CGR	Discharge Method	Grinding Rig	Grinding Heads	Project Details
CGR-1	Ready-mix truck	DP 1500 Series	3 ft wide	50 ft section, at traffic intersection
CGR-2	Ready-mix truck	DP 1500 Series	3 ft wide	250 ft section, 4-lane undivided highway
CGR-3	Direct discharge	DP 1500 Series	3 ft wide	2–3 miles on 2-lane undivided rural road
CGR-4	Tanker truck	DP 6000 Series	4 ft wide	2–3 miles on 2-lane undivided highway
CGR-5	Direct discharge	DP 4500 Series	4 ft wide	4–5 miles on 4-lane undivided highway

2.1.3 CGR Discharge Collection Process

Five Iowa concrete grinding projects were visited, starting with the collection of CGR-1 in May 2019 and ending with the collection of CGR-5 in October 2019. CGR discharge was collected into Lowe's standard 5 gal PVC buckets with snap-on lids, which were then transported back to ISU for processing and testing. The project sites sampled were selected initially based on two primary criteria: geography and the size of the grinding job. The goal in the selection process was to obtain CGRs from projects ranging in size from small concrete pavement bump grinding jobs to larger mainline highway projects. A list of grinding contractors was created by starting from a roster of contractors who attended the Iowa Concrete Paving Association (ICPA) concrete paving workshop held in February 2019 in Des Moines, Iowa. In addition to this list, several Iowa DOT engineers recommended a few additional leads. From this list, a total of 27 concrete grinding contractors were qualified and then contacted bi-monthly in search of future concrete

grinding projects scheduled for the spring and summer of 2019. A large net was initially cast, centering on Ames, Iowa, and including a 350-mile radius from the center of ISU's main campus. This range was based on realistic travel to and from grinding jobs with a roundtrip distance that could be traveled in one to two days. However, after collecting material from the first three grinding projects within the state of Iowa, the project range was reduced to a 150-mile radius (or a search within the state of Iowa) for the last two grinding jobs. The last two grinding projects came from both the eastern and western borders of the state. Results are shown in Table 2.

Table 2. Concrete diamond grinding sites

CGR	Date	Location	Contractor(s)	Job Type, Size
CGR-1	29 May 2019	Palo, IA	Croell/Cedar Falls Construction	Bump grinding, small
CGR-2	30 May 2019	Des Moines, IA	Manatt's, Inc.	Bump grinding, small
CGR-3	6 Jun 2019	Ruthven, IA	Croell/Cedar Falls Construction	Bump grinding, moderate
CGR-4	14 Jun 2019	Muscatine, IA	West Fork Grinding	Mainline, small
CGR-5	21 Oct 2019	Sioux City, IA	Cedar Falls Construction	Mainline, moderate

On each project, 30 5 gal buckets were collected by hand, with the exception of CGR-3, where 50 5 gal buckets were collected. Each bucket was filled with CGR discharge to approximately a 10 in. fill line (marked inside each of the 14 in. tall 5 gal buckets). This equated to filling each bucket to approximately 3.6 gal, with the material weighing (on average) 40 to 44 lb per bucket. A minimum of 30 5 gal buckets was chosen for this project based on CGR quantities obtained for a Minnesota DOT (MnDOT) CGR research project performed at ISU and comparisons made between the testing requirements of the MnDOT project and the testing requirements of the compaction, rainfall, and wind erosion tests for the present study (Ceylan et al. 2019). Fifty buckets were collected for CGR-3, as mentioned above, because more water was expected in this CGR discharge due to the direct discharge collection method used on this job.

2.1.4 CGRs Collected

CGR-1 from Palo, Iowa, was generated and collected from a small bump grinding job at a roadway intersection on a two-lane undivided PCC highway. Due to county restrictions, the CGR produced on this job was collected into a cement mixing (ready-mix) truck, where it was hauled offsite to a sedimentation basin owned by a third party. Collection of the CGR-1 samples involved manually holding 5 gal buckets up to the end of the mixing truck discharge chute while the truck operator slowly rotated the mixing truck drum/barrel. The resulting CGR collected from this discharge method was deposited into a mix of buckets that contained both heavy and light CGR solids in the CGR discharge. Thirty 5 gal buckets (weighing 1,244 lb) of CGR-1 discharge were collected from this job site. Results are shown in Table 3.

Table 3. Collection method and CGR discharge comparison

CGR	Collection Method	Discharge, lb (gal)	Supernatant, lb (gal)	Cakes, lb (gal)
CGR-1	Ready-mix truck	1,244 (111.5)	508 (60.9)	736 (40.9)
CGR-2	Ready-mix truck	1,131 (93.6)	301 (36.1)	830 (46.5)
CGR-3*	Direct discharge	1,964 (193.7)	1,094 (143.2)	937 (53.0)
CGR-4	Tanker truck	1,160 (95.8)	272 (32.6)	889 (52.7)
CGR-5	Direct discharge	1,445 (112.8)	332 (39.8)	1,083 (67.0)

Cakes = Moist (saturated) CGR solids after decanting supernatant
*CGR-3 weights and volumes backcalculated from final slurry weight and volume

CGR-2 from Des Moines, Iowa, likewise came from a small bump grinding job on a 250 ft long section of a four-lane undivided PCC city highway recently replaced by Des Moines Water Works. Due to city disposal restrictions, the CGR produced on this job was also collected into ready-mix trucks and hauled offsite for disposal. The CGR was disposed of in a formal sedimentation basin owned by Manatt's Inc. Collection of CGR-2 samples similarly involved holding each empty bucket up to the end of the mixing truck discharge chute while the truck operator slowly rotated the mixing truck drum. Building on the experience from collecting CGR-1 in this manner, the CGR-2 collected from this discharge method had a slightly higher ratio of CGR solids to water. This discharge and collection method, however, produced a lot of splashes, and the ratio of CGR solids to water was random with each bucket. Thirty 5 gal buckets (weighing 1,131 lb) of CGR-2 discharge were collected from this job site.

CGR-3 from Ruthven, Iowa, was generated on a bump grinding job with a moderate amount of grinding on a new 2- to 3-mile pavement section of a two-lane undivided PCC rural road (Figure 2).

Figure 2. Direct discharge CGR collection (site CGR-3)

On this grinding job, discharge onto the roadway embankment was allowed, and there did not appear to be any CGR discharge restrictions. Since this project was a new road in the final stages of construction, the roadway embankments on this job site consisted of compacted soil with no established vegetation. As a result, the CGR discharged directly from the concrete grinding rig ran directly down the sloped embankment and soaked into the bare soil. CGR-3 discharge

collection involved holding each bucket up to the grinding rig discharge pipe while the rig operator slowly advanced in a normal grinding operation. The resulting CGR discharge collected from this discharge method contained a lot more water than CGR material (by volume). With more water anticipated in the discharge, 50 5 gal buckets of CGR-3 were collected from this job site. No offsite impoundment was required by the contractor for the balance of CGR discharge produced. Approximately 2,000 lb (50 buckets x estimated 40 lb/bucket) of CGR-3 was collected from this job.

CGR-4 from Muscatine, Iowa, like CGR-3, was generated from grinding on a 2- to 3-mile section of a two-lane undivided PCC highway. However, with the CGR-4 job, substantially more PCC grinding was required. As a result, the contractor referred to this job as a mainline job and used a larger DP 6000 Series concrete grinding rig for this grinding work. Due to project restrictions, the CGR produced on this job was collected into a large three-stage tanker/hopper truck and hauled offsite to a sedimentation basin owned by a third party. CGR-4 samples were collected from a discharge pipe from the undercarriage of the tanker truck. Collection of these samples involved holding each empty bucket up to the discharge pipe spigot while the truck operator slowly opened the discharge pipe spigot/valve. This discharge method was more controlled in comparison to the first three CGRs collected. In addition, because the CGR had settled slightly to the bottom of the tanker truck, the resulting CGR discharge from this collection method had a slightly higher ratio of CGR solids to water. The tanker truck disposed of the balance of the CGR discharge offsite into a large sedimentation basin owned by a third party. Thirty 5 gal buckets (weighing 1,160 lb) of CGR-4 discharge were collected from this job site.

CGR-5 from Sioux City, Iowa, was generated on a longer new 4- to 5-mile pavement section of a four-lane undivided PCC highway project. This roadway was closed to through traffic and only appeared to require moderate bump grinding throughout the job. Although this project primarily required bump grinding, it was classified as a mainline job, due in part to the harder rose quartzite aggregate used in the PCC pavement. The contractor selected a moderate size DP 4500 Series grinding rig for this work. On this project, like CGR-3, discharge onto the roadway embankment was allowed, and there did not appear to be any CGR discharge restrictions. Since this project was in the final stages of construction too, the embankments on this job site consisted of compacted soil with minimal established vegetation. As a result, the CGR discharged directly from the concrete grinding rig ran directly down the sloped embankment and soaked into the bare soil. CGR-5 collection involved holding each empty bucket up to the grinding rig discharge pipe while the grinding rig operator slowly advanced in a normal grinding operation. One notable difference between CGR-5 and the previous CGRs collected was that rose quartzite aggregate was used in the mix design. With this known prior to visiting the site, only 30 5 gal buckets were needed for collecting samples compared to the 50 buckets needed for the collection of CGR-3, where the same direct discharge method was used on the project. This was because the contractor shared that less water was typically used for concrete grinding work on PCC pavements with harder aggregates in the mix design to keep the blades hotter. The CGR discharge collected on this job contained less water (by volume) compared to the previous CGRs collected. No offsite impoundment was required by the contractor for the balance of CGR discharge produced. Thirty 5 gal buckets (weighing 1,445 lb) of CGR-5 discharge were collected from this job site.

Recall that for both CGR-1 and CGR-2, the CGR discharge was collected into ready-mix trucks and transported offsite for disposal. For these two jobs, CGR discharge was collected directly off of the discharge chute attached to the back of the ready-mix truck. The discharge collection rate for these two jobs was controlled by the truck operator, which generally allowed for the collection of a higher ratio of solids to water (by volume) in each bucket compared to direct (roadside) CGR discharge collection on a smaller bump grinding job. On grinding jobs using ready-mix trucks, the inside of the truck mixing barrel/drum is outfitted with T-shaped blades (or fins). As the drum is rotated, the ends of the fins become visible as the barrel turns, which allows clumps of CGR solid to be anticipated slightly for collection. Although less water was collected in the CGR discharge for CGR-1 and CGR-2 compared to the other CGR samples, each bucket collected still contained random amounts of CGR solids and discharge water. In comparison, CGR-3, CGR-4, and CGR-5 had roadside CGR discharge collection. For CGR-3 and CGR-5, CGR discharge was captured directly off the grinding rig. While technically CGR-4 was collected along the roadside, because CGR-4 was pumped into a tanker/hopper truck before collection, CGR-4 more closely resembled CGR-1 and CGR-2. For CGR-4, samples were collected from a spigot under the tanker truck. This provided the most control and the cleanest and most efficient means of CGR discharge collection. CGR-4 resulted in the least amount of supernatant collected (272 lb) compared to the other four CGRs collected, whose supernatant contents ranged from 301 to 1,071 lb.

Ultimately, the amount of CGR solids collected was the product of three primary factors. The type of grinding job (bump grinding verses mainline or full lane width grinding), the size of the grinding rig head (3 ft verses 4 ft widths), and the experience of the person(s) collecting the CGR discharge contributed the most to the amount of CGR solids collected. For CGR-5 (collected from a large mainline job), 852 lb of oven-dry CGR solids was collected compared to a range of 565 to 653 lb from the other CGRs collected.

2.2. Methods/Testing

The methods and testing for the rainfall erosion portion of this research involved the collection and preparation of the soils and CGRs as well as initial pH, EC, and compaction tests on both the untreated and treated (CGR-amended) soil specimens.

2.2.1 CGR Specimen Preparation

Early in this research, the idea of creating pourable (homogeneous) CGR slurries to blend with different soils was conceived. The main idea was to pour or spray CGR onto different soils similar to a hydromulch application and then test how well the CGR stabilized the soil. With this plan in mind, homogeneous CGR slurries were made with high amounts of water (and consequently high moisture contents). Little was known about CGRs and whether CGR discharge collected was a consistent material. It was known that each field-collected CGR discharge sample contained a significant amount of water. Originally it was believed that the CGR discharge collected directly from the concrete diamond grinder discharge pipe was homogeneous. This theory proved incorrect while decanting and mixing the first CGR selected (CGR-3) into a CGR slurry. Breaking up the stiff CGR cakes in a surplus of supernatant water

was difficult, and the use of garden hoes, flat-nosed shovels, and metal scoopers was required. Since too much water was kept in the mix in the first 10 buckets containing CGR-3, the next 20 buckets were partially decanted, leaving 1 to 2 in. of supernatant in each bucket with the solids before adding them to the large Rubbermaid trough used as the mixing bin. The CGR-3 solids from these buckets were not chopped up prior to adding them to the mixing bin. This was a mistake, and later all CGR cakes were broken up after decanting prior to adding any mixing water back into the solids. The final 20 buckets of CGR-3 were fully decanted, but the excessive amount of water from the first 30 buckets had already determined that the CGR-3 slurry would be too watery. The mixing of CGR-3 into a homogeneous CGR slurry took approximately 10 hours.

An early assumption was that a significant amount of supernatant would need to be retained (to add back in with the decanted solids) in order to produce a homogeneous CGR slurry. However, this assumption also proved wrong after processing the CGR-3 slurry. After producing the homogeneous CGR-3 slurry, a new mixing procedure was created. This procedure was created after struggling to break up the stiff and cohesive CGR-3 cakes. By more closely observing the settling of the particles for the next CGR sample collected, it was found that 12 to 24 hours provided sufficient time for the CGR solids to settle in each bucket (but did not make the solids too consolidated to break up by hand). Conversely with CGR-3, the solids had settled for seven days prior to mixing. After seven days, the CGR-3 solids had consolidated and coagulated into a semi-solid state in the bottom of each 5 gal bucket. The congealed CGR solids showed significant cohesive properties and proved quite difficult to remove from the buckets and break up using garden tools and a handheld mixer.

All homogeneous CGR mixes were blended in a new, clean 150 gal heavy-duty plastic Rubbermaid bin. CGR-3 was selected first for processing because this CGR discharge contained the most water of the five CGR samples collected. CGR-3 was also expected to be more workable compared to the other CGRs for the same reason. Mixing began by dumping the contents of the first 10 (of 50) buckets of settled CGR-3 solids as well as all of the supernatant from these buckets into a large Rubbermaid bin. Each CGR cake consisted (visually) of both sand-sized particles (that had settled first to the bottom of the buckets) and a few inches of a putty-like cohesive surface comprised of consolidated silt-size particles that had settled last. Figure 3 shows particles taken from a typical settled, decanted, and broken-up CGR cake.

Figure 3. Consistency of typical settled CGR solids (after decanting)

The amount of CGR solids in each 5 gal bucket varied from as little as 2 to 3 in. to as much as 8 to 9 in. deep. This was how it was determined that the CGR discharge buckets were nonhomogeneous in comparison to each other, which became a deciding factor in choosing to mix the buckets for each CGR in a large mixing bin.

After discovering the cohesive characteristics of the settled CGR-3 cakes and how well the CGR solids consolidated at the bottom of each bucket, the mixing methods were reexamined. Although a pourable CGR slurry was desired for each mix, the final CGR-3 slurry had too much water in it. As a result, a new mixing strategy and methodology was employed for the remaining mixes. Figure 4 shows the CGR solids before and after breaking up the CGR cakes (left) and the process of power mixing a homogeneous CGR slurry (right).

Figure 4. Typical CGR cakes (left) and CGR slurry mixing process (right)

For each of the remaining four CGRs processed, the following five steps were developed and followed for producing homogeneous CGR slurries. In Step 1, a visual observation was made to determine whether sufficient time had been allowed for the CGR solids to settle. Buckets judged

acceptable for decanting had clear supernatant on top of the CGR solids that had settled to the bottom of each bucket. The surplus supernatant that separated from the CGR solids was virtually clear, containing only a thin white film on the surface of the water. The supernatant water had a soapy feel to it, which was expected and attributed to the high alkalinity of the water. In Step 2, each bucket was weighed before and after decanting, with surplus supernatant kept and temporarily stored in clean 5 gal buckets for reuse. In Step 3, the decanted CGR cakes were transferred to metal mixing trays and broken down using garden hoes, flat-nosed shovels, trowels, and metal scoopers to break up the cakes into particles smaller than 1 to 2 in. This process was repeated for all 30 buckets with each separate CGR mix. In Step 4, a small amount of decanted supernatant water was added to the mix starting with 2 gal. In Step 5, additional water was added to the mix. Added water was recorded during the mixing process, and water was added only as needed to produce a moderately wet (pourable) homogeneous slurry similar in consistency to a sandy masonry grout.

A Brutus 21665Q 120 V two-speed handheld power mixer with a mortar mixing paddle (used for thinset grout and mortar mixes) was chosen to mix the initially stiff CGR clumps and added water. The amount of supernatant water added back into the CGR cakes for CGR-1, CGR-2, CGR-4, and CGR-5 was 3.5, 2, 8, and 8 gal, respectively. Supernatant water was not tracked with the first CGR mix (CGR-3) but was later estimated at 16 gal. Mixing time (excluding that needed for CGR-3) ranged from two to three hours to produce a homogenous CGR slurry. After mixing, the slurries were poured back into clean 5 gal buckets for storage and future testing. CGR slurry weights were determined by adding the initial weight of the decanted CGR cakes to the weight of the supernatant water mixed in during the homogeneous mixing process. The weight of the supernatant water was estimated at 8.34 lb/gal. Five homogeneous slurries with amounts ranging from 752.2 lb (42.9 gal) to 1,179.9 lb (75 gal) were produced for this study. The least amount of slurry was produced with CGR-1, and the most amount of slurry was produced with CGR-5. A summary of weights recorded is shown in Table 4.

Table 4. Homogeneous CGR slurry and CGR cakes comparison

CGR	Slurry (lb)	Slurry, gal (lb/ft^3)	Cakes (lb)	Cakes, gal (lb/ft^3)
CGR-1	752.2	42.9 (131.3)	735.5	40.9 (134.8)
CGR-2	859.2	50.0 (128.5)	830.0	46.5 (133.5)
CGR-3*	1,053.6	67.0 (117.7)	936.8	53.0 (132.3)
CGR-4	954.9	60.7 (117.7)	888.2	52.7 (126.2)
CGR-5	1,180.0	75.0 (114.7)	1,113.2	67.0 (120.9)

Slurry = Homogeneous CGR slurry and decanting and remixing
Cakes = Moist (saturated) CGR solids after decanting supernatant
*CGR-3 cake weight and volume backcalculated from final slurry weight and volume

In addition to the weights of the CGR cakes and homogeneous slurries produced, since the volume of the final CGR slurries and the volume of the added mixing water was known, unit weights for both the slurries and the CGR cakes for each CGR site were calculated. The unit weights for the CGR cakes ranged from 120.9 lb/ft^3 to 134.8 lb/ft^3. This range in unit weights is attributed to different sand and aggregate PCC constituents as well as the range in the degree of saturation of the CGR cakes.

2.2.2 CGR (Solids) Collection Efficiency

The following index was created to measure the weight of water and solids collected from a concrete grinding project. This index is important, as it could help a contractor estimate the costs for transporting and disposing of the CGR discharge (CGR-laden water) produced on a given project. CGR discharge consists of CGR solids and water. The volume of the CGR moist solids (or cakes) can be measured against the total gallons of CGR produced on a project.

The collection efficiency is an important measure for CGR collection because the CGR solids collected (not the surplus supernatant) are the materials that are currently landfilled in many states. CGR discharge collected from a grinding project consists of discarded cooling water and CGR solids. The total water and solids collected in a given amount of CGR discharge can vary significantly based on the duration and type of grinding job. Smaller bump grinding jobs with sporadic bump grinding, like CGR-1 and CGR-3, averaged a 30% collection efficiency, while larger mainline jobs, like CGR-4 and CGR-5, averaged around 55% collection efficiency. Results measured for the five CGR slurries produced are tabulated in Table 5. The higher the discharge water content, the lower the collection efficiency, meaning more water is expended on these projects during grinding operations.

Table 5. CGR discharge solids collection efficiencies

CGR	Discharge (gal)	Slurry (gal)	Cakes (gal)	Collection Efficiency
CGR-1	111.5	42.9	40.9	37%
CGR-2	93.6	50.0	46.5	50%
CGR-3*	193.7	67.0	53.0	27%
CGR-4	95.8	60.7	52.7	55%
CGR-5	112.8	75.0	67.0	59%

Cakes = Moist (saturated) CGR solids after decanting supernatant
*CGR-3 discharge and cake volumes backcalculated from final slurry volume

2.2.3 CGR Solids Ratio

An alternate index was also created in this research to measure the weight of the dry CGR solids produced on a given concrete diamond grinding project. In a recent MnDOT study, CGR was found to enhance plant growth in certain plants with minerals such as calcium and magnesium, providing nutritive benefits to the soil (Ceylan et al. 2019, Luo 2019, Luo et al. 2019). Based on the potential use of CGR as a fertilizer, calculating the dry CGR solids produced on a given CGR project could be important for a contractor. Knowing the solids ratios for different types of CGR projects would allow a contractor to determine the available solids on a particular project and estimate the amount of dry CGR solids that would be produced on a grinding project. The solids ratio is the ratio of the oven dry CGR solids to the total water in the CGR discharge (cake water plus decanted supernatant). For the five CGRs in this study, the solids ratio ranged from 0.30 to 0.60. CGR projects with a higher amount of water (a lower amount of solids) in the CGR discharge, like CGR-3, will produce the lowest solids ratios. In comparison, projects with less water (a higher amount of solids) in the CGR discharge, like CGR-5, will produce the highest solids ratios. Results measured for the five CGR slurries produced are summarized in Table 6.

Table 6. CGR discharge solids ratios

CGR	Discharge (lb)	OD Solids (lb)	Water (lb)	Solids Ratio
CGR-1	1,243.6	565 (45%)	679 (55%)	0.45
CGR-2	1,130.5	632 (56%)	499 (44%)	0.56
CGR-3*	2,130.9	638 (30%)	1,493 (70%)	0.30
CGR-4	1,160.2	653 (56%)	508 (44%)	0.56
CGR-5	1,445.1	852 (59%)	563 (41%)	0.60

OD = Oven dry
*CGR-3 discharge constituent weights backcalculated from final slurry weight and post-mixing measurements

Both collection efficiency and solids ratio are important because the total weight and volume of the CGR discharge on a project directly affect the transport costs of the CGR on the project. These measures are also important because the weight of the aggregates used in PCC mixes can result in much heavier CGR cakes, which affects transport costs, but not necessarily larger volumes because less water is used to grind PCC roadways with harder aggregates in the mix design (like rose quartzite and granite).

2.2.4 CGR Slurries

The final moisture contents of each CGR slurry produced were recorded, and a method for creating a pourable CGR for future CGR slurries was created. Figure 5 shows the part of the mixing process where water was added back into the decanted moist CGR solids (left) and the consistency of a typical homogeneous CGR slurry produced (right). The weights of the CGR slurries and their moisture contents were also measured and recorded, as shown in Table 7. ASTM D2216-19, Standard Test Method for Laboratory Determination of Water (Moisture) Content of Soil and Rock by Mass, was followed for oven drying of CGR slurry samples to test for moisture content. All CGRs were dried at 60°C to help avoid changing the chemical composition of the CGR.

Figure 5. Water being added to CGR solids (left) and consistency of homogeneous CGR slurries (right)

Table 7. Collected CGR discharge solids and water breakdown comparisons

CGR	Discharge (lb)	OD Solids (lb)	Net Cake Water (lb)	Supernatant (lb)
CGR-1	1,243.6	565 (45%)	171 (14%)	508 (41%)
CGR-2	1,130.5	632 (56%)	198 (17%)	301 (27%)
CGR-3*	2,130.9	638 (30%)	299 (14%)	1,194 (56%)
CGR-4	1,160.2	653 (56%)	236 (20%)	272 (24%)
CGR-5	1,445.1	852 (59%)	231 (17%)	332 (24%)

Net Cake Water = Water decanted from CGR cakes excluding supernatant added back into the mix
OD = Oven dry
*CGR-3 discharge weight backcalculated from oven dry values and additional post-mixing measurements

CGR-3 was the initial CGR slurry created, but the process for making an ideal pourable CGR slurry was not fully determined when the CGR-3 slurry was being mixed. As a result, this first extremely watery CGR slurry created had roughly four times the amount of water needed for an ideal pourable CGR slurry and had the highest moisture content at 65.2%. For the remaining four CGR slurries produced, a more controlled mixing process was used. This process involved first decanting the CGR buckets then reintroducing measured amounts of water into the moist CGR solids (or CGR cakes) during the homogeneous slurry mixing process in the larger 150 gal mixing trough.

In addition to measuring the moisture contents of the CGR slurries produced, moisture contents were also measured for the two loess soil batches, again following ASTM D2216-19. The first batch of loess (stored inside the soil mechanics laboratory at ISU) had moisture contents ranging from 4.3% to 5.3%, with an average of 4.8%. The second batch of loess (collected from Crescent Quarry) had much higher in situ moisture contents that ranged from 14.1% to 18.3%. This was due to the excavation and collection of this soil following a week of strong rain in the region. Due to the high variability of moisture contents found in both loess batches, the moisture contents of the loess specimens to be used were always tested before use to ensure that moisture content was known ahead of any compaction tests.

2.2.5 Soil Mixtures and CGR Dosages

In choosing a CGR dosage for amending Iowa loess, the UCS of CGR-amended soils was the primary selection criterion. A secondary measure was how the plasticity index (PI) of a soil was affected by the addition of CGR. In a 2019 study, Yang et al. (2019b) analyzed the feasibility of four different CGR dosages (10%, 20%, 30%, and 40% CGR by weight) as a soil stabilizing amendment for two common Iowa soils. These soils included a coarse sand (SC) and a silty clay (CL-ML). Yang et al. (2019b) found that all four CGR dosages showed improved UCS while the PI decreased with increasing CGR dosages, and the authors concluded that a 20% CGR dosage resulted in the highest UCS gains. As a result, 20% CGR (by weight) was added to loess in the present study.

2.2.6 pH (CGR)

The testing of pH for the solids (loess and CGR dry solids) in this study was performed in accordance with ASTM D4972-19, Standard Test Methods for pH of Soils. Similarly, the testing of pH for water samples in this study was performed in accordance with ASTM D1293-18, Standard Test Methods for pH of Water. pH was measured for the soil, soil amendments, and soil mixtures (untreated loess, CGRs, and CGR-amended soils) as well as for the rainwater runoff samples collected during the rainfall simulations on the loess amended with CGR-1 and CGR-2 (hereafter referred to as CGR-1L and CGR-2L, respectively).

With respect to the pH levels of the untreated loess, both batches of loess (control) had an average pH of 7.10, while the pH of the dry CGR solids ranged between 11.13 and 11.83. Amending loess with 20% CGR increased the alkalinity of the amended soil, resulting in pH values ranging from 9.59 to 10.87. Results are shown in Figure 6.
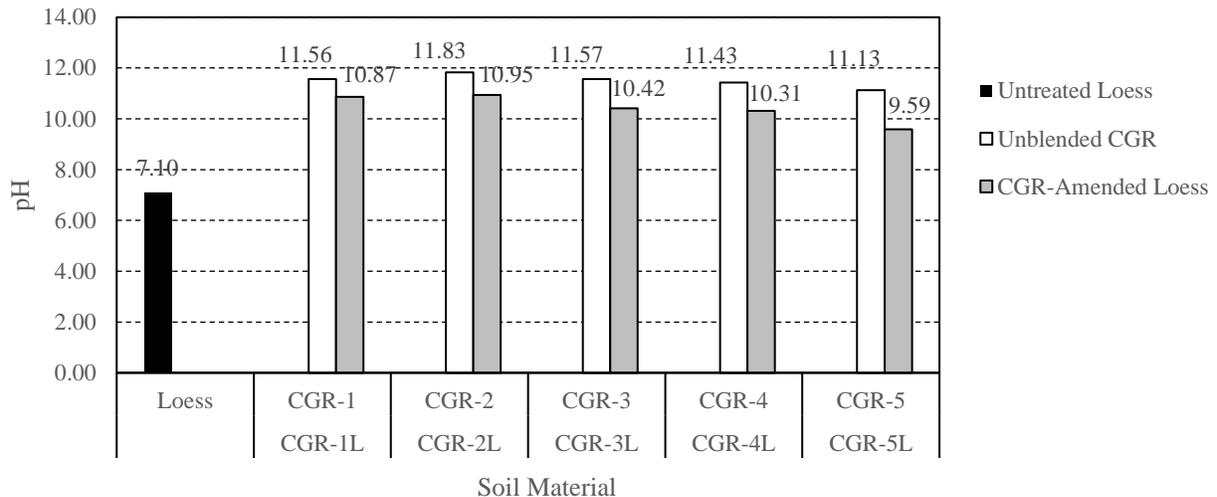
Figure 6. pH of untreated loess, oven-dried CGRs, and CGR-amended loess mixtures

The pH of the runoff water was also measured for each rainfall simulation at each of the three rainfall intensities (storms) in each of the simulated rainfall trials. The building water (the water supplied to the building by the City of Ames) was also tested for pH as well. Both the simulation water and the runoff water from the loess during the final (6 in./hour) storm of the simulation had similar, slightly basic pH values of 8.01 and 8.19, respectively. For each of the simulations with CGR-amended loess (CGR-1L and CGR-2L), the pH levels gradually increased through the course of the 60-minute simulations. For CGR-1L, the pH increased 5% over the course of the simulation, while for CGR-2L the pH increased 14%. Results are shown in Figure 7.

23
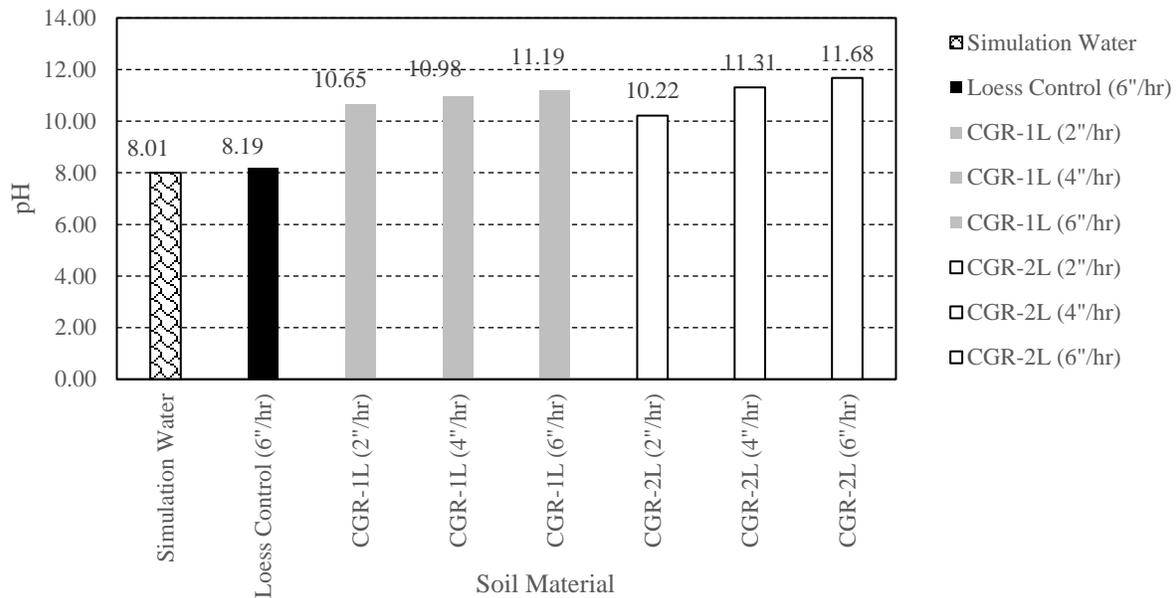
Figure 7. Post-rainfall pH of untreated loess and CGR-amended loess (by storm intensity)

2.2.7 Standard Proctor

Initial standard Proctor tests (ASTM D698-12) were performed on the untreated loess (control) as well as on the CGR-amended loess (CGR-1L and CGR-2L). The loess (control) had an optimum moisture content (OMC) of 16.8% and a maximum dry density (MDD) of 105.6 lb/ft^3. The CGR-amended soils produced mixed results. With CGR-1L, the OMC decreased 1% to 15.8% with a virtually unchanged MDD of 105.5 lb/ft^3. The OMC for CGR-2L, on the other hand, increased 0.5% to 17.3% with a slightly improved MDD of 106.8 lb/ft^3. The average OMC for the loess (control) and both CGR-amended soils was 16.6% with an average MDD of 106.0 lb/ft^3, with a standard deviation of 0.76% and 0.72 lb/ft^3 for the measured OMC and MDD values, respectively. Results are shown in Figure 8.
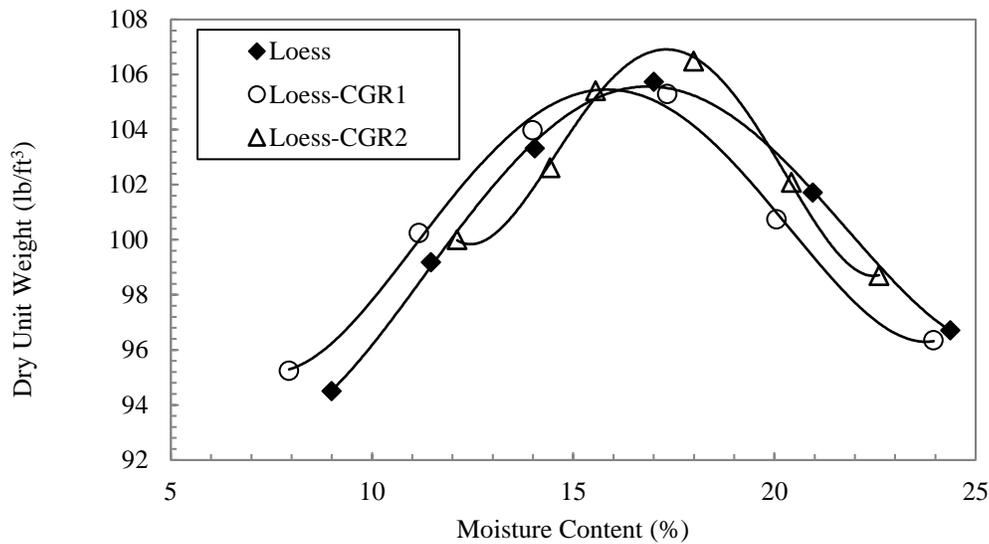
Figure 8. Standard Proctor results for loess and CGR-amended loess

2.3. Compaction

Compaction of the soil specimens in this rainfall erosion study required the design and construction of soil forms with drainage funnels and supporting racks as well as the design, construction, testing, and calibration of a uniform compaction (tamping) apparatus. Lastly, a method of tamping was required for compacting the soil forms tested in this study.

2.3.1 Rainfall Racks and Soil Forms

In order to perform rainfall simulations and erosion testing, the design and fabrication of soil forms, supporting racks, and compaction methods were each required. Soil forms specifically for this use have been made in the past using many different configurations and soil depths. For this study, the soil media being tested included both loess (soil) and CGR-amended loess mixes. Due to the high alkalinity of the CGR, there was a high potential for corrosion using metal forms. For this reason, combined with the significant weight and cost of materials, metal forms were eliminated from consideration. Plastic forms were considered as well, but wood was ultimately selected due to its durability, low cost, and feasibility for building a custom-sized soil form. Soil forms with inside dimensions of 24 in. (wide) x 48 in. (long) x 3½ in. (deep) were selected, with the size modeled after soil forms built by Shoemaker (2009) and later by Wilson (2010) in their respective master's theses research studies at Auburn University. The choice of this size allowed for a comparison of CGR-amended soils to soil treated with other erosion mitigating materials.

In both Wilson's (2010) and Shoemaker's (2009) research, rainfall simulations were also performed on compacted soil forms. However, in these studies, the focus was on testing the erosivity of different surface-treated products over exposed soils. Wilson's (2010) research tested four types of hydromulch against two conventional straw mulch products, while Shoemaker's (2009) research tested the effectiveness of different applications of anionic polyacrylamide

(PAM), a well-known chemical soil stabilizer and flocculating agent. In comparison, this study looked at the viability of amending soils with CGR to potentially stabilize the soil and reduce soil erosivity. The design of the soil forms and tamping methods used by both Shoemaker (2009) and Wilson (2010) were also improved upon in this study. Construction photos of the soil forms and supporting rack are shown in Figure 9.
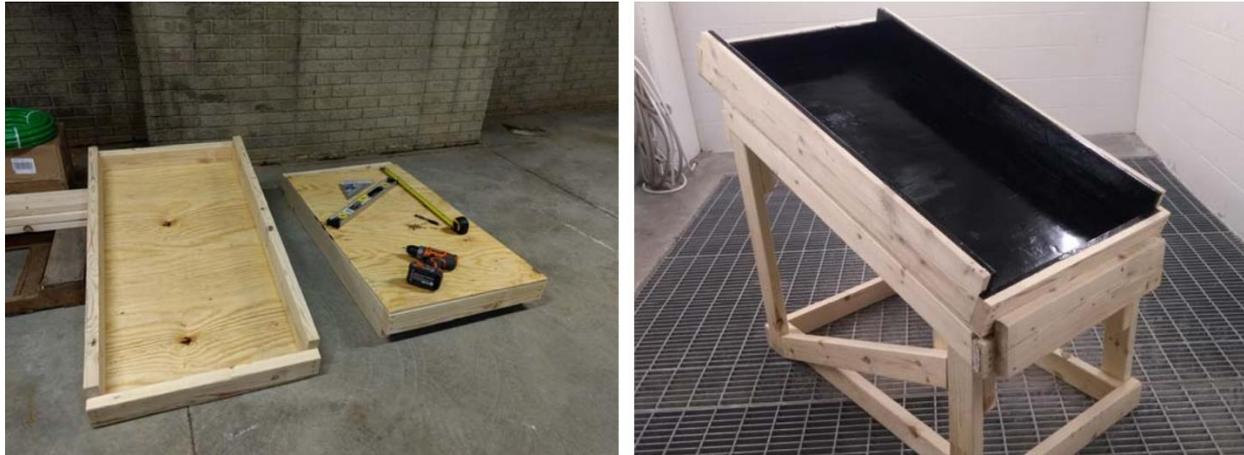
Figure 9. Construction of wooden rainfall soil forms (left) and supporting rack (right)

Like Wilson's (2010) soil forms, new wooden soil forms were built with 2x4s (1½ in. x 3½ in. lumber) for the end rails and 2x6s (1½ in. x 5½ in. lumber) for the side rails and ½ in. plywood for the soil form bases. The increased height of the side rails was to avoid wash-out and soil loss over the side rails during rainfall simulations.

To protect the untreated plywood and lumber, the interior of each soil form was treated (sealed) with a durable waterproof coating. Three waterproof sealers were evaluated along with outdoor acrylic and latex-based paints. The three waterproof sealers reviewed included Swift Response's Flex Seal (a rubberized sealer), Henry's white roofing sealant (an elastomeric roof coating), and Gardner Coating's Leak Stopper (an asphalt-based sealer). Although each product had merit, Flex Seal was chosen for this project. Key features of Flex Seal include its waterproofing properties, ease of application (no prime coat needed), low amount of volatile organic compounds (VOCs) and off-gassing during application, durability, and moderately low cost. Since only water resistance was needed on the outside of the wood forms, two coats of KILZ-2, a water-based, mildew-resistant primer, was used. In lieu of stacked blocks and sawhorses used in Shoemaker's (2009) and Wilson's (2010) research, a more substantial braced wooden rack was required for this project. A conceptual wooden rack was envisioned next and then turned into a conceptual design with the help of ISU structural engineering graduate student Nathan Miner (Figure 10).

Figure 10. Conceptual design sketch (left) and completed (built) version of rainfall test apparatus (right)

This final structural rack design included 2x4 diagonal bracing in both the X and Y axes as well as removable lateral all-thread rods to provide lateral stability to prevent failure under loading.

In order to design a structural wooden rack capable of supporting heavy forms (filled with wet compacted soil) the MDD of the compacted loess soil at OMC was required. An MDD of 16.7 kN/m^3 (107 lb/ft^3) was determined for a similar western Iowa loess in previous research performed at ISU (Coban 2017, Mahedi et al. 2019). Multiplying 107 lb/ft^3 times an 8 ft^2 soil form with a depth of 3½ in., adding in the weight of the empty 40 lb soil form, and applying a safety factor of 1.2 produced an estimated 350 lb weight requirement for each compacted soil form. This design concept was then finalized and built using 2x4 lumber and heavy-duty, corrosion-resistant exterior deck screws. A fixed 3:1 slope (18.4 degrees) was built into the wooden racks for this study (Figure 10). This slope was selected based on typical embankment foreslopes shown in Iowa DOT roadway design drawings and based on embankments detailed in Section 2107 of the Iowa DOT's *Standard Specifications for Highway and Bridge Construction* (Iowa DOT 2020).

The top edge of each rack was built to a height of 22 in. to allow for a 6 in. clearance from the metal funnel to the top of a typical 5 gal bucket. The drainage of each soil form was also engineered and improved upon in this project. The rainwater collection gutter used by Shoemaker (2009) as well as the metal flume used by Wilson (2010) installed at the base of each soil form both appeared to successfully collect the rainwater samples; however, each did not appear to be very easy to clean or reset after a rainfall event. Moreover, the fine-grained loess and CGR soil particles in this project required an improved method of collection and handling. Shoemaker (2009) utilized a PVC gutter and downspout and the end of his soil forms, while Wilson (2010) chose a metal flume. These gutters and flumes were secured directly to the wood soil forms, which then required extra handling and care with removal, cleaning, and reattachment after each rainfall simulation. With the prospect of significant test repetitions, a more durable detachable funnel was designed to address these product limitations. A new funnel design was

modeled and dimensioned in AutoCAD and then given to Drexel Metals, Inc., which fabricated a prototype. The main features of this new funnel were that it allowed for easy removal and cleaning and provided a more seamless way to direct and capture rainwater runoff samples.

The final design included a welded (not pop riveted) aluminum funnel with a U-shaped back (that snuggly fit over the bottom end rail), a triangular-shaped design with 1½ in. high side walls, a rectangular drainage outlet, and an open top (to provide visibility during testing for addressing any clogs that might occur) (Figure 11).
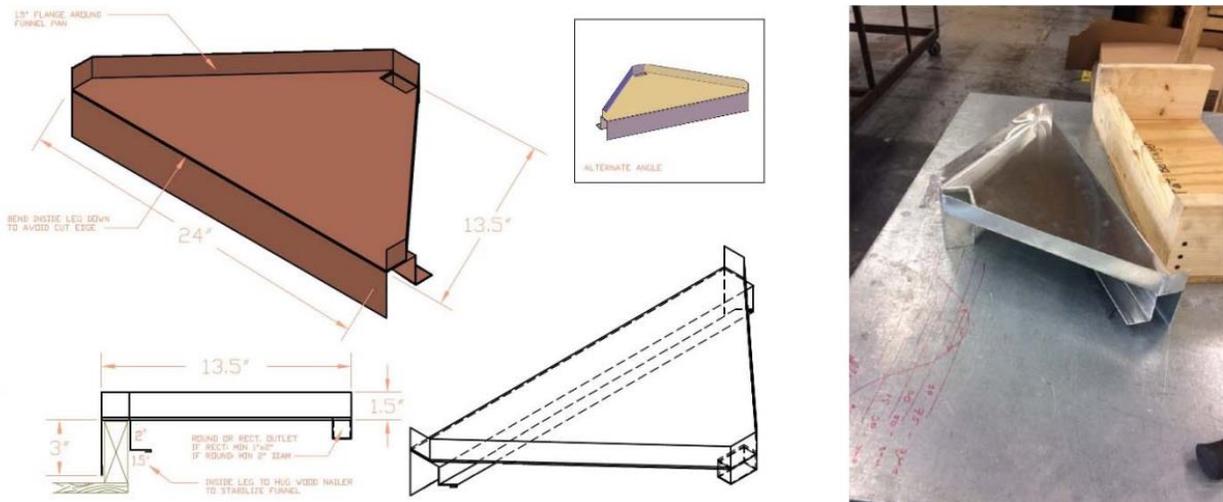
Figure 11. AutoCAD drawing (left) and actual aluminum soil form funnel (right)

Testing of the funnel prototype involved outfitting a soil form with a plexiglass cover and then running a maximum 6 in./hour maximum rainfall simulation to check for leakage and/or any overflow issues. The results of the test found no functional issues with the prototype. After this rainfall test, an easier attachment method was added to the transparent plexiglass covers fitted over the funnels. The exposed wood on the racks was also primed with two coats of KILZ-2 primer to better protect it from water penetration.

2.3.2 Uniform Tamping Apparatus

With the soil forms, supporting racks, and collection funnels designed and fabricated, focus turned to the design of a uniform tamping device/apparatus. Both Shoemaker (2009) and Wilson (2010) shared the same tamping methods, which involved lifting and dropping a hand tamper in a series of drops to achieve 95% compaction. The hand tamper used appeared to be an effective soil compaction tool in both of these studies. Wilson (2010) and Shoemaker (2009) each achieved the desired compaction in similar Alabama sandy clay loams with 80 drops and 90 drops (per square foot), respectively. Both researchers also determined optimum drop counts for each of their projects through regression analyses of the drops, which involved graphing the unit weights achieved through compaction using a smaller 12 in. x 12 in. (1 ft^2) test form. Shoemaker (2009) and Wilson (2010) each manually tamped their smaller test forms in trials consisting of 10, 20, 30, 50, and 60 drops to determine the optimum number of drops.

The challenge with any manual drop compaction method is ensuring that the energy from each drop is both uniform and repeatable. Important drop factors, including drop height, drop angle, and landing position of the tamper/weight, each need to be kept reasonably constant for each drop to deliver the same amount of compaction energy to the soil. The tamper also needs to be gravity dropped (not thrust down) so the impact delivered to the soil does not dramatically vary with each drop sequence. In addition to drop factors, the maneuverability of the tamper and/or soil form is another important design consideration. With a larger 8 ft^2 soil form footprint, compared to 10 in. x 10 in. (0.69 ft^2) or 12 in. x 12 in. (1 ft^2) tamper footprints, for example, repositioning of the form and/or the tamper is required during compaction. An automated compaction apparatus could better account for this repositioning in the design. These important design considerations were incorporated into the design and construction of the uniform tamping apparatus (UTA) created for this study (Figure 12).

Figure 12. Wooden uniform tamping apparatus

Like the soil forms, the UTA frame was fabricated primarily from 2x4 nominal wood lumber. Borrowing from Shoemaker's (2009) and Wilson's (2010) process, a 13.05 lb hand tamper with a 10 in. x 10 in. square footprint was also incorporated into the UTA. A fixed drop height of 12 in. above the top of the soil surface was built into the UTA frame, and a 24 in. (wide) x 48 in. (long) rolling platform with eight heavy-duty casters was built to allow the soil forms to be repositioned easily on the floor. Horizontal casters were added to the UTA frame to restrict movement of the rolling soil forms in the longitudinal (8 ft) direction.

With respect to the tamping angle, a PVC pipe sleeve was integrated into the UTA frame to confine the tamper to a fixed, vertical/plumb position. A horizontal slot was added for horizontal movement of the tamper, with removable check blocks added to hold the tamper (horizontally) in one of two positions in the slot during tamping. This allowed for free tamping in variable horizontal positions if needed. Vertically, the PVC pipe containing the tamper also served as a limiter to fix the maximum drop height to 12 in. from the fully raised (set) position of the tamper

down to the top surface of the soil. Lastly, a hole was drilled in the metal tamper handle for safety. A removeable carriage pin was installed in the hole to hold/lock the tamper (safely) in a raised position. This pin was used when the soil form was repositioned during compaction.

2.3.3 Uniform Compaction

Uniform compaction that could be easily replicated was required for the soil forms used in the rainfall trials in this research. Creating the UTA discussed above provided the equipment to achieve uniform compaction, but determining a repeatable uniform tamping method to compact the soil forms was also required. To test the UTA's compaction capability to produce uniform compaction over a series of test trials, a smaller 12 in. x 12 in. (x 3½ in. deep) wood test form was built. This small 1 ft^2 test form was also waterproofed with Flex Seal to simulate a scaled-down version of the full size 8 ft^2 rectangular soil form. The purpose of the UTA compaction trials was to determine the degree of compaction from an increasing amount of compaction effort. Compaction trials were performed with 50, 75, 100, 125, and 150 (gravity) drops per 1 ft^2 form with the 13.05 lbf tamper built into the UTA. This tamper was raised and then dropped (not thrust down) for each tamp (or drop) (Figure 13).

Figure 13. Calibration test trials of the UTA

The UTA compaction trials were performed on loess samples prepared with an 11.5% (-5.3% OMC) constant moisture content. This moisture content (on the dry side of optimum) was chosen to help ensure that no excess pore water pressure would adversely affect compaction while still providing enough moisture to achieve good (soil) compaction. Using the data from the UTA compaction trials and linear regression, a linear relationship with a high degree of confidence (R^2 = 93.3%) was found between the drop trials and the dry unit weights measured for all five test trials (50, 75, 100, 125, and 150 drops). Extrapolating from these data, the theoretical number of drops to achieve 90% and 95% compaction was found to be 175 and 240 drops per 1 ft^2 form, respectively. The theoretical number of drops required to reach a theoretical 100% or maximum compaction was determined to be 305 drops/ft^2. Multiplied by 8 (for an 8 ft^2 soil form), to achieve 90%, 95%, and (a theoretical) 100% compaction would require 1,400, 1,920, and 2,440

drops, respectively, for these degrees of compaction at OMC. Since this number of drops per soil form would be extremely difficult to achieve for dozens of soil forms, the prospect of compacting the soil forms required a lower, more manageable number of drops.

Included in the test trials were 150 drops/ft^2 (1,200 drops per soil form) and 125 drops/ft^2 (1,000 drops per soil form). The drops in these two trials achieved 88% and 86% compaction, respectively (Figure 14). Although 90% compaction was desired for these trials, 125 drops/ft^2 (1,000 drops per soil form) was selected for the compaction standard for the rainfall trials. This reduced number of drops was believed to still provide adequate compaction of the soil forms for erosion testing. In hindsight, changing from one lift of soil to two lifts of soil (theoretically) with 125 drops/ft^2 would have produced sufficient compaction energy to achieve 90% compaction at this same number of drops.
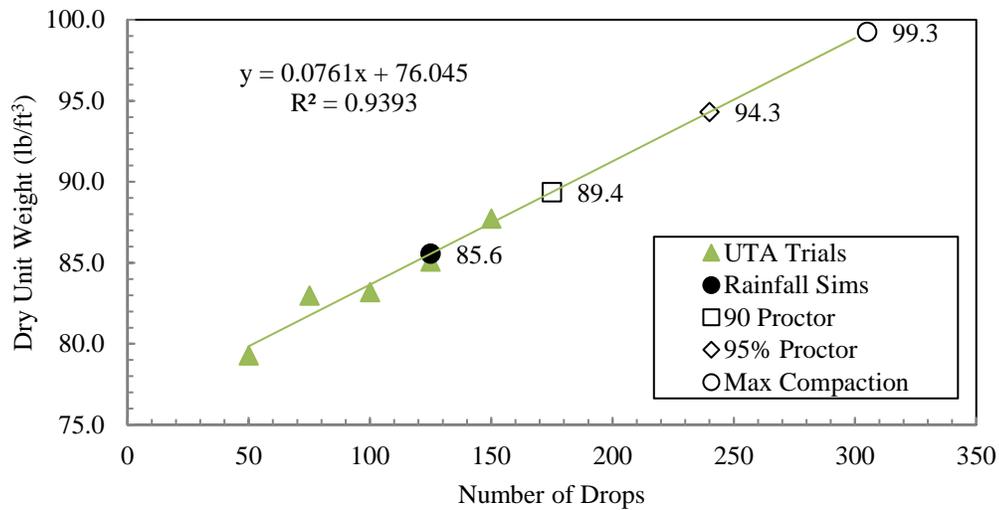
Figure 14. UTA test trial data (degree of compaction per number of drops)

2.3.4 Tamping Pattern

During the selection of the number of drops per square foot, a pattern involving 125 drops/ft^2 over 8 drop locations in the soil form was ultimately chosen. Initially, the soil form was divided into a grid of 15 overlapping drop locations. However, if the number of drop locations in the soil form were increased to 15, the total number of drops would increase to 1,875 (15 locations x 125 drops per location). Based on this dramatic increase in the total number of drops required, the number of drop locations was kept at 8, and a serpentine pattern (shown in pattern C in Figure 15) was adopted to provide an alternating pattern to the tamping and to minimize the amount of time the soil form needed to be shifted longitudinally under the UTA tamper.
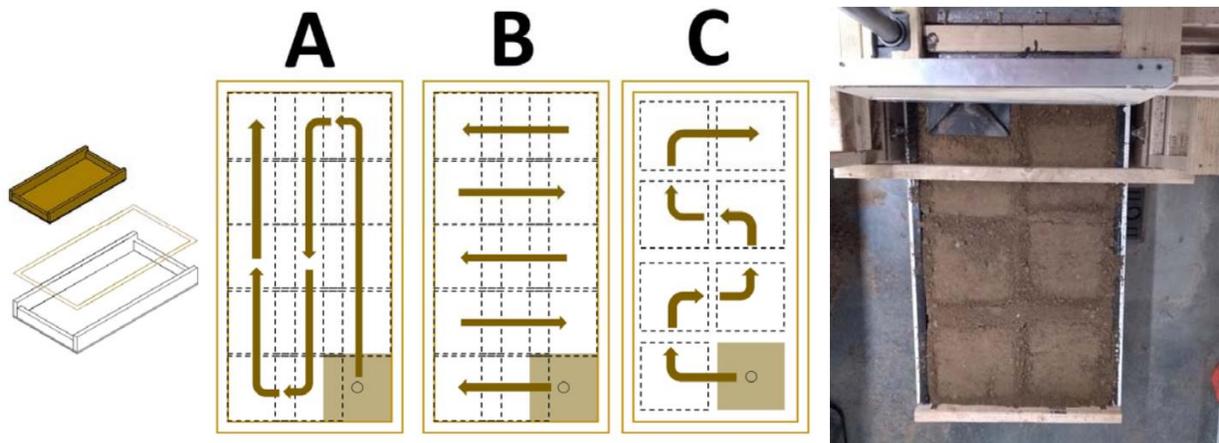
Figure 15. Rainfall soil form tamping patterns (pattern C chosen)

2.4 Rainfall Erosion Simulation

With respect to the ISU rainfall simulator used in this study, an understanding of the devices and mechanisms involved in the simulator system as well as calibration and testing of this equipment were required prior to performing the rainfall erosion testing. The calibration and testing of this equipment had not previously been performed. As a result, processes were developed to accomplish this work.

2.4.1 Rainfall Simulator (ISU)

An indoor, ceiling-mounted, three-bay, nine-nozzle, Purdue-type rainfall simulator located in the Biorenewables Research Laboratory at ISU was used for this study. It employed a total of nine VeeJet Model 80100 flat-spray nozzles (three per bay), each with laminar flow fittings, to produce a fine rainfall spray with an 80-degree fan spread (Figure 16). The drainage area with metal grates area under the rainfall simulator was 11 ft wide (left to right) by 15 ft deep (front to back), with a maximum potential rainfall zone of approximately 9 ft wide by 11 ft deep beneath the rainfall simulator.
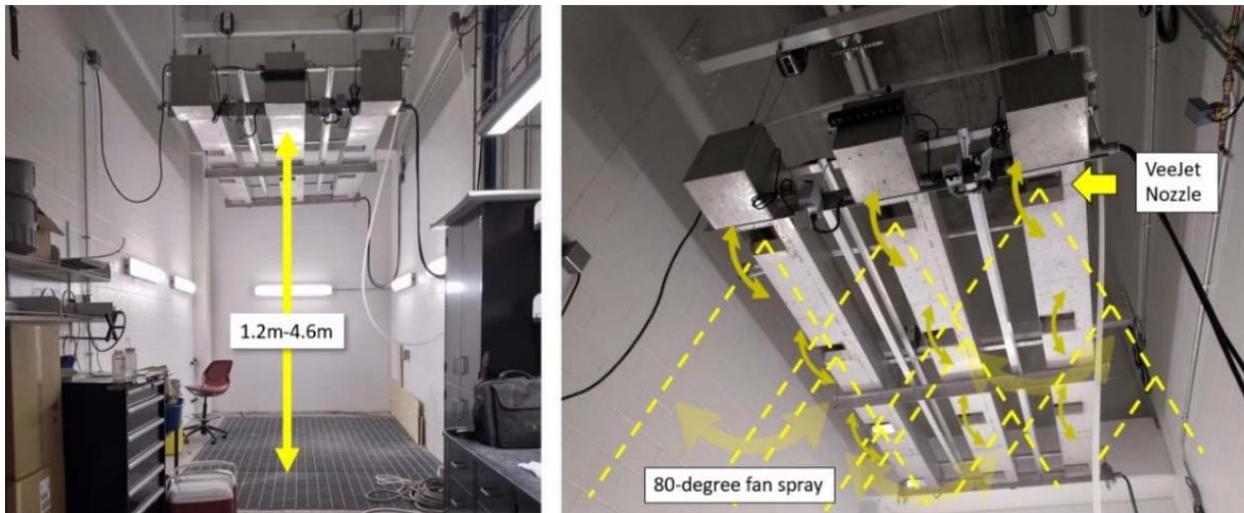
Bollinger et al. 2021

Figure 16. ISU ceiling-mounted Purdue-type rainfall simulator

Four independently controlled winches were connected to the simulator corners to control its height, which ranged from approximately 1.2 m (4 ft) to 4.6 m (15 ft) measured from the ground to the bottom of the metal simulator troughs. An optimal height of between 2.3 m (7.5 ft) and 3 m (9.8 ft) was determined by Meyer (1958) for use in rainfall simulators using the same VeeJet 80100 nozzles with 41 kPa (5.9 lb/in^2) spray pressure. Two previous nitrate leachate soils studies were performed at ISU that appeared to use the same rainfall simulator, and the height of the simulator was placed at 3.05m (10 ft) above the soil specimens tested in these studies (Nasritdinov 2003, Zhou 2004).

Since the 80100 nozzles and similar water pressures were used in the ISU simulator, a working height of 2.4 m (8 ft)—selected to be within the Meyer (1958) range—was chosen for this study. Each bay could be turned on or off with rainfall produced by one bay or a combination of two of three bays. All three bays were used for the rainfall simulations in this study.

To accommodate the variable height of the simulator, 1 in. flexible plastic tubing supplied water to the three bays in lieu of rigid pipe. This tubing transitions to a rigid PVC pipe at a valve and spigot mounted to each bay. Potable water from the City of Ames (Iowa) was controlled in the simulator with ballcocks (floats) attached to lever arms that opened and closed supply valves to regulate the amount of water supplied to reservoir tanks in each metal bay/trough. A small ⅓-horsepower submersible (recirculating) pump was located in the bottom of each reservoir tank. Additional PVC piping with adjustable 15 lb/in^2 in-line pressure gauges extended up from the pumps to the nozzles. The metal troughs had tapered cutouts with raised edges at each nozzle. This prevented any extra discharge water from flowing out of the trough between nozzle oscillations. The far end of the simulator frame was raised 2 in. higher in the back, which allowed extra water retained in the troughs to flow back to the reservoir tanks with the submersible pumps. Each pump continuously recycled water from the reservoir tanks to the nozzles. Rainfall was created by VeeJet Model 80100 flat-spray nozzles with laminar flow fittings, which produced a fine rainfall spray with an 80-degree fan spread.

Each bay contained three nozzles connected to a coupling bar, which was driven by a small motor at the back end (high side) of the troughs. This configuration produced an oscillating (or sweeping) motion in the nozzles (similar to a windshield wiper on a car). Again, the rainfall footprint generated by the simulator was approximately 11 ft wide by 15 ft deep (front to back), with a workable (uniform rainfall) area of approximately 9 ft wide by 11 ft deep. Because of the overlap of rainfall spray between the bays, rainfall under the center bay was generally higher than under the outside bays. However, lowering the pressure gauge to the center bay effectively lowered the rainfall intensity for this bay during calibration.

2.4.2 Rainfall Simulator Calibration

Rainfall simulations and testing for this study were modeled after ASTM D6459-15, Standard Test Method for Determination of Rolled Erosion Control Product (RECP) Performance in Protecting Hillslopes from Rainfall-Induced Erosion. Raindrop size distribution and the Christiansen uniformity coefficient detailed in this standard were calculated for each rainfall intensity in this study.

Rainfall intensities were set through a combination of adjustments to three 15 lb/in^2 pressure gauges (one per bay) and a central GraLab Model 451 electronic timer (Figure 17). By changing water pressure and timing calibration settings, rainfall intensities ranging from approximately 1 in./hour to 8 in./hour could be generated. The GraLab timer controlled the nozzle sweep timing for each bay. This sweep timing consisted of two settings, a sweeping motion (M1) and a pause time (M2). These settings together determined the oscillation frequency of the nozzles, and changes to these two settings combined with adjustments to the three in-line water pressure gauges made up a calibration set for a single rainfall intensity (storm) event. Three calibration sets were needed to create the required 60-minute, three-storm rainfall simulation. However, only one rainfall intensity could be set at one time. This meant that in order to transition between the three storm events, manual changes to the GraLab (nozzle) timer were required in real-time during a running rainfall simulation (assuming the water pressure could be kept constant for all three storms).
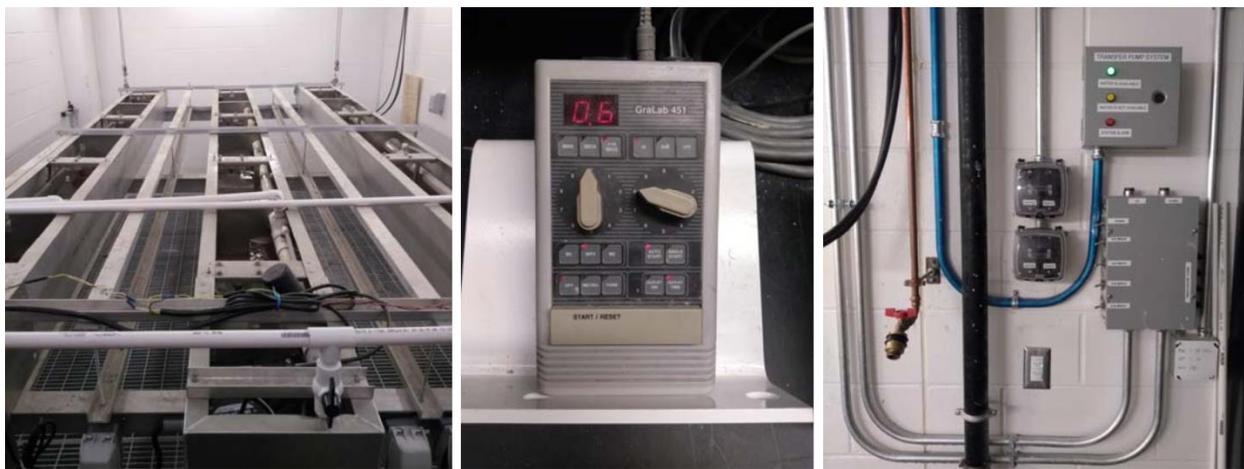
Figure 17. ISU rainfall simulator apparatus, timer, and controls

To determine the water pressure and nozzle settings required for each storm, a series of rainfall intensity trials (RI trials) was required. To measure the rainfall at different points within the rainfall simulation room, a set of graduated one-quart containers was placed in a grid on the floor under the simulator to serve as rain gauges. After each RI trial, the containers were dried on the outside and weighed, and the water depths were recorded. The goal for each RI trial was to attempt to match one of three targeted rainfall intensities within a 10% margin of error. Two patterns were used in the RI trials: a full pattern and a reduced, staggered pattern. The reduced pattern consisted of a staggered 6 x 7 grid that consisted of 21 containers, 24 in. on center, with 7 rows and 6 columns covering a uniform rainfall area of 42 ft² (the estimated area for three compacted soil forms). The full pattern consisted of an 11 x 9 grid of 99 containers, spaced 12 in. on center, with 11 rows and 9 columns covering the full (nonuniform) rainfall area of 99 ft². The full pattern (99 containers) was used to first determine the most uniform rainfall section within the full rainfall area. The reduced pattern (21 containers) was then used to determine the water pressures and nozzle timer settings required to produce the three required rainfall intensities (2 in./hour, 4 in./hour, and 6 in./hour storms).

After a series of 28 RI test trials, three calibrations sets were selected that most closely matched the desired 60-minute, three-storm rainfall simulation with a 2 in./hour, 4 in./hour, and 6 in./hour increasing rainfall storm sequence (three successive 20-minutes storms). The best RI trials for both the 2 in./hour and 4 in./hour rainfall intensities had great results, with margins of error in the volume of water collected in each of the 21 containers calculated at 1.08% and 0.94%, respectively. The best RI trial for the 6 in./storm produced a higher (but still acceptable) margin of error at 8.36% from the targeted rainfall intensity volume desired. Table 8 shows the calibration sets for the first three RI trials as well as the three (best) selected RI trials from the 28 RI trials.

Table 8. Initial and selected rainfall intensity trial calibration sets

Trial ID	Timing Settings	Pressure Settings	Bay1 (in./hr)	Bay2 (in./hr)	Bay3 (in./hr)	Total (in./hr)	Target (in./hr)	% Error
1	Manual (max rainfall)	N/A - Not tracked	6.69	9.94	7.38	8.00	-	-
2	Manual (max rainfall)	L: 12.5 lb/in² C: 12.5 lb/in² R: 12.5 lb/in²	5.04	4.61	5.10	4.92	-	-
3	Manual (max rainfall)	L: 12.5 lb/in² C: 8 lb/in² R: 12.5 lb/in²	7.25	5.83	6.92	6.67	-	-
7 *	M1 (0.5s) M2 (0.8s)	L: 12.5 lb/in² C: 6 lb/in² R: 12.5 lb/in²	1.85	2.24	1.97	2.02	2.00	1.08%
18 *	M1 (0.7s) M2 (0.1s)	L: 12 lb/in² C: 7 lb/in² R: 12 lb/in²	3.64	4.48	3.99	4.04	4.00	0.94%
22 *	M1 (0.4s) M2 (0.1s)	L: 12 lb/in² C: 7 lb/in² R: 12 lb/in²	6.16	7.13	6.22	6.50	6.00	8.36%

* Settings selected for the three rainfall intensities (2 in./hour, 4 in./hour, and 6 in./hour)

Figure 18 shows a spatial graph of the rainfall depths recorded for the grid with 99 containers measured for the 4 in./hour rainfall intensity (storm) facing the simulator. The X-axis represents the width of the rainfall simulation room from 1 to 9 ft.
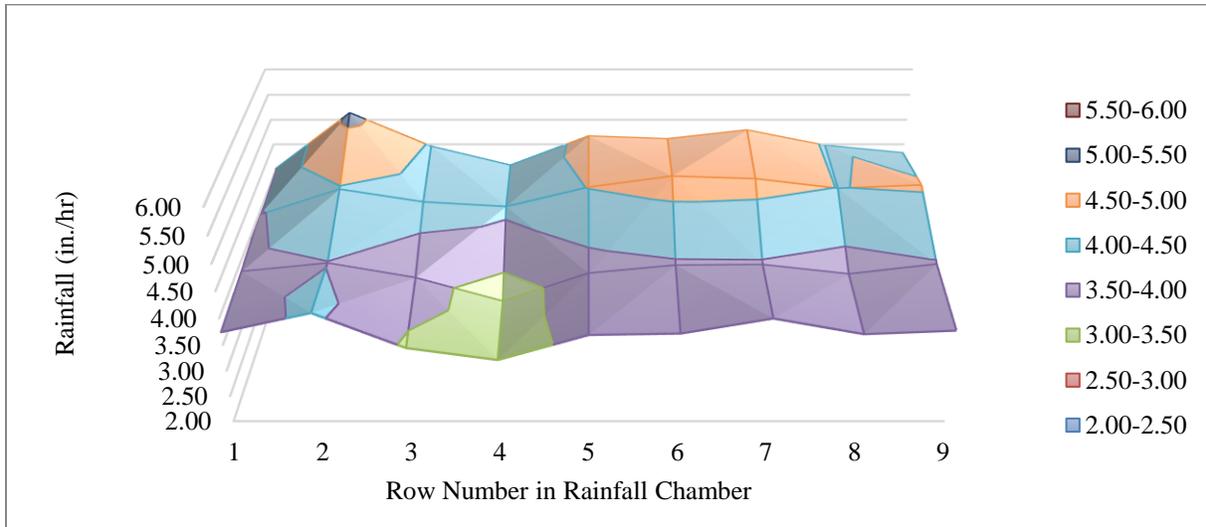
Figure 18. Rainfall uniformity data for 4 in./hour rainfall intensity

With the three best calibration sets selected, a final rainfall simulation at each rainfall intensity (2 in./hour, 4 in./hour, and 6 in./hour storms) was run with the full pattern (99 containers). Using data from these three full pattern simulations, the final placement of the soil forms in the most uniform rainfall area within the simulator room was performed. In addition, the rainfall data from these simulations allowed the Christiansen uniformity coefficients for the 2 in./hour, 4 in./hour, and 6 in./hour storms to be calculated.

The Christiansen uniformity coefficient is a commonly used measure for assessing the uniformity of water distribution from a sprinkler or irrigation system. This procedure was used for each rainfall intensity produced by the rainfall simulator on this project. These coefficients were determined from the rainfall depths measured during the full-pattern (99-container) RI trials performed after choosing the final simulator timing and pressure settings (calibration sets) for the three desired storm events. The Christiansen uniformity coefficient was calculated as 88.1%, 82.44%, and 57.41% for the 2 in./hour, 4 in./hour, and 6 in./hour storms, respectively. The coefficients for the 2 in./hour and 4 in./hour storms indicated a high degree of uniform rainfall distribution, while the coefficient for the 6 in./hour storm was deemed to indicate moderate to low uniformity. This disparity in uniformity for the 6 in./hour storm is attributed to equipment limitations in being able to produce this last heavy storm event. However, since the simulator was able to produce the required volume of rainfall with a low margin of error with the volumetric rainfall test (detailed below), the 6 in./hour storm calibration set was deemed satisfactory for the purposes of this study.

A volumetric rainfall test was created to calculate the volume of water landing on the surface of the targeted 8 ft^2 compacted soil forms. For this test, a 20-minute rainfall simulation was

performed for each of the three rainfall intensities (using the calibration sets selected for each storm). During each volumetric rainfall test simulation, the soil form was fitted with a plexiglass cover that allowed the total rainwater runoff from the 8 ft^2 soil form to be collected and weighed. Rainfall volumes for each simulated storm (2 in./hour, 4 in./hour, and 6 in./hour) were then calculated. Results showed a margin of error of less than +/- 5% for each simulation, under the 10% maximum margin of error desired. A summary of volumetric test results is shown in Table 9.

Table 9. Calibration rainfall intensity (storm) volumetric test results

Rainfall Intensity	Trails, Wt (Vol)	Total, Wt (Vol)	Error, Wt (Vol)	% Error
2 in./hour	10569 g (3.28 gal)	10723 g (3.28 gal)	-154 g (-0.04 gal)	-1.43%
4 in./hour	22403g (6.95 gal)	21447g (6.65 gal)	956g (0.30 gal)	4.46%
6 in./hour	31733 g (9.84 gal)	32170 g (9.97 gal)	-437 g (-0.13 gal)	-1.36%

A raindrop gradation (or flour test) was also performed to measure the raindrop particle size distribution of the rainfall generated by the rainfall simulator. This test was performed for each of the three rainfall intensities (2 in./hour, 4 in./hour, and 6 in./hour) in this study. For this test, three 8 in. aluminum pie pans were filled and screened flush with the top of the pie pans. The pans were then covered with aluminum foil and staggered inside the rainfall room (Figure 19). The rainfall simulator was then started, and each of the flour pans was uncovered for a brief 3- to 4-second period and then recovered. This allowed the raindrops to impinge into the flour. Nine pans in total were tested, three pans per storm intensity, with the rainfall simulator reset between each test.

Figure 19. Raindrop particle size distribution test (flour test)

The flour was allowed to air dry for 12 hours before gently screening off the dry pellets that formed from the raindrops. These pellets were then oven dried at 110°C for 2 hours before sieving the drop pellets with a fine grain set of 8 in. diameter sieves. The sieve sizes used included #4, #8, #10, #20, #30, #40, #60, #80, #100, #200, and a pan. According to the American Meteorological Society (AMS), the average raindrop has a diameter between 1 to 2 mm (AMS

2021). The AMS also describes drizzle drop sizes, which are smaller drops ranging from 0.2 to 0.5 mm in diameter.

The rainfall simulator used for this study produced uniquely different sized raindrops and drizzle drops in each of the three rainfall intensities tested. If 1 mm is used as the distinction between raindrops and drizzle drops, the 6 in./hour storm produced the greatest percentage of raindrops (79%) compared to the 2 in./hour storm (24%) and the 4 in./hour storm (34%). On the other hand, the 2 in./hour storm produced the greatest percentage of drizzle drops (76%) compared to the 4 in./hour storm (66%) and the 6 in./hour storm (21%) (Figure 20).
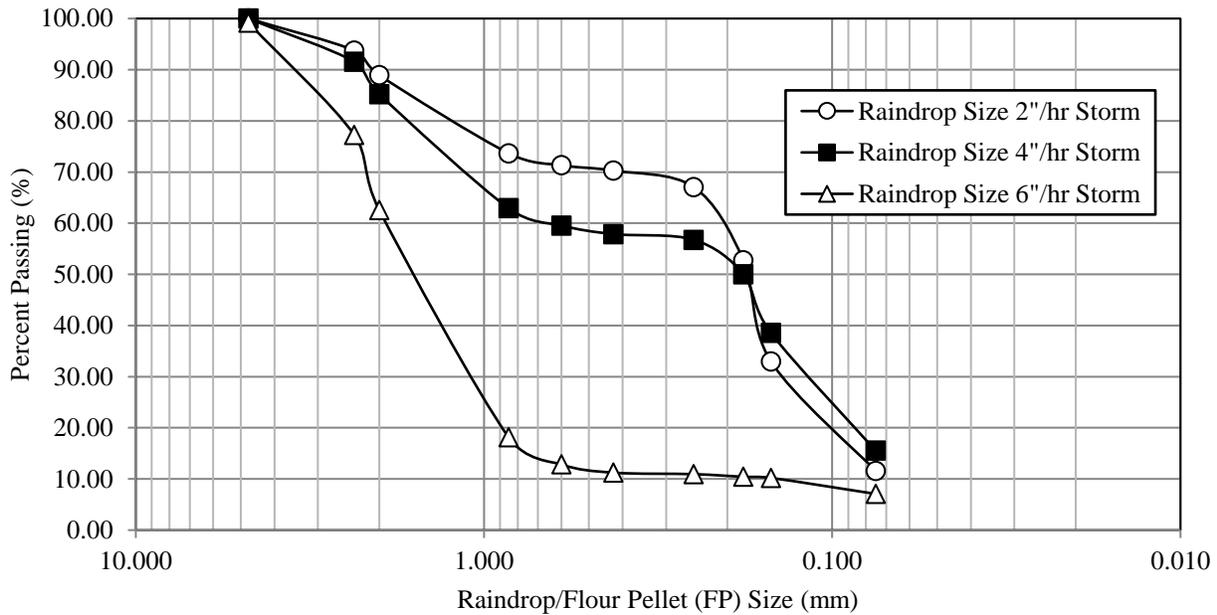
Figure 20. Raindrop gradation curves for each rainfall intensity (storm)

2.4.3 Rain Erosion Test Procedure

The test procedure for each rainfall simulation involved stepping through a series of manual timer and rainfall intensity settings to produce a real-time, three-storm, 1-hour rainfall event while also collecting turbidity and TSS samples at fixed increments for three soil forms tested at the same time in the rainfall simulation room (Figure 21). Setup for each new rainfall test involved first lifting the three compacted soil forms up onto the structural wood racks located inside the rainfall room. Plastic sheeting was placed over the three racks and soil forms to prevent contamination while setting up and pretesting the rainfall simulator.

Bollinger et al. 2021

Figure 21. Typical rainfall simulation and captured sediment-laden water runoff

The purpose for pretesting (or priming) the simulator was to ensure that the water pressure gauges, pumps, and rainfall intensity and timing equipment were all set to the proper settings and functioning properly. This usually involved running the rainfall simulator through a quick 1-minute rainfall simulation. After verification, the rainfall was turned off and the plastic sheeting was removed. Buckets were then placed under the drainage funnels attached to each soil form, and a stopwatch was reset. It took three people in rain ponchos to properly collect the turbidity samples every 3 minutes and exchange the 5 gal buckets at the transition between each of the three 20-minute storm events. The entire sequence for a single rainfall test took 60 minutes.

During this time, pressure gauges also needed to be monitored along with the level arms to the submersible pumps in each of the three rainfall simulator troughs to ensure a successful test. Care was taken to ensure that both the turbidity grab samples and 5 gal buckets were collected, capped, and sealed to avoid cross contamination during the test. Each completed rainfall test captured approximately 15 5 gal buckets and 60 50 ml grab samples of sediment-laden water for future testing. Each grab sample and bucket was labeled prior to performing the rainfall test to prevent any mix-up of the samples after the rainfall simulation was completed.

Water quality (turbidity) testing was performed in accordance with ASTM D7315-17, Standard Test Method for Determination of Turbidity in Static Mode. Turbidity tests were performed on sediment-laden runoff water collected during four indoor rainfall simulations, with turbidity (grab) samples collected at 3-minute intervals (from three separate soil forms) over the duration of a 60-minute rainfall simulation. A HACH 2100Q portable turbidimeter was used to test turbidity readings for each grab sample, with results reported in nephelometric turbidity units (NTUs). The 2100Q unit was calibrated using 10 ml sealed cells (comprised of 0, 10, 100, and 800 NTU specimens). The maximum range for the turbidimeter was 1000 NTUs, so dilution was required (as much as 40 times) for each grab sample using filtered water retrieved from an Elkay drinking water station. Water quality measurements (12 in total) were randomly taken of the Elkay dilution water to ensure that clean dilution water was being used for testing. Low turbidity values ranging from 0.39 to 1.97 NTUs were measured across all 12 dilution water samples, with only two values greater than 1 NTU and an average of 0.78 NTUs across the samples. These low

NTU values for the Elkay dilution water are consistent with the EPA's National Secondary Drinking Water Regulations (NSDWR) for turbidity, which state that potable water should not exceed 5 NTUs and filtration systems should yield a turbidity no higher than 1 NTU (EPA 2022b).

In total, 60 grab samples per simulation (20 samples from each soil form) were collected into 50 ml clear plastic centrifuge tubes with screw-top caps. The remaining stormwater runoff flowing off the surface of each soil form was collected into 5 gal buckets (separated by rainfall intensity) for the duration of the simulation. Three 20-minute rainfall (storm) events were run back to back with continuous rain throughout the simulation. Each 20-minute storm progressed in intensity, beginning with a 2 in./hour storm, proceeding to a 4 in./hour storm, and finishing with a 6 in./hour storm. Buckets were changed at the transition point between each storm event. Extra empty buckets were also used (when needed) to ensure that none of the 5 gal buckets overflowed during each simulation. Snap-on lids were used to seal each bucket to prevent cross-contamination and protect against evaporation prior to testing. Buckets stored for an extended period of time were also sealed with packing tape.

2.5. Results

All rainfall trials were performed in triplicate using three identical compacted rainfall soil forms. The first three compacted soil forms tested in the rainfall simulator were of loess with a moisture content of 11.5% (Control-1). The soil forms were covered with plastic (after compaction) to provide a 24-hour rest/curing period for the soil prior to rainfall testing. A second loess control (Control-2) with a moisture content of 16.5% was tested second, with the three compacted soil forms also covered with plastic for 24 hours prior to testing. The last two rainfall simulations for CGR-1L and CGR-2L were prepared with moisture contents of 16.5%. For these two tests, the compacted soil forms were also covered for a 24-hour curing period prior to testing. An average OMC of 16.5% was chosen for the last three simulations (Control-2, CGR-1L, and CGR-2L) to simplify soil and CGR-amended soil preparation, since the OMCs of the CGR-amended soils (CGR-1L and CGR-2L) fell within 1% of the OMC for the untreated loess (Control-2).

Turbidity testing of the grab samples collected for the loess at an 11.5% moisture content (Control-1) did not show consistent water runoff between the three soil forms tested in the first loess control trial. The compacted soil forms in Control-1 absorbed virtually all of the rainwater runoff during the first 10-minutes of the simulation, which led to a saturated, loosely compacted soil and erratic turbidity results across the three soil forms throughout the simulation. A second test was performed with the loess with a 16.5% moisture content (Control-2). The compacted soil forms in Control-2 at a moisture content close to OMC produced much more consistent water quality samples between the three soil forms tested. A side-by-side comparison of both controls, Control-1 (top) and Control-2 (bottom), is shown in Figure 22.
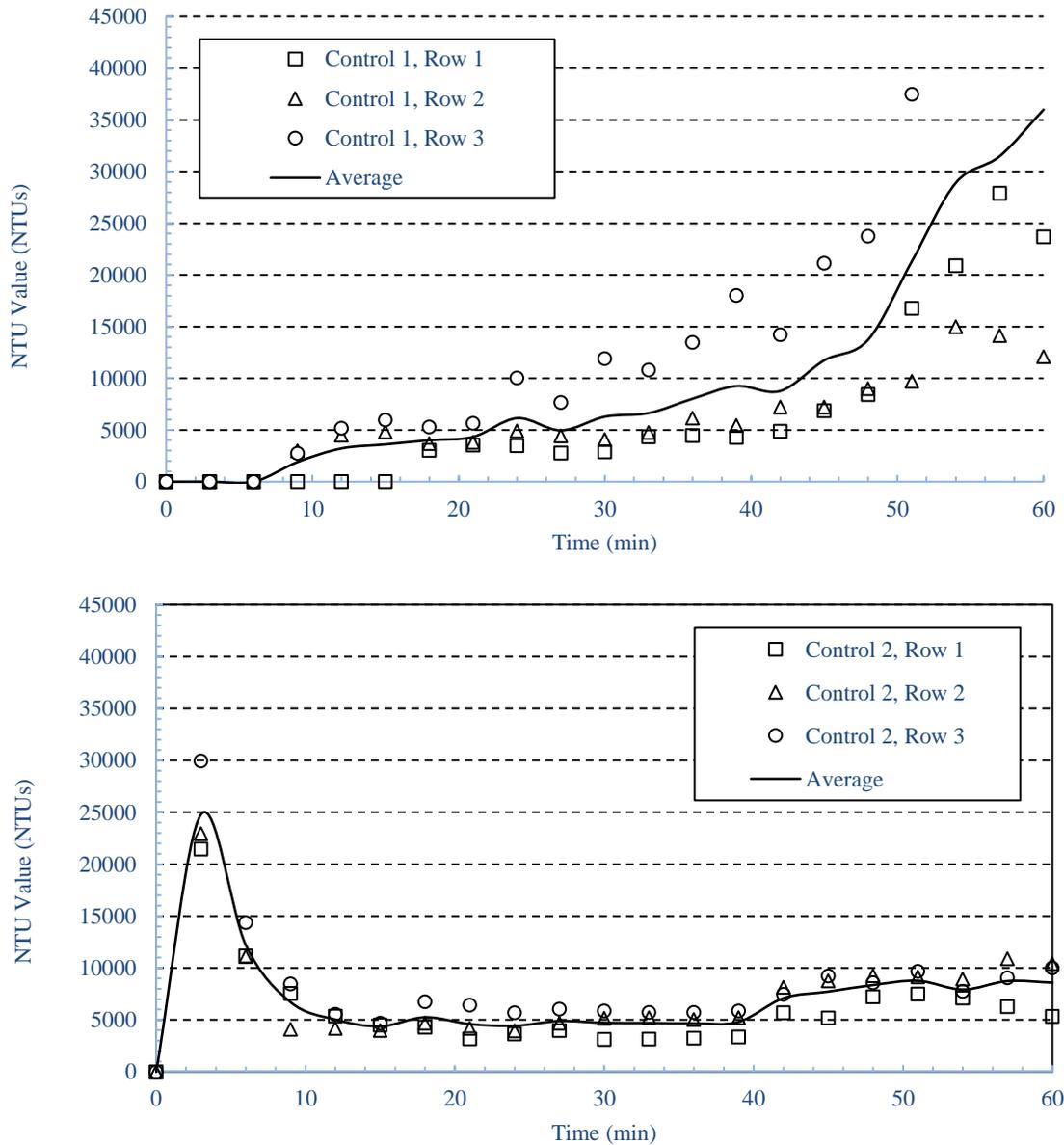
Figure 22. Water quality for loess Control-1 (top) and Control-2 (bottom)

With respect to Control-2, the short spike in turbidity for the first two readings (3 minutes and 6 minutes) is attributed to loose fines initially washing off the surface of the soil at the beginning of the rainfall simulation. The turbidity values for Control-2 leveled off starting at the 12- to 15-minute mark of the simulation, indicating relatively uniform erosion throughout the simulation. Control-2 ended with a consistent (average) turbidity value of 8,500 NTUs as the simulation finished.

Conversely, CGR-1L showed high turbidity values throughout the test, with multiple peaks crossing 39,000 NTUs throughout the duration of the simulation. CGR-1L also leveled off at 38,400 NTUs from just after the middle of the simulation to the end. CGR-2L had behavior

similar to the turbidity trends for both Control-2 and CGR-1L, but to a lesser degree. A side-by-side comparison of both CGR-amended soils, CGR-1L (top) and CGR-2L (bottom), is shown in Figure 23. CGR-2L peaked at 18,400 NTUs at the 9-minute mark and then gradually decreased in turbidity for the remainder of the simulation, plateauing at 14,400 NTUs from 30 to 48 minutes before decreasing to its lowest value of 11,400 NTUs at the end of the trial. The turbidity results in general showed that the untreated loess at OMC (Control-2) produced samples with much lower water quality values compared to both CGR-amended soils (CGR-1L and CGR-2L).
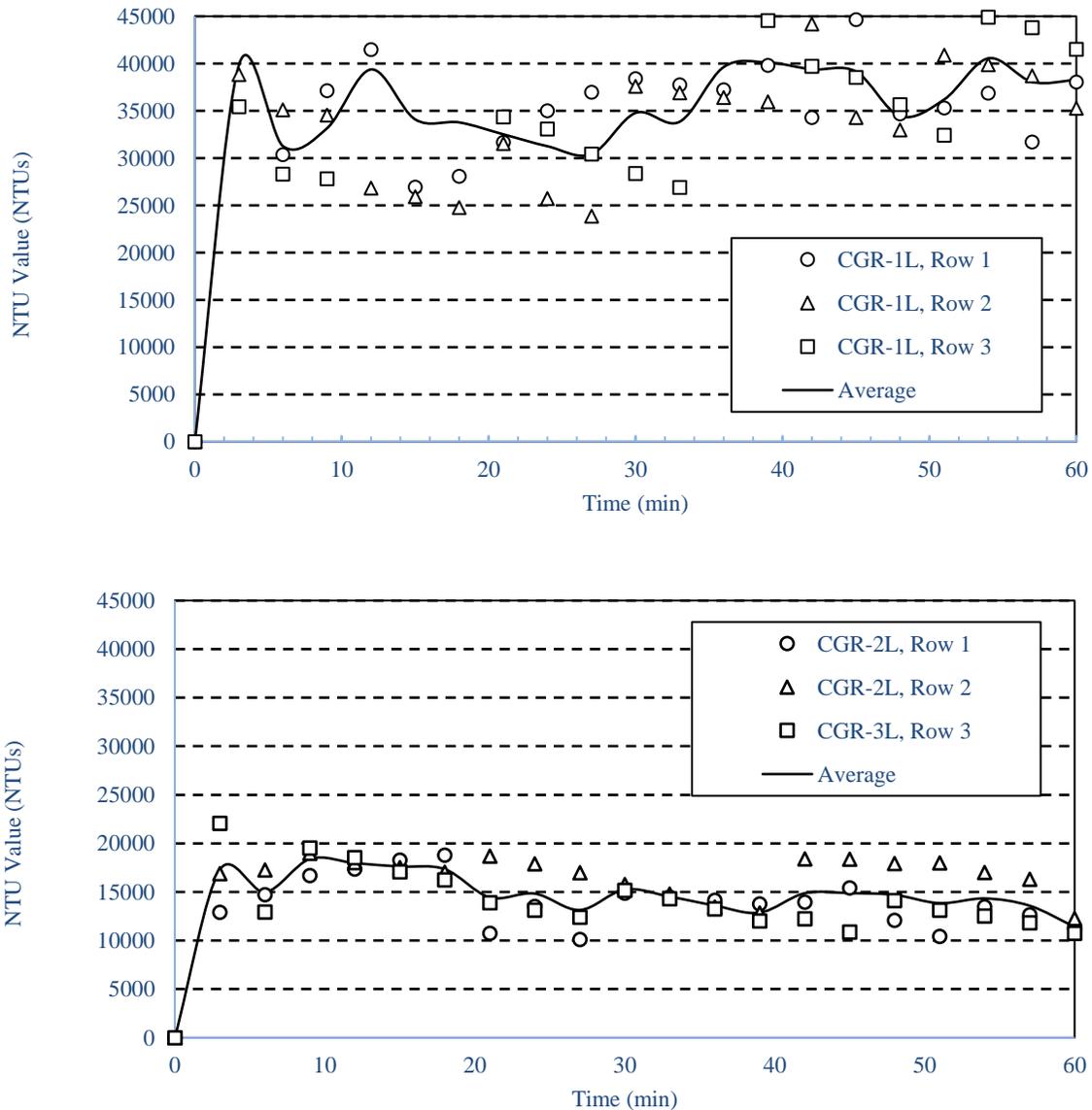
Figure 23. Water quality for CGR-amended loess, CGR-1L (top) and CGR-2L (bottom)

For the TSS testing, each bucket of sediment-laden runoff water was allowed to settle for a minimum of 24 hours prior to decanting and testing for total solids. For each bucket, the supernatant was vacuumed off using a ¼-horsepower pump and an innovative 3D-printed J-shaped straw designed by graduate student Jaime Schussler at Auburn University. This unique straw allowed the supernatant to be decanted more easily without disturbing the settled fine-sized particles from the rainwater runoff. From the vacuumed supernatant, a 50 ml sample was collected for each bucket tested, oven dried at 110°C, and weighed for sediment particulates. The remaining solids were vacated from each bucket using deionized water (as required) to effectively rinse and capture the fine particles from the sides of the buckets. These solids were then baked and weighed to determine the remaining solids within the original sediment-laden runoff water. An additional degree of granularity was created by separately collecting the rainfall runoff buckets by row and by storm event for each rainfall simulation. TSS were processed in the civil engineering environmental laboratories at both ISU and MSU on this project. At ISU, Nanopure water (deionized water) having less than 18.2 megohm ionic purity was used for rinsing to capture the fine particulates from the buckets. At MSU, laboratory-produced deionized rinsing water was used. NTU readings were not taken of the MSU deionized water.

Similarities were found between the TSS and turbidity trends in the rainfall simulations for Control-2, CGR-1L, and CGR-2L. For example, Control-2 showed the least amount of soil loss and lowest turbidity values, while CGR-2L fell in the middle and CGR-1L had the highest soil loss and turbidity readings. Control-2 showed a consistent (average) soil loss of 24,600 PPM for the first 40 minutes before increasing 60% to an average final peak value of 39,500 PPM at the end of the simulation. CGR-2L mirrored the trend for Control-2 except with higher values, averaging 79,300 PPM through the 40-minute mark and then increasing 24% to an average peak value of 98,500 PPM at the end of the simulation. In contrast, CGR-1L exhibited much more significant soil loss, averaging 99,600 PPM at 20 minutes and increasing 80% to 179,400 PPM at 40 minutes. CGR-1L started to level off as it approached the end of the simulation (the 60-minute mark) with a more gradual 10% increase in soil loss through the end of the simulation, with an ending peak value of 197,500 PPM.

Figure 24 shows two plots of the same TSS data. The top graph is a traditional bar graph with trendlines showing the increases in erosion rates with each storm intensity, while the bottom graph shows a spatial graph with pivot points at the transition points between storm events. Both graphs show the magnitude of the significantly higher soil loss for CGR-1L compared to the untreated loess and CGR-2L. The reason for the contrasting results between CGR-1L and CGR-2L is hypothesized to be the result of a greater hydration reaction between the CGR-2 and the loess. However, this has not been confirmed through additional testing of the compounds present in both CGRs.
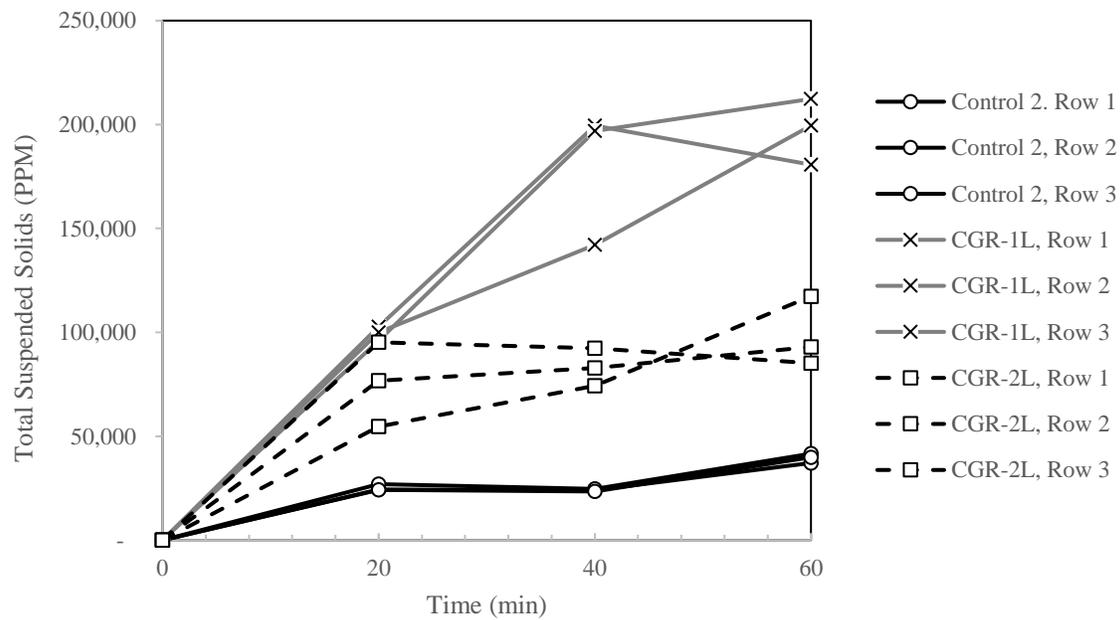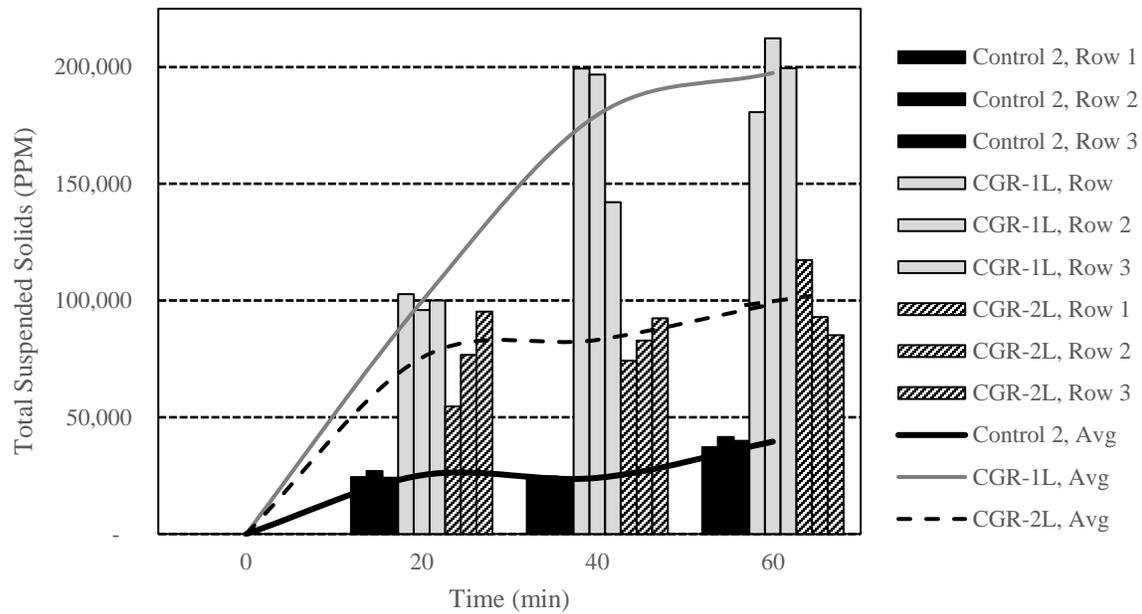
Figure 24. TSS soil loss data from rainfall simulations

Figure 25 shows turbidity results plotted against TSS results for each rainfall simulation. This composite graph clearly shows elevated turbidity levels and increased TSS erosivity trends for the CGR-amended soils compared to the untreated loess from the rainfall simulations performed. This graph also indicates that water quality (grab) samples taken over a rainfall event can be a good predictor of TSS (or total soil loss) resulting from the same rainfall event.
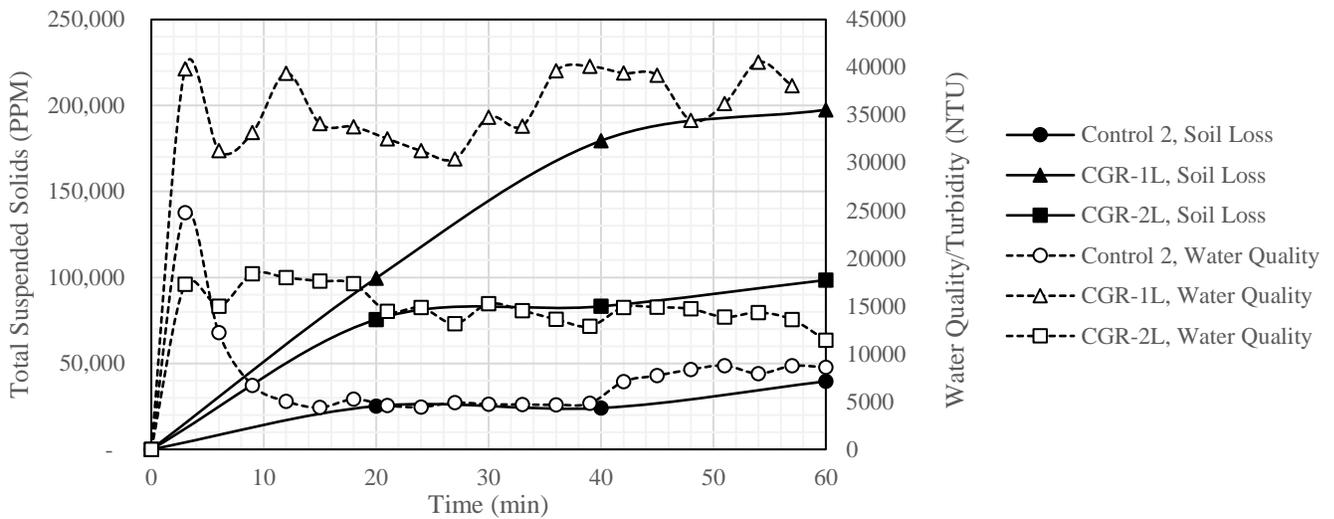
Figure 25. Soil loss and water quality over time

For each rainfall simulation, TSS samples were collected and analyzed by row and by rainfall intensity (storm event). In Table 10, results are converted to tons/acre of soil loss during each simulation.

Table 10. TSS collected (total soil loss) in tons/acre

Row	Rain Intensity	Control-1	Control-2	CGR-1L	CGR-2L
	2 in./hour	0.00	0.66	6.82	1.38
1	4 in./hour	9.82	1.54	14.54	5.60
	6 in./hour	7.72	4.85	24.27	14.28
	2 in./hour	0.08	0.90	5.01	2.30
2	4 in./hour	0.68	1.84	13.04	6.37
	6 in./hour	3.54	5.04	22.92	10.84
	2 in./hour	0.08	0.58	4.41	3.92
3	4 in./hour	1.34	1.35	10.57	9.31
	6 in./hour	18.65	3.96	19.13	12.33
	2 in./hour	0.05	0.71	5.41	2.54
Avg	4 in./hour	3.95	1.58	12.72	7.09
	6 in./hour	9.97	4.62	22.11	12.48

Soil loss data represent the TSS collected, dried, and weighed for each 20-minute storm event during the 60-minute simulation.

Control-1 (loess at 11.5% moisture content) is included in Table 10 to show the soil loss exhibited by the same loess material as Control-2 but with drier untreated loess exposed to the same rainfall conditions. With its drier initial condition, Control-1 (as expected) exhibited a much lower soil loss, an average of -0.05 tons/acre (or -7% of the -0.71 tons/acre soil loss exhibited by Control-2) during the first 20-minute 2 in./hour storm. This rapidly changed as Control-1 soil loss jumped to an average of -3.95 tons/acre and -9.97 tons/acre during the next two rainfall intensities, or -250% of the -1.58 tons/acre and -216% of the -4.62 tons/acre soil losses exhibited by Control-2 during these final two storms, respectively.

In comparison, CGR-1L and CGR-2L generated significantly more soil loss than Control-1 and Control-2 during each of their rainfall simulations. CGR-2L lost an average of 2.54 tons/acre during the 2 in./hour storm, increasing almost fivefold to 12.48 tons/acre during the 6 in./hour storm, while CGR-1L exhibited approximately double the soil loss of CGR-2L, with average soil losses starting at 5.41 tons/acre during the 4 in./hour storm before exploding to 22.11 tons/acre during the 6 in./hour rainfall intensity stage of the simulation. The results in Figure 25 and in Table 10 show a high amount of soil loss for each soil tested, but the magnitudes of the losses exhibited by the CGR-amended soils (CGR-1L and CGR-2L) were significantly higher than those exhibited by the untreated loess.

CHAPTER 3 WIND EROSION STUDY

3.1 Materials

The soils used in the wind erosion portion of this project included the western Iowa loess also used in the rainfall erosion portion of this project as well as Class A-1 shoulder aggregates from eastern Iowa. The loess collected came from the Loess Hills, and the shoulder aggregates came from county roads in both Washington County and Clinton County, Iowa. In addition to the soils collected, CGRs were collected from active concrete grinding projects located in eastern, western, northern, central, and southern Iowa.

3.1.1 Shoulder Materials

For the wind erosion testing portion of this research, a total of five granular shoulder aggregates were collected from unpaved gravel shoulders from five county roads in two counties in eastern Iowa. Three shoulder aggregates were collected from Washington County, Iowa (Sites A, B, and C) and two were collected from Clinton County, Iowa (Sites D and E). The aggregate from Site A was collected from County Road G37 (CR G37), while the aggregates from Sites B and C were collected a few miles apart on County Road G26 (CR G26), shown in Figure 26. The aggregate from Site D was collected from County Road Y46 (CR Y46), and the aggregate from Site E was collected from County Road Z24 (CR Z24).

Figure 26. Motor grader and soil sampling from CR G37 in Washington County

All five sites where soil samples were collected were outside unpaved roadway shoulders along two-lane undivided PCC county roads with speed limits ranging from 45 to 55 mph. Additionally, all five county road specimens came from aggregate shoulders ranging from 6 to 8 ft in width located next to paved PCC driving lanes. On the outside of each shoulder were vegetated (grass-covered) embankments that dropped off from the edge of the roadway shoulders at a 3:1 slope away from the roadway. Table 11 lists all five roadway shoulder sites sampled.

Table 11. Roadway shoulder sites sampled

Site	County	Town	County Road
Site A	Washington	Washington, IA	180th Street (CR G27)
Site B	Washington	Wellman, IA	190th Street (CR G26)
Site C	Washington	Washington, IA	190th Street (CR G26)
Site D	Clinton	Delmar, IA	185th Street (CR Y46)
Site E	Clinton	DeWitt, IA	330th Avenue (CR Z24)

3.1.2 Shoulder Material Collection

Initially, the proposed collection method was to manually shovel the shoulder soil after first loosening the compacted soil with drills and heavy-duty soil auger bits. However, due to the winter weather and freezing temperatures during the data collection period, an alternate method of using motorized equipment to scarify the shoulder aggregates was needed. A motor grader was chosen as the most efficient way to blade (loosen) the compacted, frozen shoulder aggregate. At each of the five sites, both Washington and Clinton Counties provided a motor grader and motor grader operator to loosen the compacted shoulder soil. This was performed as gingerly as possibly to minimize crushing or pulverizing of the existing aggregate and to reduce any changes to the soil particle sizes and gradations of the existing soils. For each sample, the full depth of the compacted shoulder aggregate was loosened until the underlying subgrade soils were visible. Although the aggregate depth was anticipated to be 4 in., the actual depth of the compacted gravel aggregate (above the subgrade) varied from approximately 6 to 10 in. Both Washington and Clinton Counties also provided small roadway crews and backfill aggregate to fill the holes created in the shoulders where the soil samples were taken. At each of the five sites visited, 10 5 gal buckets were used for aggregate collection, ranging in weight from approximately 18 kg (40 lb) to 25 kg (55 lb) of soil per bucket. A Caterpillar CAT 140M2 (Washington County) and a Caterpillar CAT 140M3 (Clinton County) all-wheel drive motor grader with 12 ft blades was used in each county for loosening the soil. Samples were collected in two days from all five county roads in December 2019. Collection from Site E is shown in Figure 27.

Figure 27. Motor grader and soil sampling from CR Z24 in Clinton County

3.2 Methods/Testing

The methods and testing for the wind erosion portion of this project involved the collection and preparation of the shoulder aggregates as well as additional preparation and testing of the loess and CGRs used in the initial rainfall erosion study. Tests were required for the initial gradation and compaction of the additional soils as well as for the compaction of the additional CGR-amended roadway shoulder mixtures.

3.2.1 Specimen Preparation (Homogeneous Mixing) and Moisture Content

To help ensure uniform testing of the shoulder aggregate soils collected from each site, the soils from each site were blended into five separate homogeneous batches. This was accomplished by first combining the 10 5 gal buckets collected for a given site into a large 150 gal mixing trough. The entire aggregate sample was then gently mixed for 2 minutes using a Brutus 21665Q 120 V two-speed hand-mixer with a three-flight steel mortar paddle and then gently turned over (mixed) with spade shovels repeatedly for 5 minutes to thoroughly rotate the soil into a homogeneous soil. The homogeneous soil was then returned to the 10 original buckets for future laboratory testing and analysis. No water was added or removed during this mixing process. Due to the snow and ice present on the ground when the samples were collected, each of the five soils collected was moist during mixing and had sufficient moisture to prevent the loss of fines from airborne dust during mixing.

The in situ moisture content tested for each of the five soils collected ranged from 7.9% to 9.2% for the Washington County soils (Sites A, B, and C) and from 9.7% to 11.8% for the Clinton County soils (Sites D and E). The Clinton County soils had higher initial moisture contents due to a light snowfall the night before the samples were collected. Two buckets from each shoulder sample were oven dried prior to performing a sieve analysis on each specimen. The oven drying temperature used was 110°C, and the drying time varied from 24 hours for the Washington County aggregate soils to 48 hours for the slightly more saturated Clinton County soils. After drying, a rubber mallet was gently used to break up clumps of dry soil so that no initial clump

was larger than 1½ in. diameter, larger than a visual observation of the maximum aggregate size for each soil specimen. One bucket of each CGR slurry (CGR-1 through CGR-5) was also oven dried for testing. Since over time each sealed bucket of stored CGR had separated into layers of sand and silt-sized particles with water also separating and rising to the top of the specimen, the CGR required remixing to return it to a viscous liquid (pourable slurry) state prior to any testing. Drying time for each of the CGRs was 72 hours at 60°C. Lower baking temperatures were used for each CGR to help minimize any change to the chemical composition of the CGR. ASTM D2216-19, Standard Test Methods for Laboratory Determination of Water (Moisture) Content of Soil and Rock by Mass, was followed for oven drying procedures and moisture content testing.

3.2.2 Sieve Analysis and Soil Classification

On each of the five roadway shoulder aggregates (Sites A through E), a sieve analysis was performed using ASTM C136/C136M-19, Standard Test Method for Sieve Analysis of Fine and Coarse Aggregates. The purpose of this test was to determine the initial gradation (particle size distribution) of each shoulder material as well as the USCS and AASHTO soil classifications. With this information, a compaction standard could then be chosen for each shoulder aggregate material. After a trial sieve test using 1½ in., 1 in., and ¾ in. sieve sizes, the nominal maximum aggregate (NMA) was determined as ¾ in. for Sites A, B, and C, while the NMA for Sites D and E was 1 in. Based on these values, the minimum sieve analysis sample of 5 kg (11 lb) was required for Sites A, B, and C, while 10 kg (22 lb) was the required minimum sieve sample for Sites D and E. With smaller sample sizes required for sieving Sites A through C, Site A was selected for initial sieving trials to test the accuracy of the sieve shakers and sieve equipment available at MSU.

Two different Gilson sieve shakers were available in the civil engineering laboratories at MSU, one with 8 in. diameter round sieves (hereafter Gilson 8D) and one with 14 in. x 14 in. square sieves (hereafter Gilson 14x14). After homogeneous mixing and oven drying, the weight of the oven-dried soil in each bucket of Site A shoulder aggregate weighed slightly more than 20 kg. With only 5 kg (or approximately one-fourth of the homogeneous oven-dried sample) required for the sieve analysis of the Site A soil, and to conserve soil, a Gilson soil splitter was then used in an attempt to uniformly divide (split or quarter) one bucket of Site A shoulder material. After splitting the material in accordance with ASTM C702/C702M-18, two sieve tests were performed using the Gilson 8D on half of the split soil sample and the Gilson 14x14 shaker on the other half of the split sample. Additionally, a second full 5 gal bucket of Site A soil was sieved in a single batch using the larger Gilson 14x14 shaker for comparison with the results of the smaller samples split and sieved. Results showed that the smaller Gilson 8D shaker produced slightly more accurate results (measured in terms of loss of fines) but was limited to smaller batch sizes per sieve test. In one case, two sieve tests were needed to sieve a single 5 kg sample in accordance with ASTM C136/C136M-19. In contrast, the larger Gilson 14x14 shaker processed larger batch sizes per sieve test, but the loss of fines (for particles passing the #4 sieve) was greater with the Gilson 14x14 shaker.

The Gilson 14x14 shaker was limited to five sieves sizes plus one solid pan for each sieve sequence. This meant that although larger samples could be sieved with the Gilson 14x14 shaker,

a transfer of fines passing the #4 (4.76 mm) sieve into a separate container was required before running the sample through a second sequence of finer sieves to process the soil samples down to a #200 (0.074 mm) sieve. Since the loss of fines (specifically soil particles smaller than a #4 sieve) influences the soil particle distribution and possibly affects the USCS and AASHTO soil classifications, care was taken during the transfer of soil to minimize the loss of fines during this exchange. The loss of fines for the smaller 5 kg samples using the Gilson 8D shaker ranged from -0.12% to -0.45%. With the larger 20 kg samples using the Gilson 14x14 shaker, the loss of fines had a range of -1.55% to -5.00%. The sieve sizes used for both the Gilson 8D and the Gilson 14x14 shakers included 1 in., ¾ in., ½ in., ⅜ in., #4, #8, #16, #50, #100, #200, and a pan.

Additionally, a sieve analysis was performed on the same material after drying the same Site A material collected after running a standard Proctor compaction test on the same soil as well. These results are graphed in Figure 28. A difference between the gradation curves for the same Site A material was found for each of the like materials tested. The primary difference in the curves is visible (as expected) for material below the #4 (4.75mm) sieve, at the transition between course and fine grain material. This is attributed to the loss of fines experienced during testing. Although the mechanical sieve shakers were responsible for dusting and the loss of fines during sieving, soil splitting is believed to have contributed an initial slightly uneven distribution of fines in the reduced (5 kg) soil samples compared to the full (20 kg) samples.
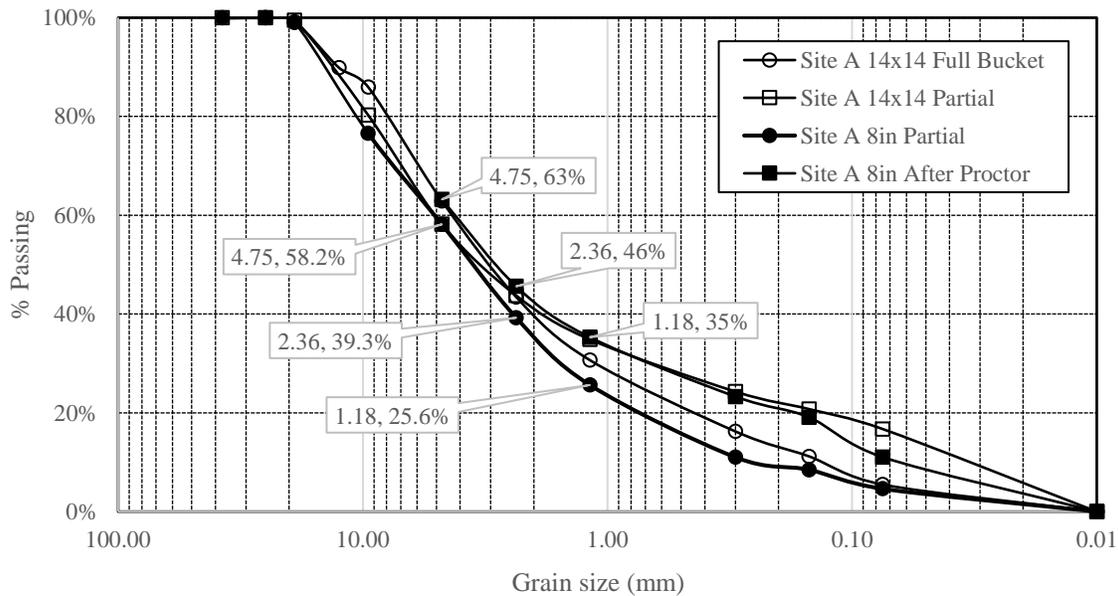
Figure 28. Sieve analysis equipment test trials with Site A soil

AASTHO T27, Standard Method of Test for Sieve Analysis of Fine and Coarse Aggregates, was used to validate the sieve tests performed on the shoulder aggregates. AASHTO T 27 limits soil loss (loss of fines) to less than -0.03% during sieving operations to validate a successful sieve test. Under AASHTO T 27, only one of the two Gilson 8D shakers passed this sieve test validation guideline. However, since the purpose of this sieve analysis for the wind erosion

portion of this research was simply to provide a broad (general) soil classification of each shoulder aggregate, the Gilson 14x14 shaker, even with the slightly higher loss in fines, was preferred to process larger batches and limit excess handling of the samples. Additionally, it was determined that the use of the Gilson 8D and the Gilson 14x14 shakers did not significantly change the gradation curves, nor did they change the overall AASTHO and USCS soil classifications for the initial Site A soil tested. As a result, the Gilson 14x14 shaker was selected for sieve analysis for the balance of soils for Sites B through Site E. Adjustments were made to the Gilson 14x14 shaker after the first series of Site A sieve tests, and the loss of fines was reduced to a range of -0.92% to -2.12% for Sites B and C and a range of -0.95% to -1.04% for Sites D and E.

The Iowa DOT has a range for acceptable Class A-1 roadway aggregates. The upper and lower limits of this gradation range are based on the standard sieve sizes listed for "Granular Surface & Shoulder" material in the Aggregate Gradation table (English units) located under Section 4109.02 of the current Iowa DOT *Standard Specifications for Highway and Bridge Construction* (Iowa DOT 2020). These sieve sizes include 1½ in., 1 in., ¾ in., ½ in., ⅜ in., #4, #8, #30, #50, #100, #200, and a pan. This range for Iowa DOT acceptable granular material is shown in the shaded region in Figure 29.
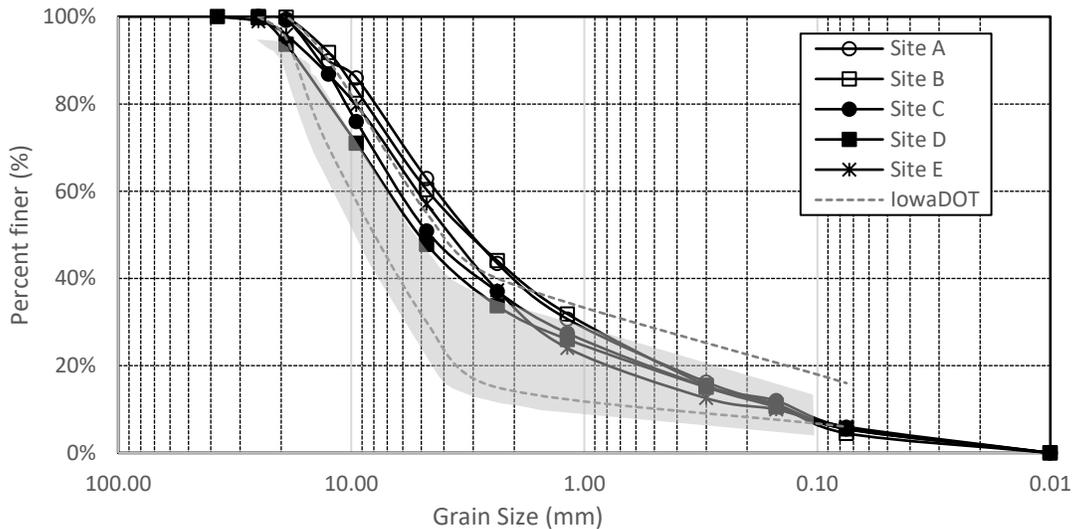
Figure 29. Sieve analysis comparison between five aggregate shoulder soils

The AASHTO soil classifications for all five county specimens were very similar Class A-1-a and Class A-1-b mixes, while the USCS soil classifications contained slight variations between the Washington County soils and the Clinton County soils. AASHTO Class A-1-a soils generally represent well-graded soils with gravel, coarse sand, and fine sand. In comparison, soils with an A-1-b AASHTO classification contain more sand compared to A-1-a soils, which contain more gravel. With respect to the USCS classification, slight differences in gravel-to-sand ratios for each soil produced both well-graded and poorly graded gravels or sands with silt, as shown in Table 12.

Table 12. Roadway shoulder site soil classifications

Site	Course Factor	AASHTO	USCS	USCS Full Soil Description
Site A	0.39	Class A-1-b	(SW-SM)g	Well-graded sand with silt and gravel
Site B	0.42	Class A-1-b	(SW-SM)g	Well-graded sand with silt and gravel
Site C	0.52	Class A-1-a	(GW-GM)g	Well-graded gravel with silt and sand
Site D	0.55	Class A-1-a	(GW-GM)g	Poorly graded gravel with silt and sand
Site E	0.46	Class A-1-b	(SP-SM)g	Poorly graded sand with silt and gravel

The collection of each of the five shoulder soils with the use of a motor grader to loosen the soil was discussed above. It was hypothesized that the use of a motor grader to loosen the soil would not detrimentally change the gradation of the shoulder soils from their in situ state. To confirm this hypothesis, a sieve analysis was also performed on the shoulder soils after performing standard Proctor compaction tests on each soil. Post-standard Proctor gradation tests revealed only minor changes to the initial aggregate soil particle distributions, and the results did not change the initial AASHTO or USCS soil classifications for each soil. Each post-compaction gradation curve also fell within the Iowa DOT range for Class-A granular shoulder material. For each initial shoulder aggregate collected, soil gradations were very close and within the acceptable range for Iowa DOT Class-A shoulder material, with upper and lower limits shown in the shaded region in Figure 29.

3.2.3 Soil Mixtures and CGR Dosages

As previously discussed, a 20% CGR dosage (to an 80% soil ratio by weight) was selected for the rainfall erosion study. To complement the rainfall erosion testing of 20% CGR-amended western Iowa loess, the same soil mixtures were included for the wind erosion testing. These soil mixtures included a loess control (with no CGR), a mixture of 20% CGR-1 and 80% loess, and a mixture of 20% CGR-2 and 80% loess. With respect to the CGR-amended shoulder aggregates, soil mixtures with Site A and Site E aggregate mixed with 20% and 40% dosages of CGR-4 and CGR-5 were selected for wind erosion testing. Site A and Site E were selected because they represented one soil from Washington County and one soil from Clinton County. CGR-4 and CGR-5 were selected because both CGRs were produced and collected from mainline CGR projects. The unique difference between CGR-4 and CGR-5 is in their PCC roadway mix design aggregates. The concrete mix design for CGR-4 contained a limestone aggregate, while the concrete mix design for CGR-5 contained a rose quartzite aggregate. With limited data on the mix design for CGR-4, this study was only able to cite the difference in gravels used in these two mix designs. CGR-5 was also collected from a newly poured PCC roadway, while CGR-4 was collected from a PCC roadway that had cured approximately 18 months prior to the time of the diamond grinding.

Since the five CGRs collected at the beginning of the rainfall study had been stored for an extended period of time, each CGR bucket required remixing to get the separated CGRs solids back into a slurry state for mixing with various shoulder aggregates.

Figure 30 shows the settled/consolidated state of a typical bucket of stored CGR. After breaking up the compacted cylinder of CGR with a garden hoe, a small amount of mixing water (kept from the original CGR discharge for each CGR) was added to the loosened solids to recreate the CGR slurries. However, after trial and error it was found that breaking up and oven drying the CGR solids was an easier solution. The CGRs solids, once broken up, were baked at 60°C to minimize any chemical changes to the slurries. Once dried, the CGRs were then gently crushed with rubber mallets to break up any remaining clumps and clods. The dry CGR was then ready to mix with the desired shoulder soils at the required 20% or 40% dosage, which in turn were hand-mixed (with mixing water added in to match OMC) to produce the homogenous CGR-amended soils ready for compaction and testing.

Figure 30. Consolidation of CGR slurry after storage for extended period of time (left) and CGR solids broken up with a garden hoe (right)

3.2.4 Standard Proctor (ASTM D698)

All soil specimens were compacted with standard compaction energy. ASTM D698-12e2, Standard Test Method for Laboratory Compaction Characteristics of Soil Using Standard Effort, was used for compaction. Using this standard, the OMCs and MDDs of both the control (untreated) soil specimen and the CGR-amended soil mixtures were found. Based on the results from sieve analysis and gradation, Method A was chosen for the shoulder aggregates from Sites A through E. This choice was based on less than 25% (by mass) of material having been retained on the #4 (4.755 mm) sieve for each soil. The OMCs for the Washington County soils (Sites A, B, and C) were 9.4%, 9.6%, and 8.5% respectively, while the OMCs for the Clinton County soils (Sites D and E) were approximately 2% lower at 7.3% and 7.6%, respectively. However, with all five soils having similar compositions of limestone-based gravel, sand, and silt, the MDDs were similar, ranging from 130.5 lb/ft^3 to 135.1 lb/ft^3 for the five soils tested from both counties. The MDDs for Site A soil (132.2 lb/ft^3) and Site E soil (132.3 lb/ft^3) were the most comparable among the soils from each county. The similarity of these MDDs was another reason for the selection of Site A and Site E soils for wind erosion testing. Proctor curves for the 13 shoulder soils and CGR-amended soil mixtures are shown in Figure 31. Although the OMCs were 2% less for the Clinton County control (untreated) soils compared to the Washington County soils, after the soils were blended with CGR-4 and CGR-5 in both 20% and 40% CGR dosages, the trends in

increasing OMCs were very similar for the CGR-amended soils for both counties, as shown in Figure 31.
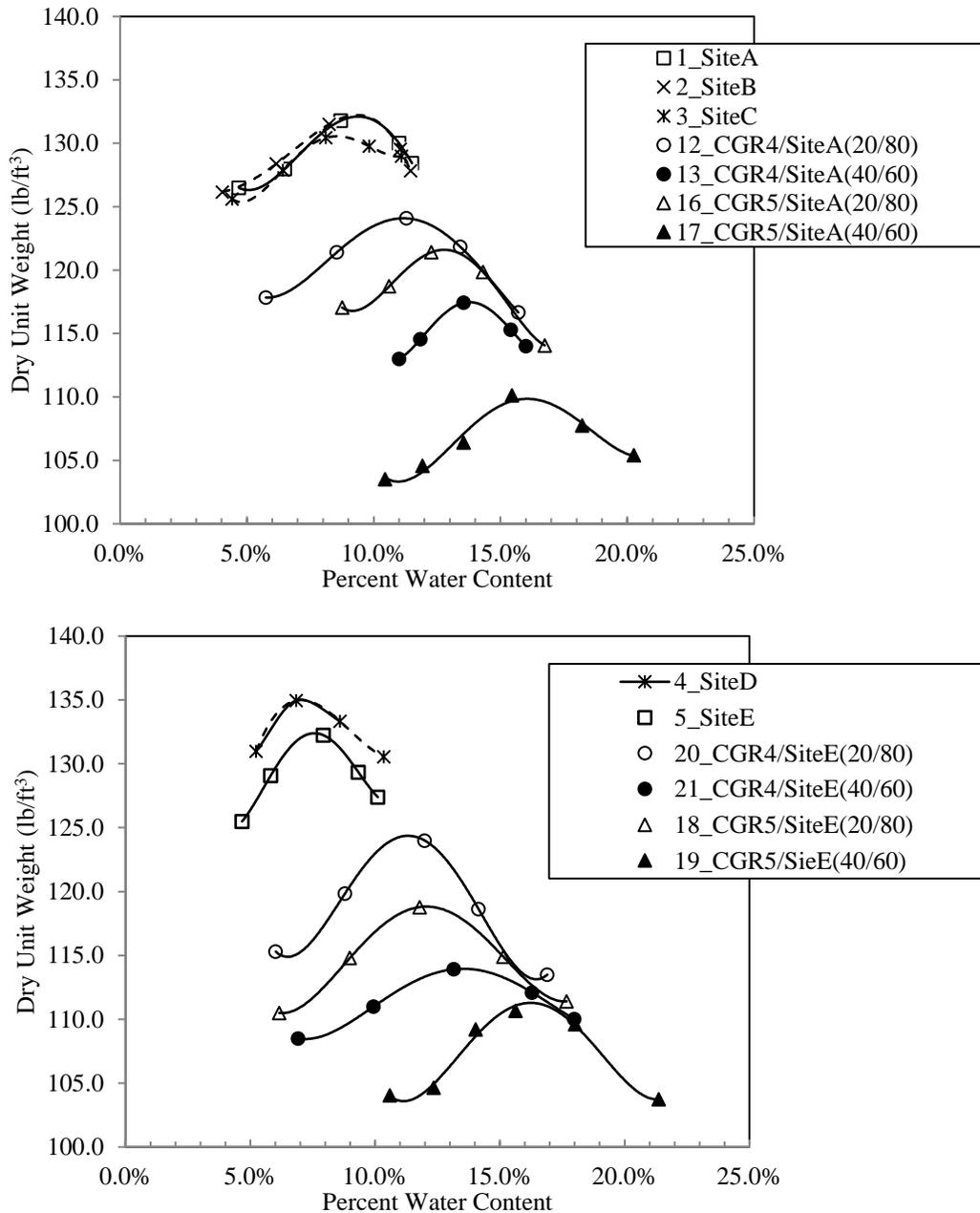
Figure 31. Standard Proctor curves for Washington County (top) and Clinton County (bottom)

Comparing the OMC points for each Proctor curve further revealed a linear correlation with a high degree of confidence with the addition of increasing dosages of CGR (0%, 20%, and 40%) to Site A and to Site E soils. This linear regression trendline was continuous with the transition from CGR-4 to CGR-5 amendments, with consistently higher moisture contents and lower

MDDs for the CGR-5-amended soils compared to the CGR-4-amended soils. Figure 32 shows these trends, with Site A soils in the top graph and Site E soils in the bottom graph.
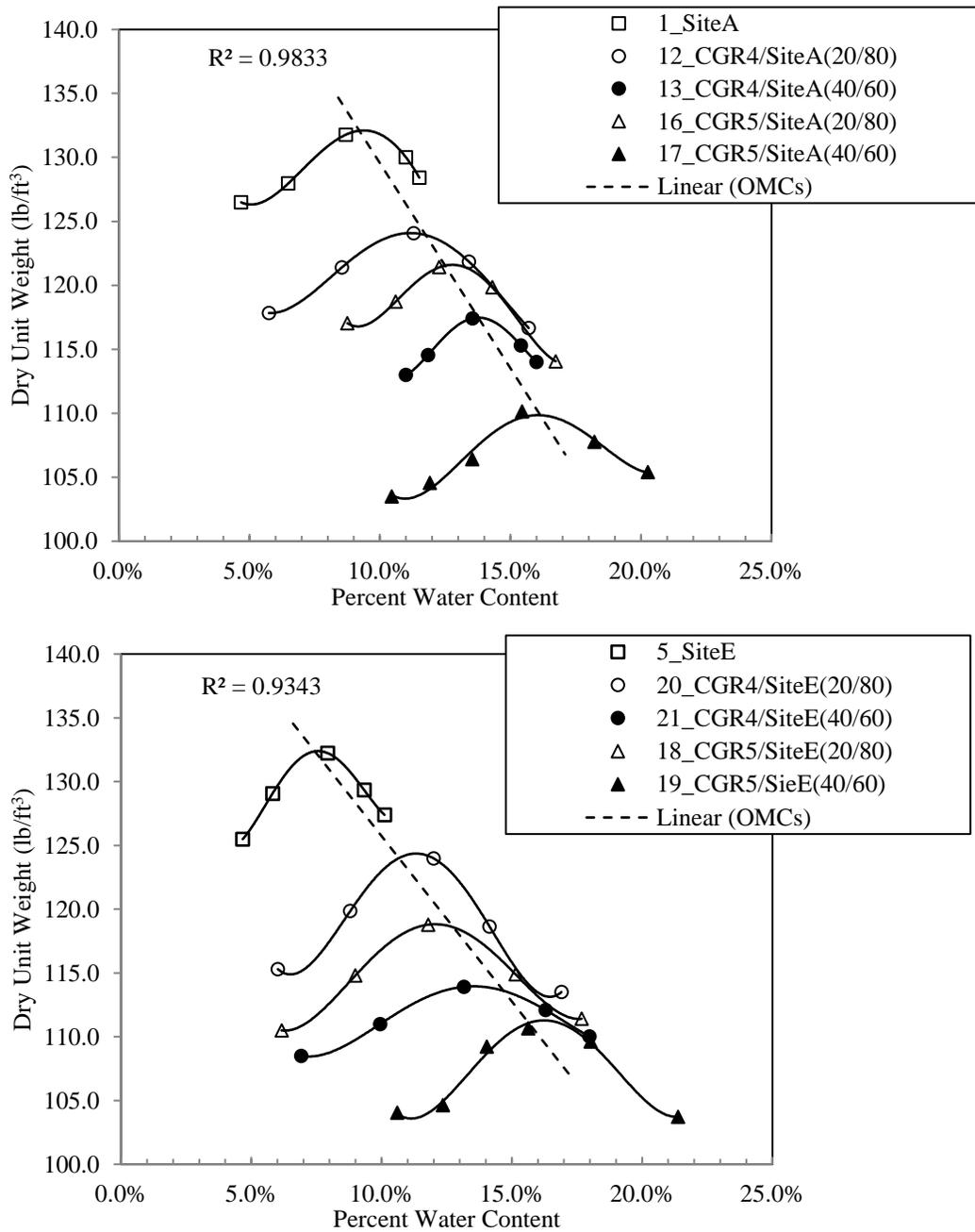
Figure 32. Standard Proctor trends for Washington County (top) and Clinton County (bottom)

3.3 Compaction

The UTA designed and built for the rainfall portion of this research was adapted and reused for the wind erosion portion of this study. The decision to use the UTA again was to both standardize and simplify the compaction of the wind erosion soil forms. As with the rainfall compacted soil forms, compaction trials were performed with 150 (gravity) drops at four drop locations (or 600 total drops) of the 13.05 lbf tamper built into the UTA (Figure 33). This tamper was raised and then dropped (not thrust down) for each tamp (or drop). The density of the soil was calculated based on the weight and volume of the rigid soil pans. Results from two initial compaction trials using Site C soil showed that 95% compaction was achieved with 150 (gravity) drops. Therefore, the number of drops was reduced to 125 (gravity) drops at four drop locations (or 500 total drops), and two successive UTA test compaction trials were run. Results demonstrated that 90% compaction (+/- 0.5%) was achieved at this tamping rate.
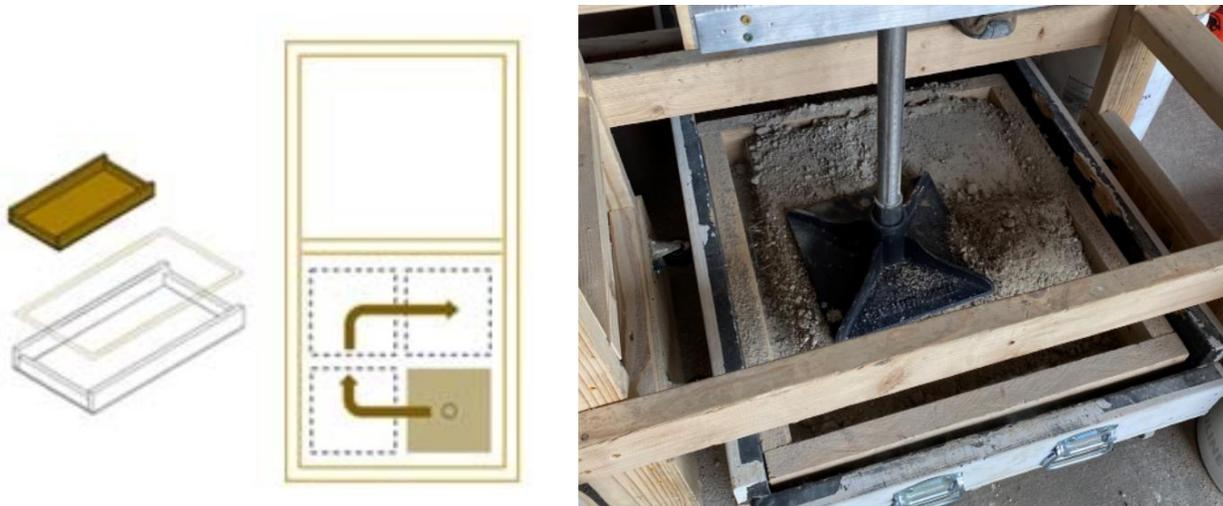
Figure 33. Tamping pattern and setup using UTA for smaller wind erosion soil forms

3.4 Wind Erosion Simulation

With respect to the wind erosion portion of this study, the design and construction of a device to wind test the compacted soil specimens was required. No standards were found for this work. As a result, equipment, calibration methods, and processes were developed to accomplish this work.

3.4.1 Wind Erosion Test Apparatus

The primary goal of the laboratory-based wind erosion test in this study was to simulate soil wind erosion caused by turbulent air flow (or wind whip) generated by large trucks passing an unpaved gravel roadway shoulder at a high rate of speed. Fugitive dust is a problem for all gravel roads and was one of the primary motivations for the wind erosion testing in this study. The overall design objective for these laboratory-based simulations was to determine whether CGR-amended Class-A shoulder aggregates as well as CGR-amended western Iowa loess would be

more resistant to wind erosion compared to untreated shoulder soils. The three primary types of wind erosion produced in these laboratory-based tests were surface creep, saltation, and suspension.

At the Civil Infrastructure Laboratory (CIL) at MSU, a wind erosion study was developed and performed during the summer of 2020. For this study, a table-mounted wind erosion test apparatus (WETA) was designed and built. This apparatus included a wooden platform complete with a removeable, recessed soil form with the top surface of the soil form designed flush with the surface of the adjacent platform. This setup mimicked the appearance of a flat roadway shoulder adjacent to a hard-surfaced driving lane. For the soil being tested, an 18 in. x 18 in. x 3 in. deep metal soil form (2.25 ft^2 surface area) was selected for multiple reasons. First, the rigidity of a metal soil form allowed compacted soil specimens to remain intact during the multiple soil form removal and weighing sequences required during each erosion test trial. The 3 in. soil form depth was chosen because it allowed for better compaction compared to shallower soil forms. Finally, test trials using baking flour and fine-grained silica sand both produced the most desirable wind disturbances over a surface area of less than 24 in. x 24 in. with the available blower (wind source). A photo of the removable recessed pan (left) and photo of the final WETA layout (right) are included in Figure 34.
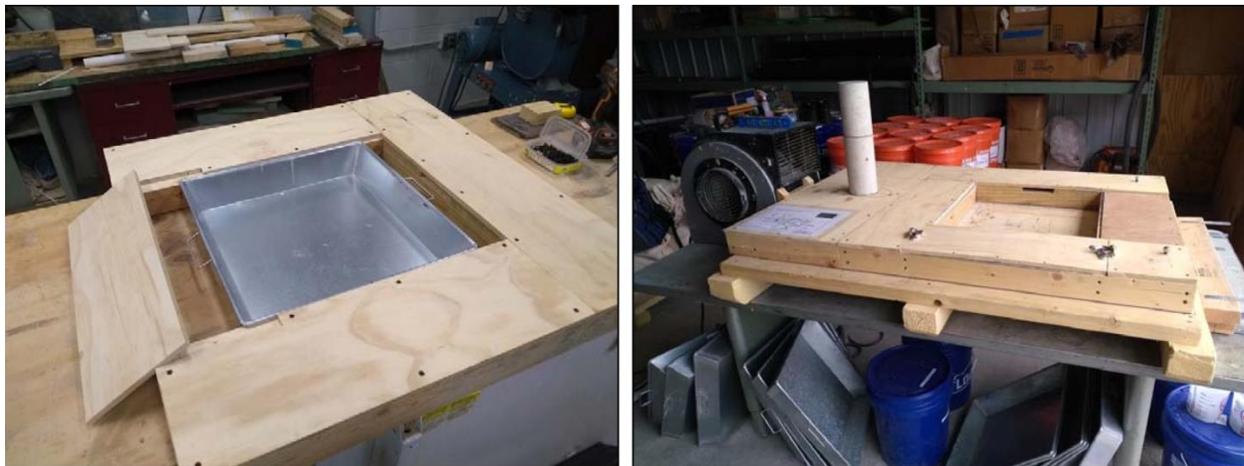
Figure 34. Wind erosion test apparatus during fabrication and final construction

The wind source used for these laboratory-based wind erosion tests was a Facso SuperCat Model 1200XL 120 V two-speed portable blower with a single-inlet, forward-curved, motorized impeller that produced a maximum 35 mph wind (1,120 CFM) across the targeted area. This maximum wind speed was best achieved by keeping the 18 in. x 18 in. soil form within 42 in. from the outlet of the blower. Using the blower alone (with no obstacles introduced into the air flow) produced a generally uniform air flow. However, for the wind erosion testing in this study, a turbulent air flow was required. Moreover, a multi-directional, repeatable, swirling (or whipping) wind event was essential.

In evaluating the type of obstacle to place in front of the blower, experiments with simple rectangular obstacles like those used as bluff objects by Murakami (1993) were first tried. This

produced a rolling flow field over the bluff object, but it reduced the airflow too much to produce noticeable erosion. Next, obstacles with rounded fronts such as those used by Hargitai (2014) were tried. This produced a desirable dual vertical vortex wind flow, but the inward motion of the vortexes deposited eroded soil behind the rounded obstacle similar to the Lee sand dunes described in Hargitai (2014).

Finally, attention was turned to fluid mechanics models that produce vortexes. The von Kármán Vortex Street classic fluid mechanics model, which includes a swirling wind pattern that produces a desirable series of repeating vortices, was considered. This naturally occurring phenomenon occurs as a result of winds being diverted around a blunt, high-profile object (Hansen 2017, Schmaltz 2016). Von Kármán Vortex Street vortices were captured by NASA in cloud formations rotating around the 6,800 ft high island of Tristan da Cunha located in the South Atlantic Ocean, as shown in Figure 35 (left) (Hansen 2017). After experimenting with one-, two-, and three-bluff object von Kármán configurations, a single cylindrical object was selected for this study to produce the desired repeating, swirling von Kármán Vortex Street wind event over the targeted soil form surface area.
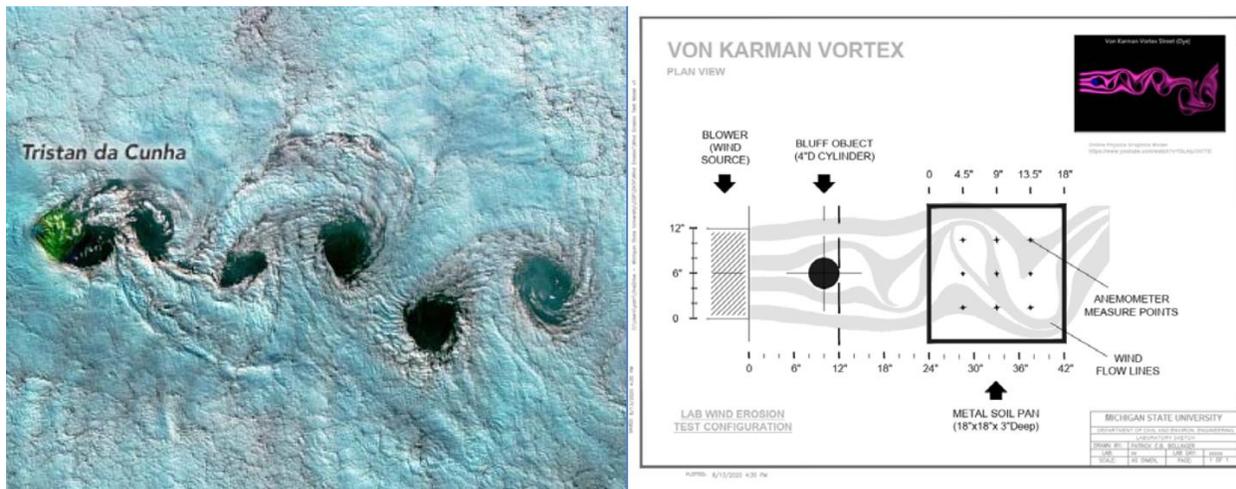
Image Joshua Stevens and Jesse Allen, NASA Earth Observatory 2017

Figure 35. Von Karman Vortex Street (left) and AutoCAD-scaled version for WETA layout (right)

Still images of the flow lines from two fluid mechanics models of the von Kármán Vortex Street, one pulled from Biju Patnaik University of Technology in India, were scaled in AutoCAD to match the 12 in. horizontal face of the Fasco blower (Ghosh 2021, Physics Graphics 2016). From here, the diameter and distance of the blunt object to insert into the windscreen were determined. The bluff object selected and placed into the blower wind stream consisted of two 4 in. diameter concrete cylinders stacked on top of each other. These cylinders were placed with the vertical tangent line located 12 in. from the face of the blower and 12 in. from the front of the recessed soil form. The total distance to the leading edge of the recessed soil form was 24 in. from the front of the face of the blower, as shown in Figure 35 (right).

3.4.2 Smoke Test and Anemometer Test Results

Validation of the creation of the von Kármán Vortex Street wind event was roughly confirmed using a smoke test and anemometer readings over a 4.5 in. grid marked on the surface of a rigid cover placed over the recessed soil form. A light smoke was produced using aerosol cans of a photography fog/haze product called Atmosphere Aerosol, and velocity readings were taken with a hand-held Davis Instruments Turbo Meter anemometer. Although basic and rudimentary, both tests confirmed that the classic von Kármán Vortex Street swirling wind patterns were produced with the WETA apparatus described above.

3.4.3 Wind Erosion Test Procedure

The procedures for the wind erosion testing involved compaction of soil forms, covering and curing of the compacted soil, and testing of the cured soil forms. For compaction, the UTA was adapted for use with the smaller 18 in. x 18 in. metal soil forms. The area within the 2 ft x 8 ft soil formed was reduced using 2x4 lumber for these tests. This allowed the smaller 18 in. x 18 in. soil form to nest nicely inside the larger wooden rainfall soil forms for compaction. Photos of a typical CGR-amended soil mixture and the setup of the modified UTA compaction layout are shown in Figure 36.

Figure 36. Steps during compaction of soil forms using UTA

After tamping compaction using the UTA, a perforated piece of rigid angled iron was used to screed the top surface of the compacted soils flush with the top edge of the soil forms. This is shown in Figure 37.

Figure 37. Preparation and screeding of compacted soil form

The screeded soil forms were then gently tamped with a rubber mallet and wooden block to compact the loose soil disturbed during screeding. Each compacted soil form was weighed and covered with shrink wrap and placed in a cool section of the CIL laboratory and allowed to cure for seven days. This part of the sample preparation process is shown in Figure 38. Soil loss due to saltation from wind erosion was measured for each of the wind erosion tests performed. After compacting each soil form at OMC and allowing each sample to cure for seven days, each compacted soil form was subjected to a three-phase wind erosion test.

Figure 38. Weighing of compacted soil (left) and curing of (sealed) compaction soil forms (right)

The wind erosion test procedure using the WETA consisted of a 30-minute wind event (Phase 1), 1 hour of air drying in the sun (Phase 2), and a 30-minute final wind test (Phase 3). The soil from each soil form was sampled immediately after conclusion of the Phase 3 wind test. Because the air drying during Phase 2 resulted primarily in moisture loss (not saltation and loss of solids), the loss in weight of the soil form during Phase 2 was recorded but was omitted from any soil erosion (soil loss) totals. Figure 39 shows two photos taken during a typical wind erosion test.

Figure 39. Views of WETA and compacted soil form during wind erosion test

The weight of the soil pan was taken and recorded before and after each of the three testing phases. Weight was measured in kilograms for each compacted soil form (kg/ft^2) and then converted to tons per roadway mile (tons/mile). One roadway mile with two 6 ft wide gravel shoulders was assumed for the conversion to a standard roadway unit of measure. Although it was not possible with the wind erosion setup to physically capture the loss of fines, a photo of the type of soil eroded is shown in Figure 40.

Figure 40. Soil loss due to wind erosion from compacted soil form (left) and loose eroded fines (right)

The formulas used in the soil loss conversion calculations are shown in Figure 41. These calculations include the minor weight loss due to moisture as well as soil loss due to erosion (saltation) off the top surface of the compacted soil forms.

$$\left(\frac{0.10kg}{2.25\,ft^2}\right)\left(\frac{2.20462\,lbs}{1\,kg}\right)\left[\left(\frac{1\,ton}{2000\,lbs}\right)\left(\frac{5280\,ft^2}{1mile}\right)\right](6ft\,wide)\,(2\,shoulders)\;=\;\textbf{3.1 tons (per roadway mile)}$$

Note: Metal Pan Surface Area: $(18in \times 18in)\left(\frac{1\,ft^2}{144\,in^2}\right) = 2.25ft^2$

Figure 41. Annotated conversion formulas for wind-eroded soil (soil loss)

After completion of the wind erosion trial, soil from each wind-eroded compacted soil form was sampled for moisture content. Soil samples were taken from the top surface of the soil form as well as the interior of the compacted soil, with one sample taken from each quadrant of the soil form. The purpose for this sampling was to measure any changes in the moisture content as a result of the wind erosion testing. Results showed an average moisture loss from the top surface of the tested soil forms for the Site A and Site E trials of -4.8% (with a maximum of -6.5% lost and a minimum of -2.4% lost). With respect to the samples taken from the middle of the tested soil forms for these same trials, an average -0.5% change in moisture content was found from the compacted soil (with a maximum of -1.3% lost and a minimum of -1.8% lost from the initial targeted OMC of the compacted soils).

3.5 Results

For this study, 20 wind erosion trials were performed, with 16 base trials consisting of three primary soil sets (Washington County soils, Clinton County soils, and western Iowa loess soils). The final 4 trials consisted of 1 confirmation retesting of the Site A Control soil, 1 test of an uncompacted (loose) Site B Control soil, and 2 trials with oven-dried Site C control soils (1 oven dried for 24 hours and 1 oven dried for 48 hours after compaction). All of the trials, with the exception of the Site B uncompacted (loose) test trial, were compacted at OMC. The 10 CGR-amended soil trials involved covering and curing the soils for seven days after compaction prior to testing.

The results for all 20 wind erosion trials are included in the graph in Figure 42. The soil loss for Phase 1 (bottom section of each bar) and the soil loss for Phase 2 (top section of each bar) were recorded for each trial. The results from Phase 1 and Phase 2 represented approximately 50% of the total soil loss in each trial, with the exception of the Site B Control trial, which exhibited greater erosion during Phase 2 after drying for an hour in the sun. For all of the soil blends tested, the (untreated) Site A Control soil resulted in the highest erosion rate at 8.07 tons/mile.
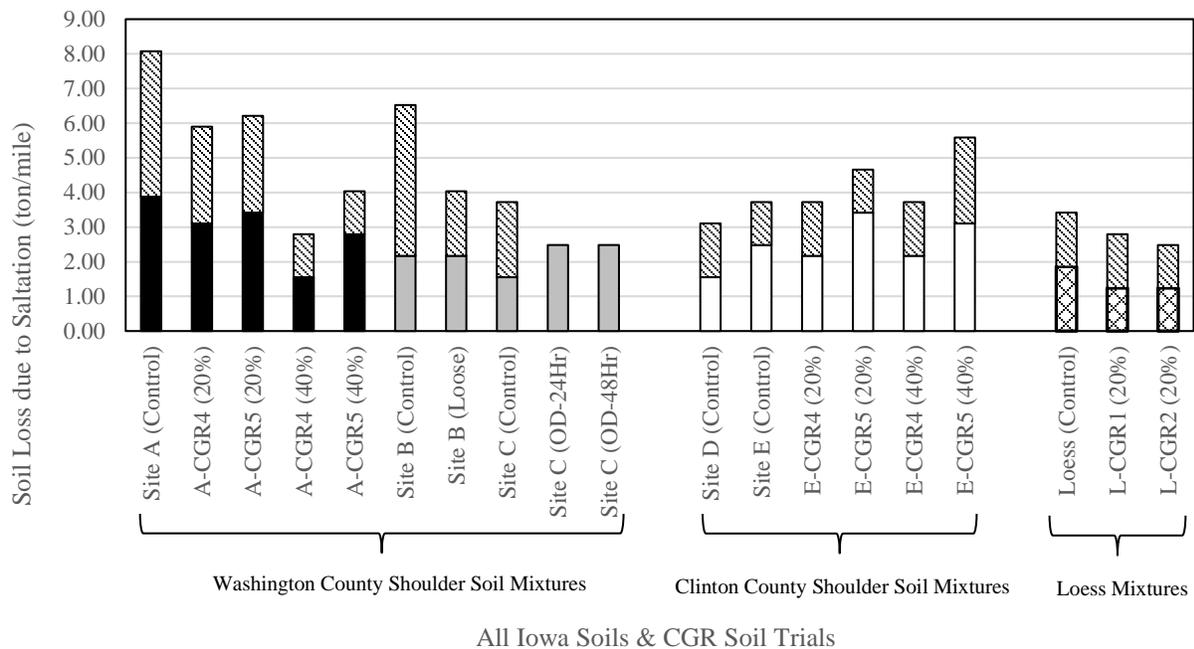
Figure 42. Wind erosion soil loss for all trials

Trials for the three primary soil sets tested were graphed separately and are shown in a side-by-side comparison in Figure 43. With respect to the Washington County soils (left graph, Site A soils), the four CGR-amended soils resulted in reduced erosion when blended with the Site A Control soil. On average, wind erosion decreased -2.17 tons/mile (-25%) and -5.28 tons/mile (-58%) with 20% and 40% CGR dosages, respectively, compared to the untreated control soil.
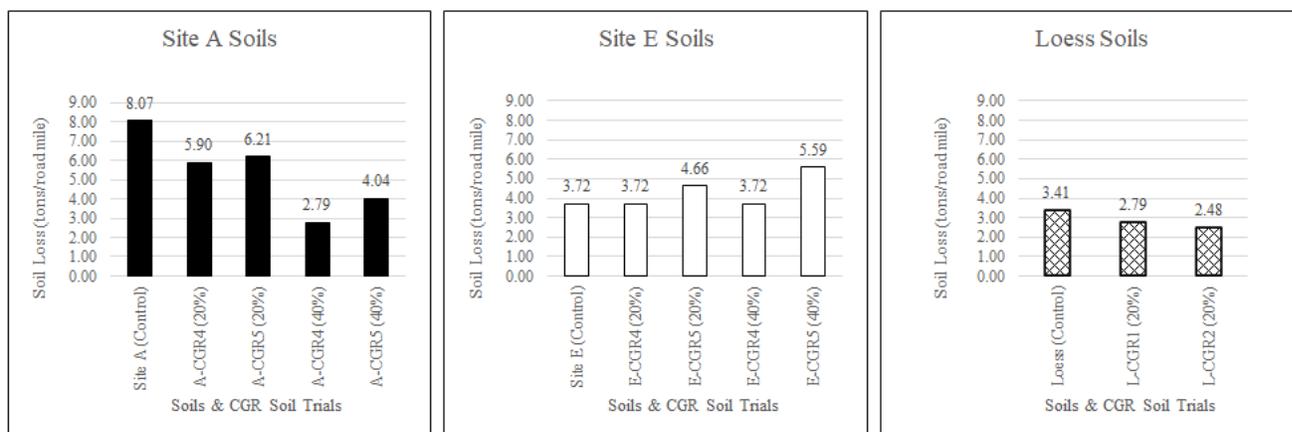
Figure 43. Wind erosion soil loss results (by soil set)

Conversely, for the Clinton County soils (center graph, Site E soils), the CGR-amended soils showed mixed results. For the CGR-4-amended soils (at both 20% and 40% dosages) soil loss was negligible. For the CGR-5-amended soils, wind erosion decreased -0.93 tons/mile, a 25% increase compared to the CGR-4-amended soils, and -1.86 tons/mile, a 50% increase compared

64

to the CGR-4-amended soils, with 20% and 40% CGR dosages, respectively, compared to the untreated control soil.

Lastly, for the western Iowa loess soil mixtures (right graph), like the Site A soils, there was improvement for the CGR-amended soils compared to the untreated control soil. Results showed that when the loess soils were amended with 20% CGR dosages, wind erosion decreased -0.63 tons/mile (-18%) and -0.93 tons/mile (-27%) compared to the untreated control soil.

Figure 44 shows a comparison of the Site A and Site E soils with the same two CGR amendments (CGR-4 and CGR-5) at 20% and 40% dosages. Results show that the Site A soils improved (stabilized) with an increase in CGR dosage, while the Site E soils worsened (eroded more) with increased CGR dosage.
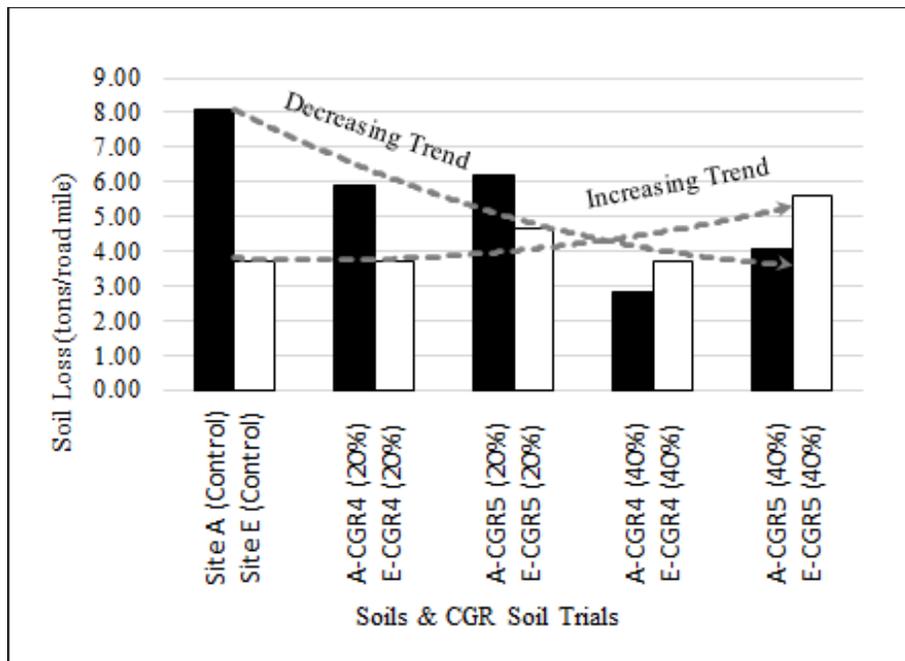
Figure 44. Wind erosion soil loss results, Site A and Site E trends

The reason for the unusual results found with the Site E soils could be due to the greater amount of in situ soil collected for this compacted Class-A roadway base. When the Washington County soils (Sites A, B, and C) were collected, the ground was hard and frozen. As a result, the motor grader was only able to loosen the top aggregate, with very little of the underlying in situ soil (the subgrade below the Class-A shoulder aggregate) collected. However, when the Clinton County soils were collected (Sites D and E), a wet snow had fallen the night before, resulting in softer, more saturated shoulder soils. As a result, the blade of the motor grader penetrated through the compacted aggregate for the Clinton County soils, slicing into the softer in situ soils beneath. This greater penetration of the blade led to the collection of more subgrade soils along with the two aggregate subbases compared to the first three Washington County shoulder soils collected.

The trials with the control soils demonstrated different behavior than expected. These control trials are shown in Figure 45. The Washington County soils all appeared to be from similar Class A-1 shoulder material, especially with Site B and Site C sampled from the same roadway shoulder a mile from each other. However, results showed significant degrees of soil erosion ranging from 3.72 to 8.07 tons/mile. The Clinton County soils also appeared to be from similar Class A-1 shoulder material although sampled from different county roads. These two sites (Site D and Site E) shared comparable wind erosion values at 3.10 and 3.72 tons/mile.
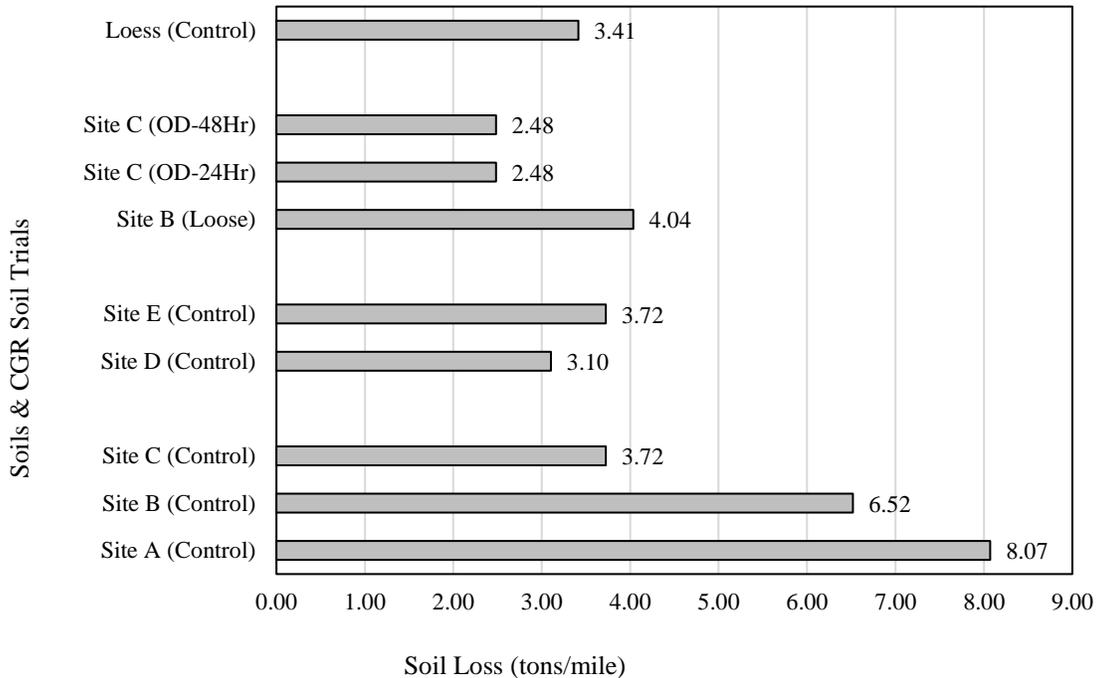
Figure 45. Wind erosion soil loss results for untreated soils

With respect to the Site B Control soil from Washington County, an unusual result was found between the two tests performed on this soil. The loose specimen eroded 38% less than the control specimen compacted at OMC. It is believed that this may have occurred because with compaction, the larger gravels and soil particles may shift down closer to the bottom of the soil form, leaving more fine particles at the top of the compacted soil form. If this was true in this case, then more fines would have been available to erode in the compacted sample compared to the loose, uncompacted Site B Control soil.

Site C had three different wind erosion trials, with each control soil compacted at OMC. The main control soil was tested immediately after compaction, while the other two Site C Control soils were oven dried at 110°C after the Phase 1 wind erosion test, one for 24 hours and the other for 48 hours, prior to the Phase 2 wind erosion test. The reason for this oven drying was to simulate compacted roadway shoulders baking in the hot summer sun. Results showed that the oven-dried soils did not experience any soil erosion during Phase 2. This resulted in 33% less wind erosion compared to the standard Site C Control soil, which was compacted and

66

immediately tested. Since oven drying eliminated the wind erosion during the second Phase 2 wind erosion test, a one-hour rest cycle was used instead, since oven drying seemed to provide stabilization to the Site C Control soils tested.

CHAPTER 4 ENVIRONMENTAL TESTING

4.1 Methods

Following materials characterization, single-batch water leach tests (WLTs) were performed to determine the leaching behaviors of the following soils and soil-CGR mixtures:

- Site A Control
- Site A soil with 20% dosage of CGR-4 (A-CGR-4 (20%))
- Site A soil with 20% dosage of CGR-5 (A-CGR-5 (20%))
- Site A soil with 40% dosage of CGR-4 (A-CGR-4 (40%))
- Site A soil with 40% dosage of CGR-5 (A-CGR-5 (40%))
- Site E Control
- Site E soil with 20% dosage of CGR-4 (E-CGR-4 (20%))
- Site E soil with 20% dosage of CGR-5 (E-CGR-5 (20%))
- Site E soil with 40% dosage of CGR-4 (E-CGR-4 (40%))
- Site E soil with 40% dosage of CGR-5 (E-CGR-5 (40%))
- Loess Control
- Loess with 20% dosage of CGR-1 (L-CGR-1 (20%))
- Loess with 20% dosage of CGR-2 (L-CGR-2 (20%))

Special attention was paid to pH, oxidation-reduction potential (Eh), alkalinity, and sulfate, nitrate, and metals concentrations. The single-batch WLTs were conducted following Cetin et al. (2012). The water quality analyses were conducted following the standardized methods shown in Table 13. It is important to note that the metals listed in Table 13 were chosen for quantitative measurement following preliminary qualitative analysis. Other metals such as Hg, Pt, and Tl were not detected in the preliminary analysis and hence were not included in the quantitative analysis.

Table 13. Summary of water quality analyses performed

Analyses	Parameters	Methods
Water chemistry analyses	Eh, EC, and pH	U.S. EPA 9045D
	Alkalinity	EPA-102-A Rev 3
	Sulfate	EPA-123-A Rev 5
	Nitrate	EPA-115-A Rev 6
Metal analyses	Al, Ag, As, B, Ba, Be, Ca, Cd, Co, Cr, Cu, Fe, K, Li, Mg, Mn, Mo, Na, Ni, Pb, Se, Si, Sr, V, and Zn	U.S. EPA 6010B

Each soil and soil-CGR mixture leachate exhibited unique water quality characteristics in the single-batch WLTs conducted following Cetin et al. (2012). In brief, all materials were air dried for 24 hours and crushed using a hammer to pass the #50 sieve (<0.297 mm) prior to leachate extractions. A liquid-to-solid ratio (L:S) of 10:1 was used, in which 200 ml of ultrapure water (leachant) was added to extraction vessels containing 20 g of dried soil or soil-CGR mixture. The

extraction vessels were rotated at 29 revolutions per minute for 24 hours at ambient temperature. Following the extraction, the supernatant was filtered through 1.5 μm pore size filters, and pH, Eh, alkalinity, nitrate, and sulfate measurements were taken. Then, the remaining leachate was acidified for metal concentration analyses.

4.2 Results

As shown in Table 14, all soil-CGR mixtures generated basic effluent solutions. Other than pH, the most notable water quality parameter of concern in the generated effluent was sulfate, for which the concentrations ranged from approximately 60 mg/L to over 150 mg/L (with a secondary maximum contaminant level [MCL] of 250 mg/L). No trend was observed between the different CGR sources for any of the CGR dosages in the mixtures.

Table 14. Water quality results of effluent from each soil and soil-CGR mixture

Specimen	pH	Redox (mV)	Alkalinity (mg CaCO$_3$/L)	Nitrate (mg N/L)	Sulfate (mg/L)
Site A Control	6.8	314	42	0.32	24
A-CGR-4 (20%)	9.4	422	64	0.45	58
A-CGR-5 (20%)	9.2	345	62	0.35	67
A-CGR-4 (40%)	10.5	456	88	0.65	89
A-CGR-5 (40%)	10.1	375	79	0.22	92
Site E Control	6.4	312	32	0.16	26
E-CGR-4 (20%)	9.1	401	67	0.39	47
E-CGR-5 (20%)	9.2	320	63	0.24	56
E-CGR-4 (40%)	10.3	447	79	0.41	86
E-CGR-5 (40%)	9.8	333	74	0.6	94
Loess Control	5.7	125	12	0.4	100
L-CGR-1 (20%)	9.1	386	45	0.17	120
L-CGR-2 (20%)	9.4	402	56	0.15	140

Of the metals quantitatively measured, Be, Cd, Cr, Cu, Li, Ni, Pb, and V were detected in reasonable concentrations in the effluents generated from the single-batch WLTs of the soil-CGR mixtures. In particular, significantly high levels of Cr, Ni, Pb, and Zn were observed (Figure 46). Most of the other metals shown in Figure 46 (Be, Cd, Cu, Li, and V) were present in relatively low concentrations.
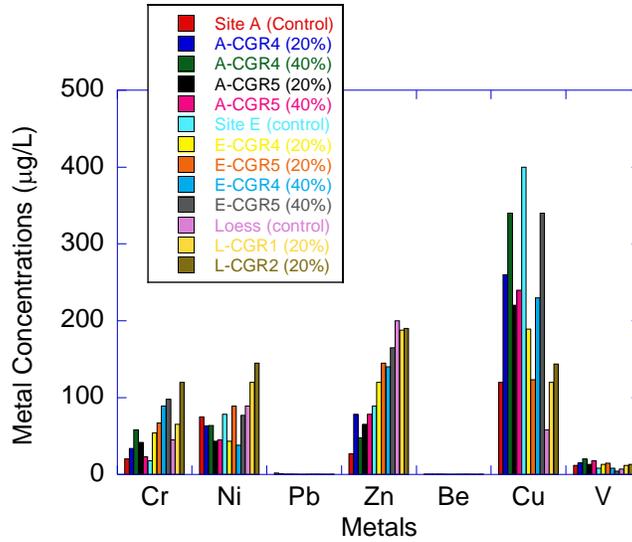
Figure 46. Select metal concentrations detected in effluents generated from single-batch WLTs of soil and soil-CGR mixtures

The known regulatory limits set by the U.S. EPA or state agencies are provided in Table 15.

Table 15. Regulatory limits of select metal analyses

Metal	Type of Regulatory Limit	Limit (mg/L)
As	U.S. EPA MCL	0.01
Be	U.S. EPA MCL	0.004
Cd	U.S. EPA MCL	0.005
Cr	U.S. EPA MCL	0.1
Cu	U.S. EPA action level	1.3
Li	N/A	N/A
Mo	U.S. EPA National Recommended Water Quality Criteria (NRWQC) (human health) limit	0.05
Ni	U.S. EPA NRWQC (human health) limit	0.61
Pb	U.S. EPA action level	0.015
Se	U.S. EPA MCL	0.05
V	CA State Water Resources Control Board drinking water notification levels	0.05

CHAPTER 5 SHEAR STRENGTH AND STIFFNESS TESTING

5.1. Methods

5.1.1 California Bearing Ratio Test

The CBR test is a penetration test for evaluation of the mechanical strength of road subgrades and base courses. The soil-CGR mixtures used in the CBR tests were prepared by mixing air-dried soil with a specified percent CGR by weight. CGR percentages were selected as 20% and 40%, as described above. All specimens for the CBR tests were compacted at their OMC using the standard Proctor effort (ASTM D 698 Method B). After compaction, the specimens were extruded with a hydraulic jack, sealed in plastic wrap, and cured for seven days at 100% relative humidity and a controlled temperature (21±2°C) before testing. All CBR tests were conducted by following the methods outlined in AASHTO T 193 and ASTM D1883. The specimens were unsoaked, and the tests were performed at a 1.27 mm/minute strain rate using the Geotest Instrument Corp S5840 Multi-Loader loading frame. The equipment had a maximum loading capacity of 44.8 kN. Duplicate specimens were tested for quality control, and the averages of these two tests were reported as the results.

5.1.2 Resilient Modulus Test

The resilient modulus test provides the stiffness of a soil under a confining stress and a repeated axial load. The procedures outlined in AASHTO T 307-99, a protocol for testing highway base and subbase materials, were followed for the resilient modulus tests. The same soils and soil-CGR mixtures used for the CBR tests were prepared in specimens that were 152.4 mm in diameter and 304.8 mm in height, and the specimens were compacted in split molds at their OMCs in eight layers using the standard Proctor energy. After compaction, the specimens were removed from the molds, sealed in plastic wrap, and were cured for seven days at 100% relative humidity and a controlled temperature (21±2°C) before testing.

An MTS loading frame and associated hydraulic power unit system was used to load the specimens. The conditioning stress was 103 kPa. The confining stress was kept between 20.7 and 138 kPa during the loading stages, and the deviator stress was increased from 20.7 to 276 kPa and applied for 100 repetitions at each stage. The loading sequence, confining pressure, and data acquisition were controlled by a personal computer equipped with the appropriate software. Deformation data were measured with internal linear variable displacement transducers (LVDTs) that had a measurement range of 0 to 50.8 mm.

The resilient moduli from the last five cycles of each test sequence were averaged to obtain the resilient modulus for each load sequence. The resilient modulus of soil is usually nonlinear and is dependent on the stress level. This nonlinear behavior was defined in this study using the common model developed by Moossazadeh and Witczak (1981):

$$\mathrm{M_R} = K_1 \theta^{K_2}$$

(1)

where M_R is the resilient modulus, K_1 and K_2 are constants, θ ($= \sigma_d + 3\sigma_c$) is the bulk stress, σ_c is the isotropic confining pressure, and σ_d is the deviator stress. A summary resilient modulus (SM_R) was computed at a bulk stress of 208 kPa following the guidelines provided in NCHRP 1-28A (Witczak 2003). This approach is consistent with the suggestions in the recent *Mechanistic-Empirical Pavement Design Guide* on providing a constant resilient modulus for chemically stabilized materials in new and rehabilitated pavement structures (ARA, Inc., ERES Consultants Division 2004).

5.2. Results

5.2.1 California Bearing Ratio Test

The CBR test results are provided in Figure 47a. All soils had CBR values lower than 50, a generally accepted limit for base applications (Asphalt Institute 2003), and therefore required stabilization for use in roadway construction. In all cases, the CBR values of the stabilized mixtures were higher than those of the soils alone. However, results showed that the CBR values of the soil-CGR mixtures were also lower than 50. Therefore, the soil-CGR mixtures cannot be used as base/subbase materials but can be used as shoulder materials.

5.2.2 Resilient Modulus Test

The SM_R values of the tested specimens are presented in Figure 47b. Similar to the CBR data, the soils alone had low SM_R values, justifying the need for stabilization with a calcium-rich binder. While the SM_R values of the soils increased with addition of CGR, the resulting mixtures were not adequate for use as a base/subbase stabilizer. Therefore, it is recommended to use these mixtures as shoulder materials.
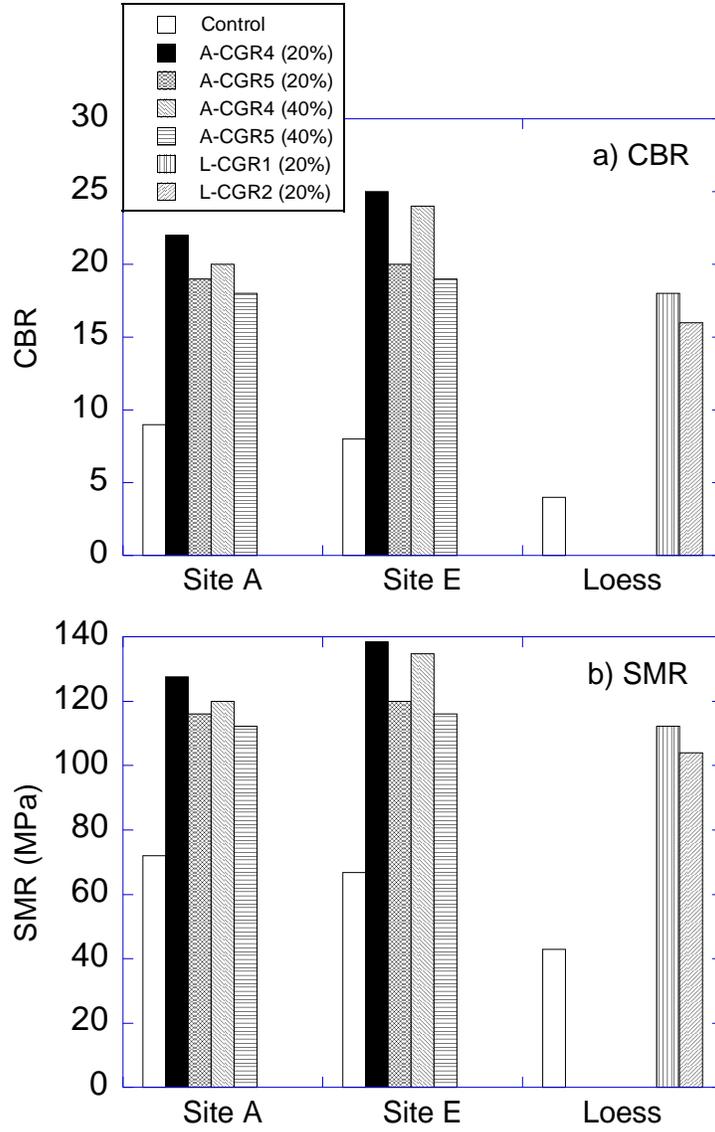
Figure 47. CBR (a) and SM_R (b) values of soils alone and soil-CGR mixtures

CHAPTER 6 DISCUSSION OF LABORATORY INVESTIGATION

6.1 Rain Erosion Discussion

The water quality of the grab samples degraded much more over time for the CGR-amended soils than for the untreated loess throughout the rainfall simulations, with turbidity values consistently ranging from 1.8 to 4.7 times greater (worse) for the CGR-amended soils. This is evidenced by studying the average turbidity values for CGR-2L (11,400 NTUs) and CGR-1L (38,400 NTUs), which outpaced the average values measured for the untreated loess in Control-2 (8,200 NTUs), even with the final average turbidity reading (8,600 NTUs) for the loess at the end of the simulation. Overall, compared to Control-2, soil loss as measured by TSS during each simulation ranged from 2.2 times worse with Control-1 to 2.7 and 4.8 times worse with CGR-2L and CGR-1L, respectively. These results showed that although soil erosion was greater for the loess compacted on the dry side of optimum compared to the loess compacted at OMC, the CGR-amended loess faired much worse compared to either of the untreated loess controls. For example, at the end of the simulation, CGR-1L lost a staggering 49.56 MT/ha (22.11 tons/acre) compared to the untreated loess in Control-2, which lost 10.35 MT/ha (4.62 tons/acre).

Yang et al. (2019b) hypothesized that the hydration reaction of the CaO within a typical CGR amendment would positively affect the cohesion and strength of the soil particles based on testing with a clayey sand and a sandy silt; however, results were opposite to these suppositions with the loess and CGRs tested in this study. The decreased cohesion (which resulted in greater erosion in this rainfall study) was attributed to the addition of the fine-grained CGR particles mixed into the already fine-grained silt-sized loess soil particles. This lower cohesion/increased erosion could also be due to the limited 24-hour cure time allowed for the CGR-amended soils, which limited the time available for hydration reactions for the CaO contained within the CGR slurries. Furthermore, differences between the compounds contained within the CGRs used in this study and the 2016 CGR used in Yang et al. (2019b) could also explain the lack of cohesion between the CGR and the loess tested in this study.

Additional testing of loess and CGR samples cured for seven days would more conclusively determine the impact of amending loess with CGR. Testing for the percentage of CaO compound in the five CGRs used in this study would also add clarity to the mechanism behind the increased erosion exhibited by the CGR-amended loess in this rainfall study. Additional research to explore and characterize the mechanisms behind the erosivity of CGR-amended loess due to rain is needed.

6.2 Wind Erosion Discussion

With respect to the wind erosion study, CGR testing was performed on the same loess soil mixtures tested in the rainfall erosion study. However, the wind erosion portion of this study was extended to include five Class A-1 roadway shoulder aggregates collected from two counties in eastern Iowa, and CGR dosages were doubled to include both 20% and 40% CGR dosages for the shoulder aggregates tested. The curing time for the CGR-amended soils was also extended to

seven days (in lieu of the limited 24-hour curing time during the rainfall erosion study) prior to wind erosion testing.

A sieve analysis was performed on all five Class A-1 roadway shoulder aggregates, and results showed that the shoulder soils sampled fell within the gradation limits established by the Iowa DOT for these aggregate materials. Wind tests, however, had mixed results. For the Washington County soils tested (Site A Control and Site A CGR-amended soils), erosion was reduced with the addition of CGR, and wind erosion lessened to a greater degree with the increase in CGR dosage from 20% to 40%. This confirmed the hypothesis for this study that the reduction in soil loss can be attributed to possible hydration reactions resulting in better cohesion in the CGR-amended soils compared to untreated soils. The hypothesis was also validated with the CGR-amended western Iowa loess, whose soil loss due to wind erosion also decreased with the addition of 20% CGR.

However, for the Clinton County soils (Site E Control and Site E CGR-amended soils), the addition of CGR-4 resulted in no appreciable changes in wind erosion, while the addition of CGR-5 resulted in greater wind erosion as well as an increase in soil loss with increasing dosages of CGR (from 20% to 40%). One reason for this disparity could be differences in the concrete mix designs for CGR-4 and CGR-5. CGR-4 had a limestone aggregate, while CGR-5 had a rose quartzite aggregate, which is more inert and less reactive during the curing process. Another reason for the trends observed in the Clinton County soils could be that more subgrade soil was captured when the shoulder soils were sampled. The portion of underlying subgrade soils collected with the aggregate shoulder samples for Site D and Site E from Clinton County appeared to have more organic material present. This was not confirmed through any laboratory testing but was noticed both in the texture of the samples as well as the strong organic smell of these two soils during drying. It was also observed that mold grew in one partial bucket of Site D soil and one partial bucket of Site E soil purposely left open to the air for a few weeks. These buckets were discarded, but these results confirmed suspicions that these two soils contained organic material.

6.3 Effects of CGR on pH

It is expected that CGR would have elevated pH values similar to those of hardened PCC. The increase in pH during the hydration process of fresh PCC is attributed to the release of Ca^{2+} and OH^- ions from several contributing compounds, each of which includes CaO. Portland cement initially contains a high percentage of CaO, ranging from 60% to 67% (Coban 2017), while CGR produced from roadway diamond grinding has a lower but broader range of CaO content, ranging from 17% (Yang et al. 2019b) to as high as 31% (Kluge et al. 2017).

Although CaO content was not tested for the five CGRs used in this study, tests for pH were performed. The average pH for the five CGRs collected for this project was 11.50, with a low pH of 11.13 and a high pH of 11.83. The average pH for the 20% CGR-amended loess was 10.43, with a low pH of 9.59 and a high pH of 10.95. Measurements of pH were also taken during the rainfall simulations. The initial pH of the simulation water was 8.01, while the stormwater runoff of the untreated loess had a slightly increased pH of 8.19 (compared to an initial pH for the

untreated loess of 7.10). This slight increase in the pH of the untreated loess is attributed to the pH of the recirculated simulation water used in this study. The average pH for the stormwater runoff of the 20% CGR-amended loess was 11.01, with a low pH of 10.22 and a high pH of 11.68. This showed that the average pH for the stormwater runoff from the CGR-amended loess soil forms after the rainfall simulations was close to the initial average pH of the CGR-amended soils prior to the rainfall simulations (discounting the slight increase in pH due to the simulation water).

6.4 Effects of CGR on Compaction Characteristics with Loess

The CGR-amended soils tested in this study were expected to be drier and possibly stiffer due to the water used up in the pozzolanic reaction of the CaO in the CGR during hydration. Amending the fine-grained loess with 20% CGR in this study resulted in only slight changes in OMC and MDD. The untreated loess had an initial OMC of 16.8% and an MDD of 105.6 lb/ft^3. The two different 20% CGR-amended loess mixtures had a comparable average OMC of 16.6% and an average MDD of 106.2.

6.5 Effects of CGR on Compaction Characteristics with Shoulder Materials

In comparison to the CGR-amended loess, mixing 20% and 40% CGR with the five different Class 1-A roadway shoulder aggregates produced more substantial changes in OMC and MDD. Untreated Washington County soils had an average OMC of 9.2% and an average MDD of 131.7 lb/ft^2, while untreated Clinton County soils had an average OMC of 7.5% and an average MDD of 133.7 lb/ft^2. Despite the approximate 2% difference between the average OMCs for the soils from these two counties, after blending these untreated aggregates with 20% CGR, the average OMC increased to 11.9% while the average MDD decreased to 122.2 lb/ft^2 across all five 20% CGR-treated shoulder soils. With 40% CGR, the average OMC further increased to 14.9% while the average MDD further decreased to 113.2 lb/ft^2 across all five 40% CGR-treated shoulder soils. Note that the maximum moisture content was the highest for 40% CGR-5-treated soils, with an averaging OMC of 16.1% and the lowest average MDD of 110.7 lb/ft^2. This difference is attributed to CGR-5, which was collected from a newer concrete road. It is hypothesized that the CaO content in CGR-5 was higher than in the other CGRs collected because the road was only recently completed at the time of grinding, producing CGR with a higher hydration potential.

In general, CGR had a much broader drying effect on the Class 1-A granular shoulder aggregates in comparison to the CGR-amended loess. This is attributed to the greater amount of air voids in the coarse-grained shoulder aggregates, which allows more water to infiltrate the soil blended with the fine-grained CGR material compared to the already fine-grained silty loess. The coarse-grained shoulder aggregates from Clinton County, although not formally tested for organic and clay content, exhibited a bit more initial cohesion compared to the Washington County soils. When handling and manipulating the untreated moist soils from Clinton County, these soils held together slightly better than the aggregate from Washington County when a small portion of the soil was rolled into a ball. However, the Clinton County soil did not hold together when trying to further roll the soil balls into cylinders. In comparison, the Washington County soils did not hold together when pressed by hand into balls.

76

CHAPTER 7 FIELD DEMONSTRATIONS

7.1 Washington County Site

The gravel shoulder area of the eastbound lane of County Road G-26 in Washington County was selected for a field demonstration of the soil stabilization potential of CGR. A concrete diamond grinder was used on this road to reduce the roughness of the concrete surface in the summer of 2020. The CGR material was collected from the concrete diamond grinder and used for shoulder stabilization on the same roadway. The routine field evaluation of the site included LWD and DCP tests. The details of field construction and the results of the evaluation are discussed in the following sections.

7.1.1 Site Information and Construction Plan

County Road G-26 has a 24 ft wide concrete pavement and 8 to 10 ft wide gravel shoulders on both sides. The location of the field demonstration site in Washington County, Iowa, is shown in Figure 48.
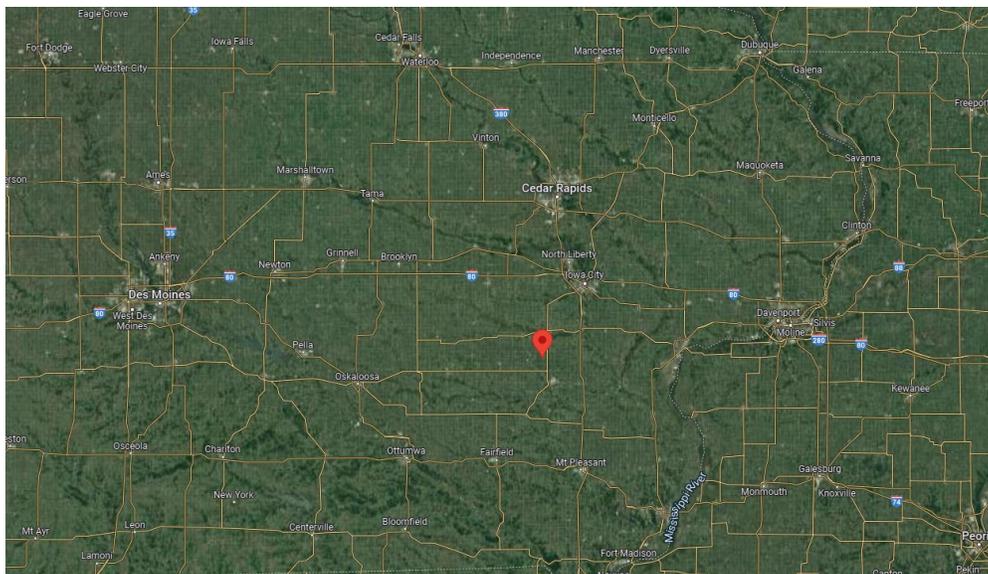
Image © Google Earth

Figure 48. Location of field demonstration site in Washington County

A total of four test sections were considered for the Washington County field demonstration site, including a Base One-treated section (Base One), a section in which CGR was mixed with shoulder material (CGR Reclaimed), a section that received CGR on its surface without reclamation (CGR Top), and a control section without treatment (Untreated). Base One is a proprietary liquid stabilizer invented by TEAM LAB Chemical Co. that has been commonly used for unbound pavement material stabilization in Iowa and Minnesota.

The four test sections were built in the shoulder area, and each section was 250 ft in length and 5 ft in width. Figure 49 shows the layout and dimensions of each section of the field demonstration site in Washington County.
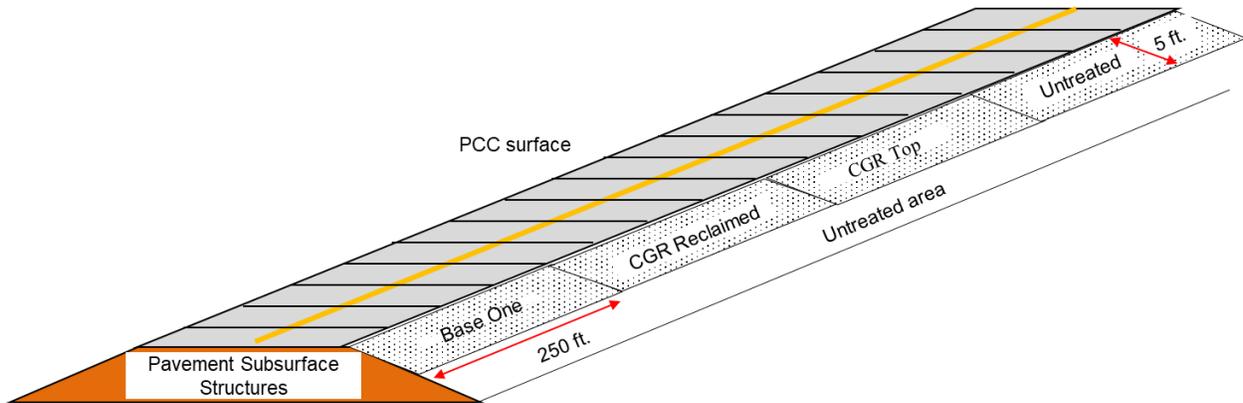
Figure 49. Schematic diagram of field demonstration site in Washington County

7.1.2 Construction Methods and Steps

The construction of the test sections began with a preliminary design plan describing the CGR application rate, CGR settling time, CGR and shoulder materials density, CGR collection and storage process, and construction steps. The preliminary design was discussed with the county engineers from Washington County and finalized. From laboratory tests conducted by Ceylan et al. (2019), it was determined that the CGR slurry should contain 68% solids with a moisture content of 46% by weight. Also, based on the findings from Yang et al. (2019b), 20% dry CGR by weight was determined as the optimum CGR application rate in terms of maximum strength improvement. Considering the settlement rate, solids-to-liquid ratio, and density of the CGR and the field moisture content of the shoulder materials, 3 tons of settled CGR were required for each of the test sections to achieve the target 20% CGR application rate. The maximum dry density, optimum moisture content, and field moisture content of the shoulder materials were estimated to be 123.6 lb/ft^3, 12.3%, and 4%, respectively.

The CGR produced during the diamond grinding operation was collected in 210 gal heavy-duty super bags placed within containments. The process of CGR collection from the concrete diamond grinding operation is shown in Figure 50.

Figure 50. CGR collection at diamond grinding project site in Washington County: (a) preparing the super bags with containment, (b) transporting the super bags to the diamond grinding site, (c) diamond grinding operations, (d) filling the super bags with CGR, (e) securing the bags, and (f) transporting the bags to the construction site

The collected CGR was stored in the bags for at least 3 hours to settle the particles. Once the CGR particles were settled, the clear water from the top of the bag was drained to obtain the settled CGR slurry. Figure 51 shows the dewatering process of the CGR slurry. According to the preliminary design, five bags of settled CGR slurry were required for each of the test sections to accumulate 3 tons of settled CGR. In each bag, the target settled CGR thickness was 15 in.
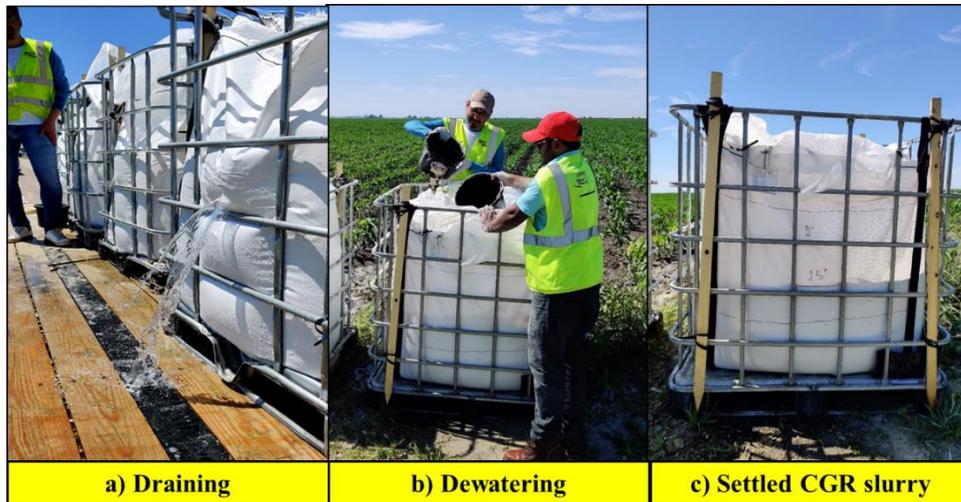
Figure 51. Dewatering process for CGR slurry at the demonstration site in Washington County: (a) draining water from bags, (b) manual dewatering, and (c) settled CGR slurry

For the CGR Reclaimed section, the required amount of CGR was mixed with the top 3 in. of the existing shoulder materials. For the CGR Top shoulder section, the settled CGR was poured onto the shoulder materials and uniformly distributed to a target CGR thickness of 0.5 in. Finally, a section of the pavement shoulder was treated (top 3 in.) with Base One for comparison purposes. The construction steps for each of the prepared sections are explained below.

CGR Reclaimed Section

- Construction occurred on June 8, 2020.
- A 5 ft area of the shoulder was reclaimed using a RoadHog, and the section was leveled using a motor grader.
- A forklift was used to apply CGR from the bags. Initially, the bags were filled to a height of 32 in., and the settled CGR heights in the bags were 20 in., 15 in., 18 in., 18 in., and 15 in. (with a target of 15 in.).
- The CGR was distributed using a motor grader, and the CGR was mixed with the shoulder gravel using road milling equipment (RoadHog).
- Again, a motor grader was used to level the surface.
- The section was compacted using a rubber tire compactor with nine passes.
- Figure 52 illustrates the detailed construction steps for the CGR Reclaimed section.

Figure 52. Construction of CGR Reclaimed section in Washington County: (a) placing CGR bags at the designated distance, (b) dumping CGR, (c) reclaiming soil with CGR using a RoadHog, (d) distributing CGR by blading, (e) leveling the surface, (f) compaction, and (g) completed CGR Reclaimed section

CGR Top Section

- Construction occurred on June 8, 2020.

- The section was leveled using a motor grader with two passes.
- A windrow at the side of the test section was made using a motor grader to avoid the loss of CGR outside the section width.
- CGR from the super bags was applied to the section using a forklift. The settled CGR heights in the bags were 15 in., 15 in., 13 in., 13 in., and 15 in. (with a target of 15 in.). Initially, the bags were filled to a height of 28 in.
- The CGR was distributed using a motor grader.
- Surface materials were added on top of the CGR using a motor grader.
- The section was compacted using the rubber tire of a motor grader in three passes.
- Figure 53 shows the detailed construction steps for the CGR Top section.

Figure 53. Construction of CGR Top section in Washington County: (a) creating windrow, (b) dumping CGR, (c) mixing and blading CGR, and (d) completed CGR Top section

Base One Section

- Construction occurred on June 4, 2020.
- A RoadHog was used to reclaim the existing surface up to a 3 in. depth.
- Base One was applied using six sprinklers with an application rate of 0.005 gal/yd^2/in. A total of 100 gal of Base One was applied for the stabilization of the section.
- The section was sprayed with water to bring it to optimum moisture content.

- Again, a RoadHog was used to mix the stabilizer with the shoulder material.
- The edge and surface were leveled using a motor grader.
- The section was compacted using a rubber tire compactor with a total of nine passes.

7.1.3 Field Data Collection and Results

LWD and DCP tests were performed to evaluate the efficacy of using CGR in shoulder stabilization. The data were collected and reported at four different time periods that included before construction and seven days, one year, and two years after construction. Figure 54 shows the appearance of the Washington County site two years after construction, as well as the LWD and DCP field evaluation tests. From the appearance of the surface conditions, it was observed that the treated sections had a lower loss of aggregate than the untreated section.

Figure 54. Washington County site appearance after two years: (a) Base One-treated section, (b) CGR Reclaimed section, (c) CGR Top section, (d) untreated section, (e) LWD testing, and (f) DCP testing

The LWD and DCP tests were performed at three points in each section at intervals of 50 ft.

The Zorn 3000 LWD device used in this study features a 22 lb hammer with a drop height of 28.5 in. and a base plate diameter of 11.81 in. Since the zone of influence of an LWD is 1.5 to 2 times the diameter of the LWD plate, the elastic modulus determined by the LWD in these tests is considered to be the composite elastic modulus of both the surface and subgrade layers. Figure 54e shows the LWD test setup used in this study. The composite elastic modulus values of the pavement shoulder sections were calculated using the following equation (Schwartz et al. 2017):

$$E_{LWD} = \frac{(1-\vartheta^2)\sigma_0 A f}{d_0}$$ (2)

where E_{LWD} is elastic modulus as calculated from the LWD tests, σ_0 is the vertical stress applied on top of the LWD plate, ϑ is Poisson's ratio (assumed as 0.4), d_0 is the diameter of the plate, A is the stress distribution factor (assumed value of $3\pi/4$), and f is the shape factor (assumed to be two for a uniform stress distribution).

Figure 55 shows the composite elastic modulus values of the constructed test sections determined from the LWD test results.
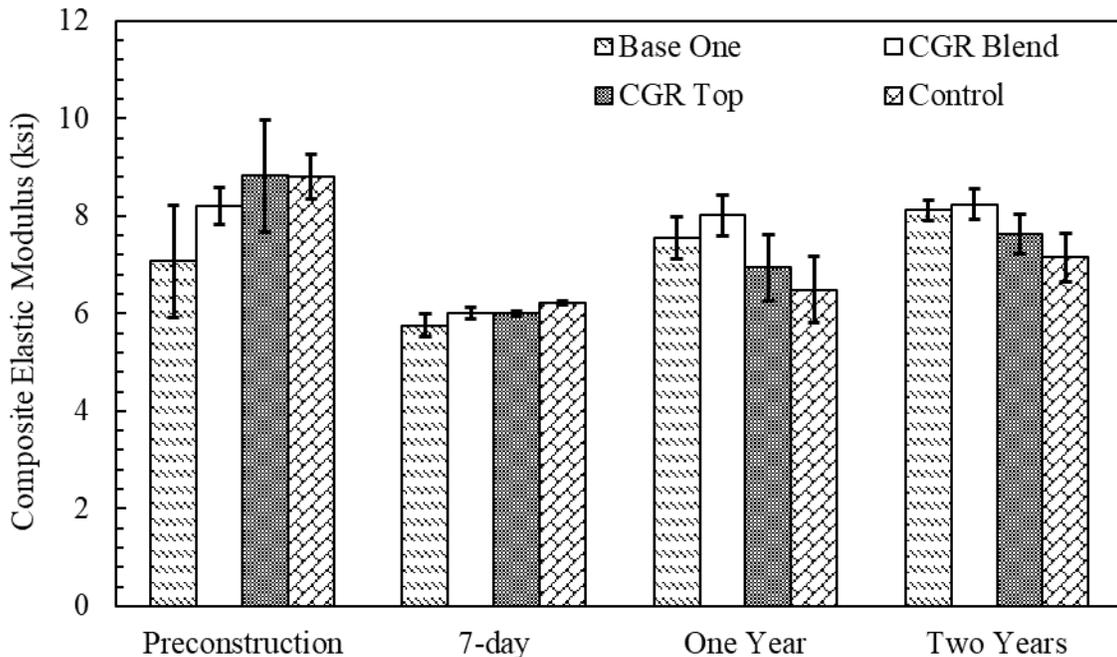
Figure 55. LWD results at demonstration site in Washington County

The highest elastic modulus values were found during the preconstruction test for all sections except the Base One section. Compared to these initial values, the composite elastic modulus values of the test sections were found to be lower during the test conducted seven days after construction. Similar observations were also made for the control section. It was concluded that

the differences in the elastic modulus values between these two tests resulted from higher moisture contents during the second test. The preconstruction test was performed in May 2020. The construction of the test sections was completed in June 2020. The test performed seven days after construction was conducted on June 16, 2020. It was concluded that the higher rainfall observed in the month of June increased the subgrade moisture content, which eventually decreased the composite elastic modulus values of the test sections seven days after construction.

One and two years after construction, the composite elastic modulus values for all sections increased. The average composite elastic modulus of the Base One section was found to be lower in the preconstruction test than in later tests, with higher variations in measurements (shown in error bars). Between the test conducted seven days after construction and the tests conducted one and two years after construction, the elastic modulus values of all sections increased noticeably. The rates of increase in the composite elastic modulus values were similar for all sections. In addition, significant differences in the modulus values of the test sections were observed between the tests conducted seven days after construction and one year after construction. But the differences in elastic modulus between the tests conducted one year and two years after construction were not significant.

From these results, it can be concluded that the CGR Reclaimed section exhibited improved performance compared to the control section. Moreover, the CGR Top section showed slightly higher composite elastic modulus values compared to those measured for the control section. However, as indicated by the standard deviations, these increases were not significant. In addition, the CGR Reclaimed section provided a very similar modulus to that of the Base One-treated section.

The DCP tests were performed following the standard designated by ASTM D6951. DCP testing was performed to determine the CBR and thickness of the shoulder materials. A DCP cone with a 0.79 in. base diameter was used to penetrate the pavement layers up to a depth of 24 in. The hammer used for the DCP test weighed 7.6 lb. Figure 54f shows the DCP test process performed at three different locations in each test section.

The DCP results were used to calculate the DCP index (DCPI) as the penetrations per blow for each of the test points. Using the DCPI as the rate of penetration and empirical correlations based on the ASTM D6951 standard, the CBR values for each layer were calculated. The empirical equations used for the calculation of CBR were as follows:

$$CBR = \frac{292}{DCPI^{1.12}} \tag{3}$$

when the calculated CBR is higher than 10.

$$CBR = \frac{1}{(0.017019 \times DCPI)^2} \tag{4}$$

when the calculated CBR is lower than 10.

Figure 56 shows the average CBR values obtained from the DCP tests conducted at different times, including before construction of the test sections and one week, one year, and two years after construction. Note that each plot presents the average CBR values of three test points in each section.
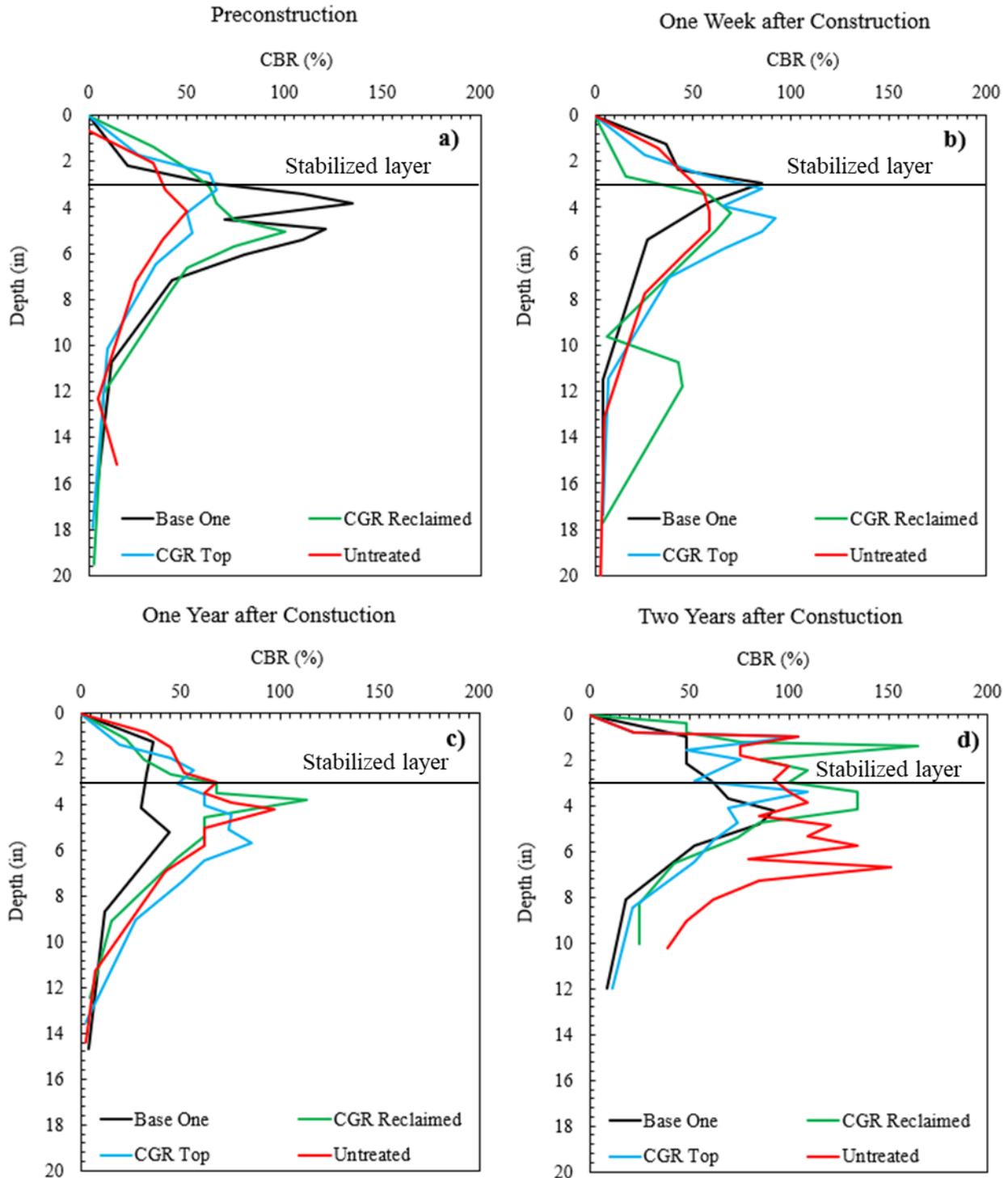

Figure 56. DCP results at demonstration site in Washington County

The CBR values gradually increased with an increase in penetration depth. At depths between 3 in. and 6 in., higher CBR values were measured. It was anticipated that the compacted pavement base layer would increase the CBR values in this zone. As the base layer was passed, the CBR values subsequently decreased with an increase in depth.

This study focused on the CBR values calculated to a depth of 3 in. (within the stabilized layer), since the use of CGR was restricted to this zone. As illustrated in Figure 56a, the CBR values before construction were similar among the different test sections. The CBR values one week after construction, shown in Figure 56b, were lower than those measured during the preconstruction period for all sections; this finding could be explained by the rainfall observed in the month of June, which reduced the strength of the stabilized layer. One week after construction, the surface treatments did not show significant improvement in CBR values compared to the untreated section. Figure 56c and Figure 56d indicate that a similar outcome was found one year and two years after construction, with no significant improvement in the CBR values of the treated layers compared to those of the untreated section. However, the CGR Reclaimed section exhibited slightly higher CBR values compared to the untreated section. The difference in CBR values between the CGR Reclaimed and Base One-treated sections was significant, with higher CBR values obtained for the CGR Reclaimed section.

7.2 Clinton County Site

Another field demonstration site was constructed in Clinton County, the easternmost point in the state of Iowa, near the Mississippi river. Similar to the Washington County site, this field demonstration site was constructed in May 2021 to explore the benefit of using CGR as a stabilizer for unbound pavement material. The routine field evaluation of the site included LWD and DCP tests, and the surface condition of the test sections was documented over time to assess the sections' field performance. The following sections provide detailed information on the construction of the field demonstration site and the results of the field evaluation.

7.2.1 Site Information and Construction Plan

County Road Z-24 in Clinton County, Iowa, was selected for the field demonstration site. Figure 57 shows the location of the test sections. County Road Z-24 is a two-way, two-lane concrete road with a 22 ft wide pavement and 8 to 10 ft wide gravel shoulders on both sides. The test sections were constructed in the shoulder on one side of the road.
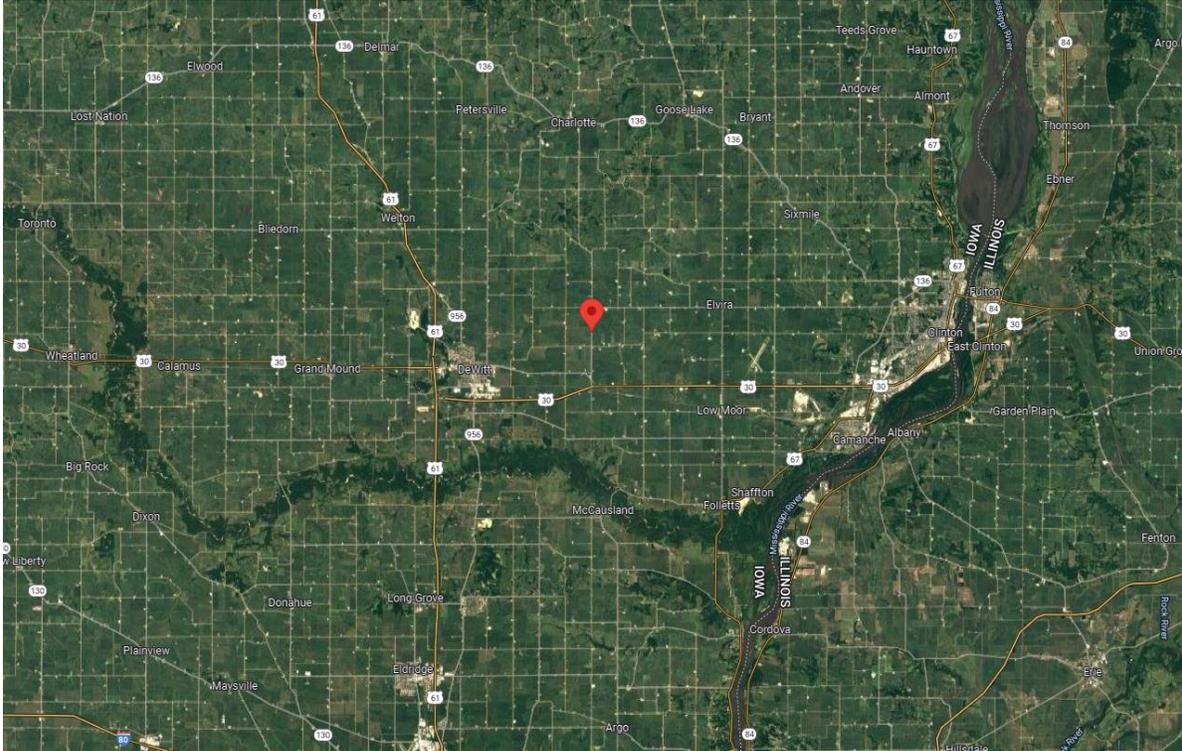
© 2022 Google

Figure 57. Location of field demonstration site in Clinton County

Figure 58 illustrates the schematic of the field demonstration site, with the detailed dimensions of each test section. The field demonstration site in Clinton County consisted of four test sections similar to those constructed in Washington County, including a Base One-treated section (Base One), a section in which CGR was mixed with shoulder material (CGR Reclaimed), a section that received CGR on its surface without reclamation (CGR Top), and an untreated control section (Untreated). Each section was 250 ft in length and 5 ft in width, and a 50 ft gap between sections was provided to avoid overlap between the sections during construction. The shoulder located on the other side of the road from the treated sections was considered an untreated section for field performance evaluation.
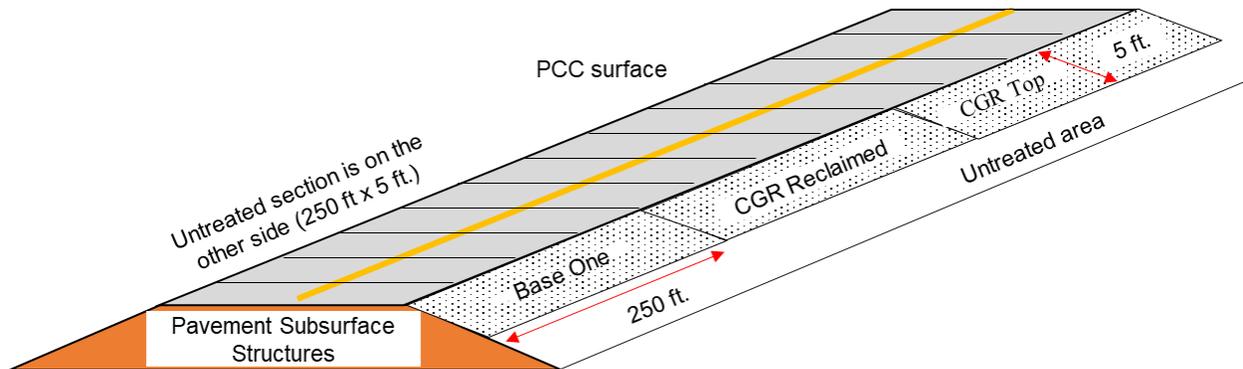
Figure 58. Schematic diagram of field demonstration site in Clinton County

7.2.2 Construction Methods and Steps

For the field demonstration site in Clinton County, a construction method similar to that used in Washington County was adapted to build the test sections. The amount of CGR required for the sections was determined after finalizing the application rate, settlement rate, solids-to-liquid ratio, and density of the CGR and the field moisture content of the shoulder materials. A 20% CGR application rate was selected as the optimum application rate based on a laboratory investigation by Yang et al. (2019b). The maximum dry density and optimum moisture content of the shoulder materials alone were determined to be 133 lb/ft^3 and 8%, respectively. The estimated maximum dry density and optimum moisture content of shoulder materials mixed with 20% CGR were estimated to be 130 lb/ft^3 and 9.2%, respectively, for the field construction.

The CGR was collected from a nearby diamond grinding operation on County Road Y-46, approximately 8 miles away from the field demonstration site. The CGR material was collected in 210 gal heavy-duty super bags to a height of 28 in. Figure 59 illustrates the CGR collection process from the concrete diamond grinding operation in Clinton County.

Figure 59. CGR collection at diamond grinding project site in Clinton County: (a) preparing the super bags with containment, (b) diamond grinding operations, (c) filling the super bags with CGR, and (d) dewatering the CGR bags

The CGR collected in the heavy-duty super bags was allowed to settle for 3 hours, and the water from the top of the bags was drained manually before the CGR was applied to the CGR-stabilized sections. The height of the settled CGR in each bag was determined to be approximately 15 in. A total of five bags of settled CGR were used for each of the CGR Reclaimed and CGR Top sections, and the estimated total weight of the CGR was 3 tons for each section. The steps for constructing the CGR Reclaimed, CGR Top, and Base One-treated sections in Clinton County were similar to the steps used in Washington County. The CGR material was poured on top of the shoulder material for the CGR Top section, while CGR Reclaimed and Base One-treated sections were reclaimed up to 2.5 in. and mixed with CGR and Base One, respectively. The detailed construction steps are explained below.

Base One Section

- Construction occurred on May 25, 2021.
- A RoadHog was used to reclaim the existing surface up to a 2.5 in. depth.
- A total of 100 gal of Base One and 250 gal of water were applied for the stabilization of the section. Base One was applied using six sprinklers with an application rate of 0.005 $gal/yd^2/in$.
- Again, a RoadHog was used to mix the stabilizer with the shoulder material.
- The edge and surface were leveled using a motor grader.
- A total of 18 passes of a rubber tire compactor were used to achieve the target density of the Base One section.

CGR Reclaimed Section

- Construction occurred on May 25, 2021.
- The shoulder was leveled to a 5 ft width using a motor grader before CGR application.
- The CRG bags were brought to the section using a forklift, and the CGR was spread throughout the section. Initially, the bags were filled to 28 in., and the settled CGR height in the bags was approximately 15 in.
- The CGR was distributed using a motor grader.
- A RoadHog was used to reclaim the existing surface up to a 2.5 in. depth, and the CGR was mixed with the shoulder gravel.
- The surface was leveled using a motor grader.
- A rubber tire compactor was used to provide adequate compaction with a total of 18 passes.
- Figure 60 shows the step-by-step construction process for the CGR Reclaimed section.

Figure 60. Construction of CGR Reclaimed section in Clinton County: (a) leveling site before CGR application, (b) dumping CGR, (c) reclaiming soil with CGR using a RoadHog, (d) distributing CGR by blading, (e) rolling compaction, and (f) completed CGR Reclaimed section

CGR Top Section

- Construction occurred on May 26, 2021.
- A motor grader was used to make a windrow at the edge of the section to avoid the loss of CGR outside the section width.
- A total of five bags of settled CRG was poured on top of the section using a forklift.
- The CGR was uniformly distributed using a motor grader.
- Surface materials were added on top of the CGR using a motor grader, and the top surface was leveled.

- No additional compaction using a rubber tire roller was applied apart from the compaction provided by the motor grader tires.
- The steps for constructing the CGR Top section are illustrated in Figure 61.

Figure 61. Construction of CGR Top section in Clinton County: (a) section appearance before CGR application, (b) creating windrow, (c) dumping CGR, (d) section appearance after CGR application, (e) blading CGR Top section, and (d) completed CGR Top section

7.2.3 Field Data Collection and Results

The efficacy of using CGR for pavement shoulder material stabilization at the Clinton County site was evaluated by conducting LWD and DCP tests along with a visual survey of the surface conditions. Figure 62 shows the surface conditions of the field demonstration site in Clinton County one year after construction. From the appearance of the surface conditions, it was observed that the stabilized sections had a lower loss of aggregate than the untreated section.

CGR stabilization is hypothesized to reduce the aggregate loss from the shoulder of the road due to the wind generated by high-speed truck traffic.
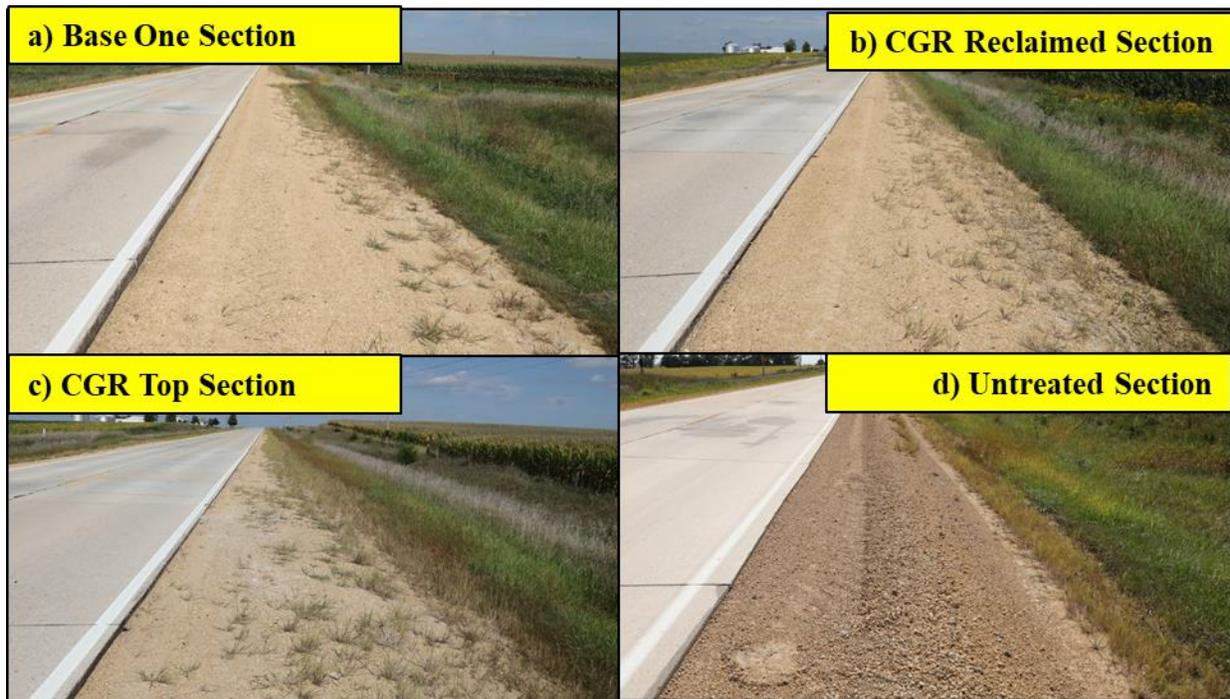
Figure 62. Clinton County site appearance after one year: (a) Base One-treated section, (b) CGR Reclaimed section, (c) CGR Top section, and (d) untreated section

The LWD and DCP tests were conducted at three test points in each section to measure the composite elastic modulus and CBR values of the test sections, respectively.

The same LWD device with the same configuration was used for the evaluations of both the Washington County and Clinton County field demonstration sites. The LWD tests were conducted before the construction of the test section and one week, six months, and one year after construction to document the field performance of the treatments at different times. The composite elastic modulus values of the test sections were estimated using Equation (2). Figure 63 documents the average LWD test results for each section from the Clinton County demonstration site.
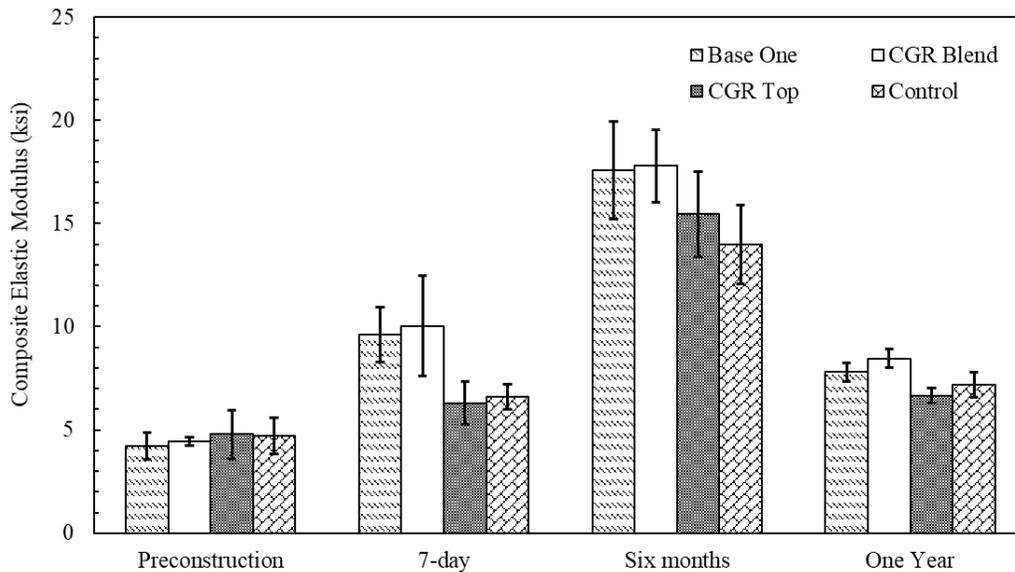
Figure 63. LWD results at demonstration site in Clinton County

The LWD test conducted one week after construction shows similar composite elastic modulus values for each section, with the highest variation observed in the CGR Top section. The composite elastic modulus values of the CGR Reclaimed, CGR Top, and Base One sections increased over time compared to the control section. Improved strength was obtained for the treated sections because of the stabilization of the surface layer provided by the CGR mix and the Base One additive. The composite elastic modulus values measured six months after construction were significantly higher than the values measured at other times because of the frozen condition at the site during this test. The tests performed six months after construction were conducted in December 2021, when the surface temperature was documented to be 21°F. The frozen soil layer resulted in higher composite elastic modulus values for all sections. The CGR Reclaimed section demonstrated a 20% to 40% improvement in composite elastic modulus compared to the control section.

The DCP tests were conducted at the same time as the LWD tests, and measurements were taken at three test points located 50 ft apart within each section. Equations (3) and (4) were used to estimate the CBR values from the DCP test results. Figure 64 indicates the average CBR values for all test sections during all four testing periods, including before construction and one week, six months, and one year after construction.
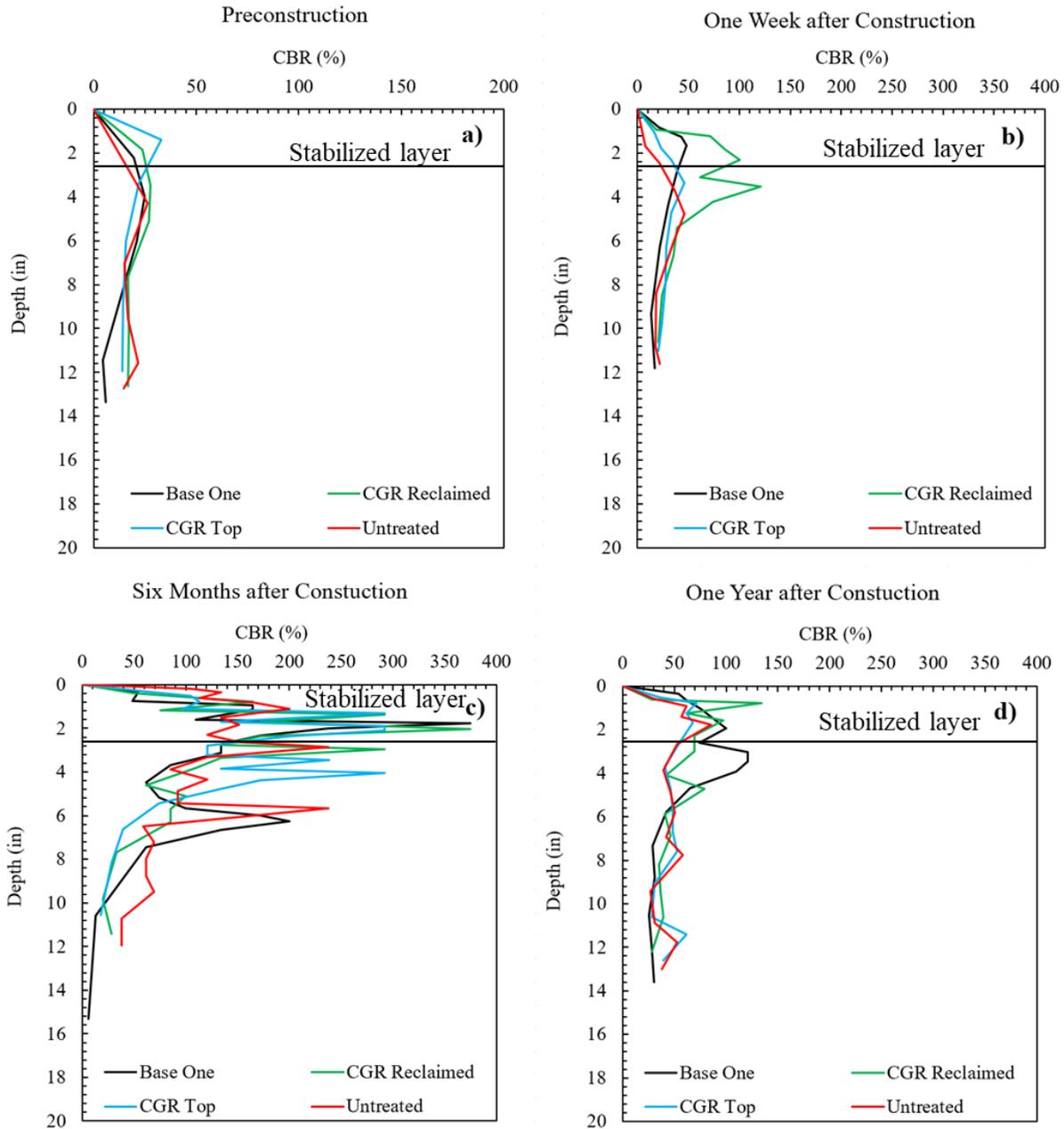
Figure 64. DCP results at demonstration site in Clinton County

The average CBR values measured one week after construction did not show significant variability among the sections; however, slightly lower CBR values were documented for the control section. At one week and one year after construction, the CBR values of the Base One-treated and CGR Reclaimed sections were higher than those of the control section, which can be attributed to the beneficial use of CGR and Base One in shoulder stabilization. The CGR Reclaimed section may also have gained strength with curing time due to the hydration of the remaining cementitious compounds in the CGR. In addition, the CGR Reclaimed section demonstrated better performance compared to the Base One-treated section. However, the CBR

values measured six months after construction were mainly influenced by the frozen condition of the site at this time.

7.3 Summary

Two field demonstration sites were selected to assess the benefits of using CGR in pavement shoulder stabilization. One site was located in Washington County and the other was located in Clinton County, Iowa. Four test sections were built at both sites, including a Base One-treated section, a CGR Reclaimed section, a CGR Top section, and an untreated section. The CGR Reclaimed and CGR Top sections demonstrated two different methods of CGR application. The CGR Reclaimed section was constructed by mixing the CGR with the top 3 in. of shoulder material, whereas the CGR Top section was built by pouring the CGR on the top of the shoulder. The Base One-treated section was selected to compare the stabilization performance of the CGR with that of a commercial additive.

LWD and DCP tests were performed at both sites to evaluate the field performance of the test sections. The LWD and DCP test results in Washington County indicate that the application of CGR to the pavement shoulder material did not improve the performance significantly. However, the CGR Reclaimed section in Clinton County demonstrated a 20% to 40% improvement in strength compared to the untreated section. In addition, the CGR Reclaimed section in Clinton County exhibited higher stiffness compared to the Base One-treated section.

CHAPTER 8 CONCLUSIONS

Utilizing waste materials to help stabilize problematic soils is a creative and sustainable idea. One abundant waste material is CGR slurry, which is produced in large quantities on concrete diamond grinding (roadway) projects in the United States. In lieu of recycling, the two primary means of disposal are discharge of the CGR slurry directly onto adjacent roadway shoulders or collection and transport to local sedimentation pits or local landfills.

It seems unusual to still see CGR discarded, since CGR is merely concrete fines with a high lime content, while it is also classified as a nonhazardous waste product by EPA standards (provided the pH is less than 12.0). CGR has been collected and tested in numerous studies, and its mineral composition and chemical properties are well known. More importantly, several major studies have concluded that CGR does not have long-term effects on soil chemistry, soil infiltration, or vegetation growth or any detrimental effects on fish and the environment (Ceylan et al. 2019, Yang et al. 2019b, Luo et al. 2019); however, the recycling uses for CGR still remain largely unexplored.

In this research, two distinct laboratory erosion studies, one using wind and one using rain, were performed to observe CGR-amended soil and determine the effect of CGR amendment on erosion. Supporting laboratory tests performed on both untreated (control) soils and CGR-amended soils included sieve analysis (gradation), moisture content analysis, standard Proctor testing, pH measurement, turbidity measurement, and the measurement of eroded soil loss.

In addition, two field demonstration sites were constructed in Iowa to determine the benefit of using CGR as a stabilizer for pavement shoulder materials. Two different CGR stabilization techniques were evaluated: (1) mixing CGR with shoulder material (CGR Reclaimed sections) and (2) pouring CGR on top of shoulder material (CGR Top sections). The performance of the CGR-stabilized sections was compared with that of an untreated section and a section treated with a proprietary additive.

The key findings from both the rain and wind erosion studies and the field demonstrations are as follows:

- The pH for the untreated loess was 7.10. A close range of pH values was found for the five CGRs collected, with a low pH of 11.13 and high pH of 11.83. Similarly, the average pH for the 20% CGR-amended loess ranged from a low pH of 9.59 to a high pH of 10.95.

- The initial pH of the rainfall simulation water was 8.01, which is presumed responsible for the slight increase in pH of the stormwater runoff from the untreated loess (8.19). The average pH for the stormwater runoff from the 20% CGR-amended loess ranged from a low pH of 10.22 to a high pH of 11.68 across the six CGR-amended soil forms tested.

- The water quality of the 20% CGR-amended loess was much poorer compared to that of the untreated loess grab samples collected. The average turbidity values ranged from as low as

1.8 to as high as 4.7 times higher (worse) across all 120 water quality grab samples collected from the 20% CGR-amended loess rainfall simulations. This translates to an average of 410% poorer water quality for the grab samples collected from the CGR-amended loess trials compared to the samples collected from the untreated loess. The water quality was the poorest during the middle third of the test (during the 4 in./hour storm) for all trials of the 20% CGR-amended loess. During this storm, the water quality averaged 530% worse for the CGR-amended soils tested.

- With respect to the rain-eroded soil collected and weighed after the rainfall simulations, the 20% CGR-amended loess eroded substantially more than the untreated loess during the 60-minute rainfall trials. Soil loss (erosivity) measurements showed an average soil loss of -520% for the CGR-amended soil compared to the untreated loess soil. This translates to an average of -17.30 tons/acre for the CGR-amended soil compared to -4.62 tons/acre for the untreated loess control soil. Soil loss increased from the 2 in./hour storm to the 4 in./hour storm but decreased from the 4 in./hour to 6 in./hour storm.

- Loess compacted on the dry side of optimum (-5.3% OMC) rain eroded -216% more than loess compacted at OMC (-9.97 tons/acre of soil loss for soil compacted on the dry side of optimum compared to -4.62 tons/acre of soil loss for soil compacted at OMC).

- With respect to the wind erosion results, for all of the soil blends tested, the untreated Site A Control soil resulted in the highest erosion rate at -8.07 tons/mile. However, for the wind erosion results for the two similar untreated soils from Washington County (Site B and Site C), the wind erosion rates were substantially lower at -3.72 and -6.52 tons/mile, respectively.

- Amending the Washington County shoulder aggregate with CGR decreased the wind erosivity of the soil. Wind erosion decreased 25% and 58% for shoulder aggregates amended with 20% and 40% CGR, respectively, compared to untreated soils. Conversely, amending the Clinton County shoulder aggregate with CGR increased the wind erosivity of the soil. Wind erosion increased 25% and 50% for shoulder aggregates amended with 20% and 40% CGR, respectively, compared to untreated soils.

- Adding 20% CGR to western Iowa loess only slightly reduced the wind erosivity of the soil. Additionally, the wind erosion rate of untreated loess mirrored the wind erosion rates of Class 1-A untreated shoulder aggregates from Clinton County.

- The field demonstration in Washington County showed that CGR stabilization did not improve the performance of the shoulder material significantly. However, a slight improvement in strength was observed for the CGR Reclaimed section. Conversely, the CGR Reclaimed section in Clinton County demonstrated a 20% to 40% improvement in terms of composite elastic modulus and CBR values. Moreover, the performance of the CGR Top sections suggests that pouring CGR on top of shoulder materials without mixing may not be an effective stabilization technique. Blending the CGR with the shoulder material appears to be the more effective stabilization technique for field application.

CHAPTER 9 RECOMMENDATIONS AND LIMITATIONS

9.1 Recommendations

A key goal of any geotechnical research study is to maximize the number of soils and soil mixtures being tested in order to maximize the amount of data available for analysis. Recommendations for future rain erosion tests would include the testing of additional Iowa soils (e.g., glacial till and alluvium) with 20% CGR dosages (as well as other CGR dosages). This would more conclusively determine whether the rain erodibility trends found would continue for other CGR-amended soils.

With respect to the rainfall simulator, enhancements to the existing simulator (e.g., increasing the number of nozzles from 9 to 12) would increase the rainfall footprint within the simulator. Additionally, changing the style of simulator from a Purdue-type simulator to a simulator style that produces uniform 3 mm gravity-driven raindrops could produce raindrops of more uniform size and distribution within the rainfall simulation room.

Although redundancy is good for test trials, with respect to future rainfall testing, the testing of a single test form of a particular soil blend (in lieu of testing three soil forms per rainfall trial) would allow more soils and more soil blends to be tested initially. This would also significantly save on the extra compaction effort required to produce three soil forms with the same soil for each test. Regarding the compaction of the soil forms, changing from a single lift to three lifts of 1½ in. of soil using the UTA compaction equipment could dramatically reduce the number of compaction tamps required per soil form, which in turn would reduce the wear and tear on the UTA. Lifting of the 350 lb compacted soil forms required the brute strength of three people. Installing a wall-mounted arm and winch to lift and set the compacted soil forms would provide a safer and more efficient way to lift the soil forms on the racks for testing.

Another recommendation for future testing is to adjust specimen curing time. The limited 24-hour curing time chosen for the rainfall erosion study (which was chosen due to time constraints) reduced the reaction time for the CGR to gain stability and strength with the CGR-amended loess soils tested. A seven-day curing time following compaction is recommended for future trials. Loess was selected for this study because of its fine particle size, low plasticity, abundance in Iowa, and the poor drainage and strength characteristics (generally) associated with silts and loams, which in turn makes loess a problematic soil for use in roadside embankments. However, utilizing the same Iowa soils used in previous CGR studies would allow for more direct correlation of the results with these other studies. Complementing these additional soils with extended curing times could lead to promising uses for CGR as a soil stabilizing amendment.

With respect to the duration of each rainfall simulation, extending each simulation beyond the 60-minute limit would be helpful in determining whether any leveling-off trends would continue or change for some soil types. Having the flexibility and extra equipment to collect additional samples is recommended.

Finally, rainfall simulations using other sustainable soil amendments such as corncob ash, rice husk ash, and bamboo ash (and/or CGR-amended soils with these materials) could be performed to determine whether the pozzolanic characteristics in these materials might serve as a catalyst for improving the cohesive properties of loess and other Iowa soils.

Recommendations for future wind erosion testing with CGR-amended soils would include testing the three remaining soils (Sites B, C, and D) with CGR as well as testing the western Iowa loess with a 40% CGR dosage. This would better confirm the wind erosion behavior of the soils collected for each county road sampled. Extending wind erosion testing to additional Iowa soils (e.g., glacial till and alluvium) with both 20% and 40% CGR dosages could more definitively determine wind erosion trends between different types of soils.

With respect to future research recommendations, increasing the velocity of the wind source to more closely match the posted speed limits (45 and 55 mph) found on roads where CGR treatments are likely to be applied would increase the degree of wind erosion produced with each soil mixture sampled. Additionally, if a lateral (perpendicular) secondary wind source were also added to the test, this could more closely produce the desired swirling "wind whip" air flow that was the targeted wind effect for this study. Finally, as in the recommendations made for future rainfall studies, wind erosion testing using other sustainable soil amendments such as corncob ash, rice husk ash, and bamboo ash (and/or CGR-amended soils blended with these materials) could create future recycling uses for these waste materials while improving the cohesive characteristics of loess and cohesionless Class A-1 roadway aggregates.

While the CGR-treated field sites in Clinton County exhibited the expected strength improvements, the field test results in Washington County did not indicate similar improvements. It is therefore highly recommended to build more field sites (a total of at least five field demonstration sites) to better assess the benefit of using CGR for shoulder stabilization. Another recommendation for future field evaluations would be to assess the material loss resulting from the wind effect of high-speed traffic and the leaching of the CGR from the shoulder material due to rainfall-related infiltration of water.

Based on the findings of the field demonstrations, another recommendation for future study is to use CGR as a stabilizing agent in the base and subbase layers of paved roads and in the gravel layer of unpaved gravel roads. CGR stabilization could provide improved stiffness and less traffic-induced deformation, thereby extending the service life of paved roads and unpaved gravel roads.

9.2 Limitations

Limitations on the laboratory portion of this project included both material and time constraints. The rain erosion study included the testing of only one soil type (western Iowa loess). Rainfall testing also only included a single dosage of CGR (20%) with only two of the five CGRs collected. The wind erosion study did extend testing to five shoulder aggregate soils, but due to time constraints only two soils (Site A and Site E) were tested at two CGR dosages (20% and 40%) with two of the five CGRs collected (CGR-4 and CGR-5). Additionally, the 2020–2021

pandemic severely limited access to laboratory facilities for the safety of students and faculty on this project.

A source of bias on the project was the selection of western Iowa loess for the initial testing. Other Iowa soils would have been good candidates for testing in this project, but loess was favored due to its abundance and ease of collection.

The main limitation of the field study was the limited number of field demonstration sites. Additionally, the field study only assessed the use of CGR for shoulder stabilization and did not assess the use of CGR for stabilizing the base, subbase, and subgrade soils of paved and unpaved roads. Finally, the performance of the CGR-stabilized sites was only monitored for one to two years, while monitoring the sites' performance for a minimum of five years would be expected to better capture the long-term benefits of using CGR for soil stabilization in the field.

REFERENCES

AC Business Media, LLC. 2013. Canada's Sixth Busiest Airport Becomes Country's First Major Airport to Groove Runway Pavement. *For Construction Pros.com*.

AMS. 2021. Raindrop. *Glossary of Meteorology*. American Meteorological Society.

ARA, Inc., ERES Consultants Division. 2004. *NCHRP 1-37A: Guide for Mechanistic-Empirical Design of New and Rehabilitated Pavement Structures*. National Cooperative Highway Research Program, Washington, DC.

ASCE. 2021. *First Concrete Pavement*. American Society of Civil Engineers, Reston, VA.

Argabright, S. M. 1991. Evolution in Use and Development of the Wind Erosion Equation. *Journal of Soil and Water Conservation*, Vol. 46, No. 2, pp. 104–105.

Asphalt Institute. 2003. *Thickness Design: Highways and Streets Manual Series, No. 1*. Asphalt Institute, Lexington, KY.

Benik, S. R., B. N. Wilson, D. D. Biesboer, D. Hansen, and D. Stenlund. 2003. Performance of Erosion Control Products on a Highway Embankment. *Transactions of the American Society of Agricultural and Biological Engineers (ASAE),* Vol. 46, No. 4, pp. 1113–1119.

Berendzen, P. B., R. M. Cruse, L. L. Jackson, R. Mulqueen, C. F. Mutel, D. Osterberg, N. P. Rogovska, J. L. Schnoor, D. Swenson, E. S. Takle, and P. S. Thorne. 2011. *Climate Change Impacts on Iowa 2010: Report to the Governor and the Iowa General Assembly*. Iowa Climate Change Impacts Committee, Leopold Center for Sustainable Agriculture, Iowa State University, Ames, IA.

BCPA. 2020. Roads: Roads Get Grinding and Grooving. *Britpave News*, No. 21, pg. 4, The British Cementitious Paving Association.

Bruce, M. E. C., R. R. Berg, J. G. Collin, G. M. Filz, M. Terashi, and D. S. Yang. 2013. *Design Manual: Deep Mixing for Embankment and Foundation Support*. FHWA-HRT-13-046. Federal Highway Administration, Turner-Fairbank Highway Research Center, McLean, VA.

Brusseau, M. L. 2019. Chapter 32. Sustainable Development and Other Solutions to Pollution and Global Change. *Environmental and Pollution Science*. Third edition. Academic Press, Cambridge, MA, pp. 585–603.

BTS. 2019. *National Transportation Statistics - Public Road and Street Mileage in the United States by Type of Surface*. Bureau of Transportation Statistics, Washington, DC. https://www.bts.gov/content/public-road-and-street-mileage-united-states-type-surfacea.

Bollinger, P. E. B., B. Cetin, H. Ceylan, and M. A. Perez. 2021. *Use of Concrete Grinding Residue as a Soil Amendment-Part II*. Recycled Materials Resource Center, University of Wisconsin-Madison, Madison, WI.

Cetin, B., A. H. Aydilek, and Y. Guney. 2010. Stabilization of Recycled Base Materials with High Carbon Fly Ash. *Resources, Conservation, and Recycling*, Vol. 54, No. 11, pp. 878–892.

Cetin, B., A. H. Aydilek, and L. Li. 2012. Experimental and Numerical Analysis of Metal Leaching from Fly Ash-Amended Highway Bases. *Waste Management*, Vol. 32, pp. 965–978.

Ceylan, H., K. Gopalakrishnan, S. Kim, and R. F. Steffes. 2013. *Evaluating Roadway Subsurface Drainage Practices*. Institute for Transportation, Iowa State University, Ames, IA. https://intrans.iastate.edu/app/uploads/2018/03/roadway_subsurface_drainage_practices_w_cvr-1.pdf.

Ceylan, H., Y. Zhang, B. Cetin, S. Kim, B. Yang, C. Luo, R. Horton, and K. Gopalakrishnan. 2019. *Concrete Grinding Residue: Its Effect on Roadside Vegetation and Soil Properties*. Minnesota Department of Transportation, St. Paul, MN.

Chepil, W. S. 1958. *Soil Conditions That Influence Wind Erosion*. Technical Bulletin No. 1185. USDA Agricultural Research Service, Washington, DC.

Chesner, W. H., R. J. Collins, and M. H. MacKay. 1998. *User Guidelines for Waste and Byproduct Materials in Pavement Construction*. FHWA-RD-97-148. Federal Highway Administration, Turner-Fairbank Highway Research Center, McLean, VA.

Christopher, B. R., C. Schwartz, and R. Boudreau. 2006. *Geotechnical Aspects of Pavements Reference Manual/Participant Workbook.* FHWA NHI-05-037. Federal Highway Administration and National Highway Institute, Washington, DC.

Cline, C., M. Anshassi, S. Laux, and T. G. Townsend. 2020. Characterizing Municipal Solid Waste Component Densities for Use in Landfill Air Space Estimates. *Waste Management and Research: The Journal for a Sustainable Circular Economy*, Vol. 38, No. 6, pp. 673–679.

Coban, H. S. 2017. *The Use of Lime Sludge for Soil Stabilization*. Master's thesis. Iowa State University, Ames, IA.

Correa, A. L. and B. Wong. 2001. *Concrete Pavement Rehabilitation – Guide for Diamond Grinding*. FHWA-SRC 1/10-01(5M). Federal Highway Administration, Washington, DC.

Cruse, R., D. Flanagan, J. Frankenberger, B. Gelder, D. Herzmann, D. James, W. Krajewski, M. Kraszewski, J. Laflen, J. Opsomer, and D. Todey. 2006. Daily Estimates of Rainfall, Water Runoff, and Soil Erosion in Iowa. *Journal of Soil and Water Conservation*, Vol. 61, No. 4, pp. 191–199.

DeSutter, T., L. Prunty, and J. Bell. 2011a. Concrete Grinding Residue Characterization and Influence on Infiltration. *Journal of Environmental Quality*, Vol. 40, No. 1, pp. 242–247.

DeSutter, T., P. Goosen-Alix, L. Prunty, P. J. White, Jr., and F. Casey. 2011b. Smooth Brome (*Bromus inermis* Leyss) and Soil Chemical Response to Concrete Grinding Residue Application. *Water, Air, and Soil Pollution*, Vol. 222, pp. 195–204.

Dispenza, K. 2020. Research Studies Show Potential Environmental Benefits of Concrete Grinding Residue: Is Slurry an Ugly Word? *Roads and Bridges*, February.

EPA. 2022a. *40 CFR, Chapter 1, Subchapter 1, Part 261, Subpart C - Characteristics of Hazardous Waste*. U.S. Environmental Protection Agency, Washington, DC.

EPA. 2022b. *Secondary Drinking Water Standards: Guidance for Nuisance Chemicals*. U.S. Environmental Protection Agency, Washington, DC.

FHWA. 2020. *Public Road Length – 2019: Miles by Type of Surface and Ownership/Functional System National Summary*. Federal Highway Administration, Washington, DC. https://www.fhwa.dot.gov/policyinformation/statistics/2019/pdf/hm12.pdf.

FHWA. 2015. *Gravel Roads Construction and Maintenance Guide*. Federal Highway Administration, Washington, DC.

Gee, K. W. 2005. *Technical Advisory T 5040.36 Surface Texture for Asphalt and Concrete Pavements*. Federal Highway Administration, Washington, DC.

Ghosh, P. 2021. *Performing CFD Analysis Over a 2D Cylinder to Visualize von Karman Vortex Shedding Using ANSYS Fluent*. Skill-Lync.com.

Goodwin, S. and M. Roshek. 1992. Recycling Project: Concrete Grinding Residue. *Transportation Research Record: Journal of the Transportation Research Board*, No. 1345, pp. 101–105.

Hansen, K. 2017. *Two Views of von Karman Vortices*. NASA Earth Observatory. https://earthobservatory.nasa.gov/images/90734/two-views-of-von-karman-vortices.

Hargitai, H. 2014. Obstacle Dunes and Obstacle Marks. *Encyclopedia of Planetary Landforms*. Springer, New York, NY.

Hibbs, B. O. and R. M. Larson. 1996. *Tire Pavement Noise and Safety Performance, PCC Surface Texture Technical Working Group*. FHWA-SA-96-068. Federal Highway Administration, Washington, DC.

Holmes and Narver. 1997. *Concrete Grinding Residue Characterization.* California Department of Transportation (Caltrans), Sacramento, CA. https://www.igga.net/wp-content/uploads/2018/08/Concrete_Grinding_Residue_Characterization_1997.pdf.

IGGA. 2013. *Diamond Grinding Slurry Handling – Best Management Practices*. International Grooving and Grinding Association, West Coxsackie, NY. https://www.igga.net/resources/diamond-grinding-slurry-handling-best-management-practices/.

IGGA. 2019. *IGGA History*. International Grooving and Grinding Association, West Coxsackie, NY. https://www.igga.net/history/.

Iowa DOT. 2020. *Specifications for Highway and Bridge Construction.* Iowa Department of Transportation, Ames, IA. https://iowadot.gov/erl/index.html.

Iowa SUDAS. 2015. *Iowa Statewide Urban Design and Specifications (SUDAS).* Iowa Statewide Urban Design and Specifications, Iowa State University, Ames, IA. https://iowasudas.org/manuals/specifications-manual/.

Jones, S. N. and B. Cetin. 2017. Evaluation of Waste Materials for Acid Mine Drainage Remediation. *Journal of Fuel*, Vol. 188, pp. 294–309.

Kenter, P. 2012. Diamond Grinding Can Go a Long Way for Road Lifespan. *Daily Commercial News by ConstructConnect*, February 24. https://canada.constructconnect.com/dcn/news/infrastructure/2012/02/diamond-grinding-can-go-a-long-way-for-road-lifespan-dcn048926w.

Kestler, M. A. 2009. *Stabilization Selection Guide for Aggregate- and Native-Surfaced Low Volume Roads.* U.S. Department of Agriculture Forest Service.

Kinnell, P. I. A. 2000. The Effect of Slope Length on Sediment Concentrations Associated with Side-Slope Erosion. *Soil Science Society of America Journal*, Vol. 64, No. 3, pp. 1004–1008.

Kluge, M., N. Gupta, B. Watts, P. A. Chadik, C. Ferraro, and T. G. Townsend. 2017. Characterisation and Management of Concrete Grinding Residuals. *Waste Management and Research: The Journal for a Sustainable Circular Economy*, Vol. 36, No. 2, pp. 149–158.

Knappett, J. and R. F. Craig. 2012. Chapter 1: Basic Characteristics of Soil. *Craig's Soil Mechanics.* 8th ed. pp. 3–5 and 13–19. CRC Spon Press, Abingdon, UK.

Li, C., J. Ashlock, B. Cetin, and C. Jahren. 2018. *Feasibility of Granular Road and Shoulder Recycling*. Institute for Transportation, Iowa State University, Ames, IA. https://intrans.iastate.edu/app/uploads/2018/07/granular_rd_and-shoulder_recycling_feasibility_w_cvr.pdf.

Luo, C. 2019. *The Effects of Road Surface Concrete Grinding Residue (CGR) on Selected Soil Properties and Plant Growth*. PhD dissertation. Iowa State University, Ames, IA.

Luo, C., Z. Wang, F. Kordbacheh, Y. Zhang, B. Yang, S. Kim, B. Cetin, H. Ceylan, and R. Horton. 2019. The Influence of Concrete Grinding Residue on Soil Physical Properties and Plant Growth. *Journal of Environmental Quality*, Vol. 48, No. 6, pp. 1842–1848.

Mahedi, M., B. Cetin, and A. Y. Dayioglu. 2019. Leaching Behavior of Aluminum, Copper, Iron and Zinc from Cement Activated Fly Ash and Slag Stabilized Soils. *Waste Management*, Vol. 95, pp. 334–355.

Mamo, M., D. McCallister, and W. Schacht. 2015. *Evaluation of Concrete Grinding Residue (CGR) Slurry Application on Vegetation and Soil Responses Along Nebraska State Hwy 31*. University of Nebraska-Lincoln, Lincoln, NE.

McGhee, K. H. 1994. *NCHRP Synthesis 204: Portland Cement Concrete Resurfacing*. National Cooperative Highway Research Program, Washington, DC.

McLaren, C. 1999. *Arkansas Highway History and Architecture, 1910–1965*. Arkansas Historic Preservation Program, Little Rock, AR.

Meyer, L. D. 1958. *An Investigation of Methods for Simulating Rainfall on Standard Runoff Plots and a Study of the Drop Size, Velocity, and Kinetic Energy of Selected Spray Nozzles*. USDA-ARS Special Report, Vol. 81, pp. 1–86.

Moossazadeh, J. and M. W. Witczak. 1981. Prediction of Subgrade Moduli for Soil that Exhibits Nonlinear Behavior. *Transportation Research Record: Journal of the Transportation Research Board*, No. 810, pp. 9–17.

Murakami, S. 1993. Comparison of Various Turbulence Models Applied to a Bluff Body. *Journal of Wind Engineering and Industrial Aeronautics*, Vol. 46–47, pp. 21–36.

Nasritdinov, A. 2003. *Using Rainfall Simulation and Tracer Anions to Study the Effects of Soil Bulk Density and Soil Moisture on Nitrate Leaching Characteristics*. Master's thesis. Iowa State University, Ames, IA.

National Geographic. n.d. Erosion, Resource Library Encyclopedia. National Geographic Society. https://www.nationalgeographic.org/encyclopedia/erosion/.

Neal, B. F. and J. H. Woodstrom. 1976. *Rehabilitation of Faulted Pavements by Grinding*. California Department of Transportation (Caltrans), Sacramento, CA.

Olson, K. R., L. D. Norton, T. E. Fenton, and R. Lal. 1994. Quantification of Soil Loss from Eroded Soil Phases. *Journal of Soil and Water Conservation*, Vol. 49, No. 6, pp. 591–596.

OSU. n.d. *AgBMPs, Ohio State University Extension: Inter-Rill and Rill Erosion*. College of Food, Agriculture, and Environmental Science, Ohio State University Extension, Columbus, OH. https://agbmps.osu.edu/scenario/inter-rill-and-rill-erosion.

Pasko, T. J., Jr. 1998. Concrete Pavements – Past Present and Future. *Public Roads Magazine*, Vol. 62, No. 1.

Physics Graphics. 2016. *Von Karman Vortex Street*. https://youtu.be/f3LmjJ1N7YE.

PCA. *Highways - History of Concrete Highways*. Portland Cement Association, Washington, DC. https://www.cement.org/cement-concrete/paving/concrete-paving-types/highways.

Rao, S., H. T. Yu, L. Khazanovich, M. I. Darter, and J. W. Mack. 1999. Longevity of Diamond-Ground Concrete Pavements. *Transportation Research Record: Journal of the Transportation Research Board*, No.1684, pp.128–136.

Rasmussen, R. O., S. Garber, R. Sohaney, P. Wiegand, and D. Harrington. 2010. *What Makes a Quieter Concrete Pavement?* Tech Brief. Concrete Pavement Surface Characteristics Program, National Concrete Pavement Technology Center, Iowa State University, Ames, IA. https://intrans.iastate.edu/app/uploads/2021/04/quieter-concrete-tech-brief_10-07-10.pdf.

Rasmussen, R. O., P. D. Wiegand, G. J. Fick, and D. S. Harrington. 2012. *How to Reduce Tire-Pavement Noise: Better Practices for Constructing and Texturing Concrete Pavement Surfaces*. National Concrete Pavement Technology Center, Iowa State University, Ames, IA. https://intrans.iastate.edu/app/uploads/2018/08/How_to_Reduce_Tire-Pavement_Noise_final.pdf.

Ricks, M. D., M. A. Horne, B. Faulkner, W. C. Zech, X. Fang, W. N. Donald, and M. A. Perez. 2019. Design of a Pressurized Rainfall Simulator for Evaluating Performance of Erosion Control Practices. *Water,* Vol. 11, No. 11, Article 2386.

Robinson, G. R., Jr., W. D. Menzie, and H. Hyun. 2004. Recycling of Construction Debris as Aggregate in the Mid-Atlantic Region, USA. *Resources, Conservation and Recycling*, Vol. 42, No. 3, pp. 275–294.

Sawangsuriya, A. and T. B. Edil. 2016. Evaluation of Soil Stiffness and Strength for Quality Control of Compacted Earthwork. *International Journal of Earth, Energy and Environmental Sciences*, Vol. 10, No. 2, pp. 114–118.

Schaefer, V., L. Stevens, D. White, and H. Ceylan. 2008. *Design Guide for Improved Quality of Roadway Subgrades and Subbases*. Iowa Statewide Urban Design and Specifications (SUDAS) and Center for Transportation Research and Education, Iowa State University, Ames, IA. https://intrans.iastate.edu/app/uploads/2018/03/subgrade_subbase_tr525.pdf.

Schmaltz, J. 2016. *Going with the Flow*. NASA Earth Observatory. https://earthobservatory.nasa.gov/images/88005/going-with-the-flow.

Schwartz, C. W., Z. Afsharikia, and S. Khosravifar. 2017. *Standardizing Lightweight Deflectometer Modulus Measurements for Compaction Quality Assurance*. Maryland Department of Transportation State Highway Administration, Baltimore, MD.

Shoemaker, A. L. 2009. *Evaluation of Anionic Polyacrylamide as an Erosion Control Measure Using Intermediate-Scale Experimental Procedures*. Master's thesis. Auburn University, Auburn, AL.

Smith, E. G. and B. C. English. 1982. *Determining Wind Erosion in the Great Plains*. Center for Agricultural and Rural Development, Iowa State University, Ames, IA.

Snell, L. M. and B. G. Snell. 2002. Oldest Concrete Street in the United States. *Concrete International*, Vol. 24, No. 3, pp. 72–74.

Snyder, M. B. 2019. *Concrete Pavement Texturing*. Tech Brief. FHWA-HIF-17-011. Federal Highway Administration, Washington, DC.

Townsend, T. G., P. Chadik, N. Gupta, M. Kluge, T. Vinson, and J. Schert. 2016. *Concrete Debris Assessment for Road Construction Activities*. Gainesville, FL.

USDA. 2011. *National Agronomy Manual (190–V–NAM)*, 4th ed. U.S. Department of Agriculture, Washington, DC.

USDA. 2020. *2017 National Resources Inventory: Summary Report*. Natural Resources Conservation Service, Washington, DC, and Center for Survey Statistics and Methodology, Iowa State University, Ames, IA. https://www.nrcs.usda.gov/sites/default/files/2022-10/2017NRISummary_Final.pdf.

White, D. J. and P. Vennapusa. 2013. *Low-Cost Rural Surface Alternatives Tech Transfer Summary*. Center for Earthworks Engineering Research, Institute for Transportation, Iowa State University, Ames, IA. https://intrans.iastate.edu/app/uploads/2018/03/rural_surface_alternatives_t21.pdf.

Willis, J. 2014. *Surface Grinding Concrete Pavements*. The British Cementitious Paving Association, 12th International Symposium on Concrete Roads 2014, Prague, Czech Republic, pp. 1–8.

Wilson, W. T. 2010. *Evaluation of Hydromulches as an Erosion Control Measure Using Intermediate-Scale Experiments*. Master's thesis. Auburn University, Auburn, AL.

Witczak, M. W. 2003. *NCHRP Project 1-28A: Harmonized Test Methods for Laboratory Determination of Resilient Modulus for Flexible Pavement Design. Vol. I, Unbound Granular Material.* National Cooperative Highway Research Program, Washington, DC.

Woodruff, N. P. and F. H. Siddoway. 1965. A Wind Erosion Equation. *Soil Science Society of America Proceedings*, Vol. 29, pp. 602–608.

Yang, B., B. Cetin, Y. Zhang, C. Luo, H. Ceylan, R. Horton, S. Kim, and M. Mahedi. 2019a. Effects of Concrete Grinding Residue (CGR) on Selected Sandy Loam Properties. *Journal of Cleaner Production*, Vol. 240, No. 118057.

Yang, Y. Zhang, B. Cetin, and H. Ceylan. 2019b. Concrete Grinding Residue: Management Practices and Reuse for Soil Stabilization. *Transportation Research Record: Journal of the Transportation Research Board*, Vol. 2673, No. 11, pp. 748–763.

Yonge, D. and H. Shanmugam. 2005. *Assessment and Mitigation of Potential Environmental Impacts of Portland Cement Concrete Highway Grindings*. Washington State Transportation Center (TRAC), Pullman, WA.

Zhang, Q., Z. Wang, Q. Guo, N. Tian, N. Shen, B. Wu, and J. Liu. 2019. Plot-Based Experimental Study of Raindrop Detachment, Interrill Wash, and Erosion-Limiting Degree on a Clayey Loessal Soil. *Journal of Hydrology*, Vol. 575, pp. 1280–1287.

Zhou, J. 2004. *Using Rainfall Simulation, TDR, and Tracer Anions to Determine Effects of Soil Properties on Nitrate Leaching*. PhD dissertation. Iowa State University, Ames, IA.

THE INSTITUTE FOR TRANSPORTATION IS THE FOCAL POINT FOR TRANSPORTATION AT IOWA STATE UNIVERSITY.

InTrans centers and programs perform transportation research and provide technology transfer services for government agencies and private companies;

InTrans contributes to Iowa State University and the College of Engineering's educational programs for transportation students and provides K–12 outreach; and

InTrans conducts local, regional, and national transportation services and continuing education programs.

IOWA STATE UNIVERSITY

INSTITUTE FOR TRANSPORTATION

Visit **InTrans.iastate.edu** for color pdfs of this and other research reports.